

Identification and characterization of glomeromycotan ammonium transporters

Dissertation
zur Erlangung des Doktorgrades der Naturwissenschaften
an der Fakultät für Biologie
der Ludwig-Maximilians-Universität München

vorgelegt von
Matthias Ellerbeck

München, 21. September 2012

Dissertation eingereicht: 21.09.2012

Tag der mündlichen Prüfung: 30.01.2013

Erstgutachter: Prof. Dr. Martin Parniske

Zweitgutachter: PD Dr. Arthur Schübler

Eidesstattliche Versicherung

Ich versichere hiermit an Eides statt, dass die vorliegende Dissertation von mir selbständig und ohne unerlaubte Hilfe angefertigt wurde.

München, den _____

Matthias Ellerbeck

Erklärung

Hiermit erkläre ich, dass die Dissertation nicht ganz oder in wesentlichen Teilen einer anderen Prüfungskommission vorgelegt worden ist. Ich habe nicht versucht, anderweitig eine Dissertation einzureichen oder mich einer Doktorprüfung zu unterziehen.

München, den _____

Matthias Ellerbeck

Veröffentlichungen in Fachzeitschriften

Teile dieser Arbeit wurden bereits zur Veröffentlichung eingereicht:

Ellerbeck M, Schübler A, Brucker D, Dafinger C, Loos F and Brachmann A (2012). Characterization of three ammonium transporters of the glomeromycotan fungus *Geosiphon pyriformis* (eingereicht bei *New Phytologist* am 10.09.2012).

Folgende Manuskripte sind in Vorbereitung:

Ellerbeck M, Schübler A and Brachmann A (2012). Root organ culture and root organ liquid culture (ROC and ROL) for AM fungi production.

Die im Manuskript beschriebene Methode verbessert die Kultivierung von AM Pilzen erheblich und soll patentiert werden. Eine Erfindungsmeldung wurde am 12.07.2012 bei der LMU eingereicht. Die entsprechenden Kapitel finden sich in der vorliegenden Dissertation unter dem Gliederungspunkt 2.4 (Seiten 61 – 66).

Ellerbeck M, Perez-Tienda J, Ait-Lahmidi N, Wipf D, Ferrol N, Schübler A and Brachmann A. Characterization of the ammonium transporter complement of the glomeromycotan fungus *Rhizophagus irregularis*.

Das Manuskript beschreibt die Identifikation des dritten Ammoniumtransporters von *R. irregularis*, die Charakterisierung der drei Transporter in *Saccharomyces cerevisiae* sowie die Lokalisation der Proteine und der mRNA-Transkripte in *R. irregularis*. Die entsprechenden Resultate finden sich in der vorliegenden Dissertation unter den Gliederungspunkten 2.2.2 und 2.3 (Seiten 34 – 36 und 41 – 60).

Für Marianne

Acknowledgements

I want to thank my thesis advisory committee (Prof. Parniske, Prof. Schübler, Prof. Jung and Andreas Brachmann) for fruitful discussions and constructive advice during the respective meetings.

I want to thank Prof. Martin Parniske for the opportunity to conduct my doctoral work in his group.

Special thanks go to Andreas Brachmann for supervision, discussion, guidance and advice through the last years.

I also want to thank Prof. Arthur Schübler for sharing ideas and giving valuable input.

I want to thank all members of the Genetics institute for the inspiring working atmosphere. Namely, I want to thank Stefan Allmann, Andreas Binder, Martin Groth, Kristina Haage, Simone Hardel, Regina Kühner, Jayne Lambert, Carolina Senes, Sylvia Singh and Kathalin Toth for discussions during coffee breaks, help and assistance whenever necessary.

Thanks to Marianne for love, support and patience!

Table of Contents

Summary	11
1. Introduction.....	12
1.1 Arbuscular mycorrhiza symbiosis (AM)	12
1.1.1 Steps in AM establishment.....	12
1.1.2 Lifestyle and organization of AMF; cultivation under laboratory conditions..	14
1.1.4 <i>Geosiphon pyriformis</i> symbiosis as a model system for AM symbiosis	16
1.1.5 Nutrient fluxes in AM	19
1.2 Ammonium transport	21
1.2.1 General facts about nitrogen and ammonium	21
1.2.2 The Amt/Mep/Rh-family of AMTs	22
1.2.3 AMTs of fungi	23
1.2.4 Bioenergetics of ammonium transport.....	25
1.2.5 Regulation of AMT proteins	26
1.2.6 Objectives of the study	26
2. Results.....	28
2.1. Identification of glomeromycotan AMTs	28
2.1.1 <i>Geosiphon pyriformis</i> and <i>Rhizophagus irregularis</i> each contain 3 AMT-like genes	28
2.1.2 Phylogenetic analysis of glomeromycotan AMTs.....	30
2.2. Functional characterization	32
2.2.1 <i>GpyrAMT2</i> and <i>GpyrAMT3</i> are not able to complement a yeast $\Delta mep1-3$ mutant	32
2.2.2 Only GintAMT1 is capable of methylammonium transport	35
2.2.3 Ammonium removal assays support ammonium transport capability of GpyrAMT1	38
2.2.4 The ammonium transport capability of GpyrAMT2 can be rescued partly by a single amino acid exchange	38
2.2.5 Summary functional characterization	41
2.3. Localization of glomeromycotan AMTs	42
2.3.1 Establishment of specific antibodies	42
2.3.2 Establishment of preparation protocol.....	44
2.3.3 Extraradical localization of fungal AMTs	45
2.3.4 Intraradical Localization of fungal AMTs	51
2.3.5 Localization of fungal AMT transcripts	58
2.3.6 Summary localization of glomeromycotan AMTs	61
2.4. Optimization of the fungal <i>in-vitro</i>-culturing system	62
2.4.1 ROC success rate (RSR) can be used to determine root colonization of mother-culture	62

2.4.2 Reduction of phosphate content in liquid MSR improves stable root colonization	63
2.4.3 A continuous liquid culture method of mycorrhizal chicory roots.....	64
2.4.4 Effect of sucrose and gellan gum concentration on fungal root colonization and RSR.....	65
2.4.5 ROL of mycorrhizal chicory positively affects the fungal growth in successive ROCs	66
2.5. Establishment of a transformation system for <i>R. irregularis</i>.....	68
3. Discussion	69
3.1 Definition of the AMT complements of two glomeromycotan fungi.....	69
3.2 The functional relevance of glomeromycotan AMTs in arbuscular mycorrhiza symbiosis	73
3.3 Optimization of the culturing system of <i>R. irregularis</i>	76
4. Material and methods	79
4.1 Material	79
4.1.1 Equipment	79
4.1.2 Chemicals and consumables	80
4.1.3 Enzymes.....	82
4.1.4 Buffers and solutions.....	82
4.1.5 Media.....	87
4.1.7 Oligo nucleotides used in this study	90
4.1.8 Plasmids used in this study	92
4.2 Methods	93
4.2.1 Strains and Cultivations.....	93
4.2.2 Molecular biological methods	94
4.2.3 Biochemical methods	99
5. References	104
6. Appendix	114
6.1 Sequences of glomeromycotan AMTs and their genes.....	114
6.2 List of figures	120
6.3 List of Tables.....	121
6.4 Abbreviations.....	122

Summary

The majority of plant species on earth are undergoing a very intimate root symbiosis with fungi of the phylum *Glomeromycota*. This symbiosis is called arbuscular mycorrhiza (AM) symbiosis. The fungal partners are obligate symbiotic organisms and feed their host with phosphate, nitrogen, micronutrients and water and, in exchange, are fed by their host with a significant portion of photosynthetically fixed carbon. Because of their specific lifestyle – arbuscular mycorrhiza fungi are multi nucleate organisms lacking a sexual phase – the research on this symbiosis mainly focused on the plant side in the past decades. The major facilitators carrying out nutrient transport between the symbiotic partners are not yet identified.

Focusing on the symbiotic nitrogen exchange, the goal of this study was the identification and characterization of glomeromycotan ammonium transporters. Therefore, an existing cDNA library of *Geosiphon pyriformis*, a glomeromycotan fungus, was screened for ammonium transporter encoding genes by functional complementation of *Saccharomyces cerevisiae*, degenerate PCR and next generation sequencing. In parallel, the transcriptome data of *Rhizophagus irregularis*, a widely used model AM fungus, was screened for ammonium transporter encoding genes.

To increase the production of fungal material for nucleic acid extraction and biochemical investigations, the traditional culture system of glomeromycotan fungi with *Agrobacterium rhizogenes* transformed host roots on two compartment Petri-dishes, was modified and a liquid cultivation step was introduced, resulting in more reliable hyphal growth on the Petri-dishes afterwards.

In total, 6 genes coding for ammonium transporter related proteins, were identified, 3 for each of the two fungi. Functional characterization and localization in yeast revealed ammonium transporter typical characteristics for only one of them, while the others showed either unusual localization or unusual transport properties in terms of ammonium or methylammonium transport – an ammonium analogue, typically used for biochemical determination of ammonium transport kinetics.

Localization studies in *R. irregularis* via immune localization and *in-situ*-RT-PCR revealed unexpected localization of the transporters and their transcripts restricted to fungal storage organs (extraradical spores and intraradical vesicles), when ammonium was present in the medium. Without surrounding ammonium, the transporters could be localized to a sub population of extraradical hyphae additional to the localization in spores, indicating a cyclic retention function instead of a direct ammonium uptake function of the investigated ammonium transporters. No ammonium transporters – neither proteins nor mRNA transcripts – were detected in arbuscules. The symbiotic nutrient exchange, however, is supposed to take place in these eponymous structures of the symbiosis with their enlarged surface area.

The lack of ammonium transporters in arbuscules leads to the idea of nitrogen release to the host plant by passive diffusion of ammonia over the arbuscular plasma membrane of the fungal symbiont to the periarbuscular space and active uptake of ammonium from the periarbuscular space by the plant host.

1. Introduction

1.1 Arbuscular mycorrhiza symbiosis (AM)

In nature, more than 90% of all land plants undergo root symbioses with varying fungal partners. Those beneficial interactions are called mycorrhiza (*gr.* μυκός, mykós = 'fungus', ρίζα, riza = 'root'). Ectomycorrhizal (*gr.* ἐκτός, ekto = outside) associations, predominantly formed by trees in temperate forests, are characterized by the fungal partner staying outside of the plant cells, while in endomycorrhizal (*gr.* ἐντός, endo = inside) associations the fungus penetrates plant root cells. The most important endomycorrhizal symbiosis is the arbuscular mycorrhiza symbiosis (AM). AM is a nearly ubiquitous plant-microorganism symbiosis in terrestrial ecosystems (Brachmann & Parniske, 2006; Wang & Qiu, 2006). About 80% of all terrestrial plants undergo AM with so-called AM fungi (AMF, Bougoure *et al.*, 2009; Gianinazzi-Pearson, 1996; Smith & Read, 2008). To date, AMF without exception belong to one distinct monophyletic fungal phylum, the *Glomeromycota* (Schüßler & Kluge, 2001; Hibbett *et al.*, 2007), and - the other way round - all glomeromycotan fungi investigated so far are able to form AM. The eponymous symbiotic structures of the AM symbiosis, the arbuscules (*lat.* arbuscula = little tree), can be observed in 400 million year (MY) old fossil findings (Remy *et al.*, 1994) and fossil AMF spores are dated to 460 MY ago (Redecker *et al.*, 2000). Therefore, AM is discussed to be one of the key acquisitions of green plants that allowed terrestrial life on earth.

1.1.1 Steps in AM establishment

AMF are obligate symbionts, this means dependent on photosynthetically fixed carbon provided by their host (Schüßler *et al.*, 2006). The only plant-independent phase of AMF is the presymbiotic growth after spore germination. This hyphal outgrowth, however, stops if no compatible plant is recognized in the environment (Logi *et al.*, 1998). The crucial steps in AM formation are shown in Figure 1. After recognition of plant-derived hormones (so-called strigolactones; Akiyama *et al.*, 2005; Besserer *et al.*, 2006) the fungus produces lipochitooligosaccharides as signal molecules (Figure 1, step 1). Those signal molecules are called Myc factors (Maillet *et al.*, 2011), referring to the rhizobial Nod factor playing a role in the root nodule symbiosis of legumes (Riely *et al.*, 2004; Parniske, 2008). Additionally, the fungal hyphae react with enhanced growth (e.g. *Rhizophagus irregularis* DAOM 197198) and/or branching (e.g. *Gigaspora magerita*). This is why strigolactones are also called branching factors (Akiyama *et al.*, 2005). The direct contact between fungal hyphae and plant roots is followed by the formation of a hyphopodium (Figure 1, step 2; wrongly termed appressorium formerly). Afterwards, the fungal hyphae are subsequently guided through the epidermal cell layers by the plant cells, which form by massive cytoskeletal rearrangements a tunnel-like structure called pre penetration apparatus (PPA, shown in Figure 1, step 3; Genre *et al.*, 2005). In the cortical cell layers, the fungal hyphae grow intercellularly and form,

depending on the plant-fungus combination, a varying number of intracellular arbuscules, which are characterized by an enlarged surface and therefore supposed to be the active organs for symbiotic nutrient exchange (Parniske, 2008). In later phases of the symbiosis, the fungus forms intercellular vesicles and (in some AMF species) even intraradical spores (Figure 1, step 4). Those structures are supposed to be fungal storage organs. In the surrounding soil, the fungus starts to grow and forms a dense hyphal network as soon as the symbiosis is established. The enlarged surface as well as the density of the network increase the nutrient and water uptake ability and significantly contribute to plant nutrition. In addition, the fungal hyphae can by their small diameter access nutrients and/or water from small pores in the soil better than roots or root hairs. In regular intervals, fungal spores are formed. The spores are on the one hand fungal storage organs and on the other hand serve as soil persisting form of AMF. Spores help the fungus to survive adverse environmental conditions like draught stress, disruption of the hyphal network etc.

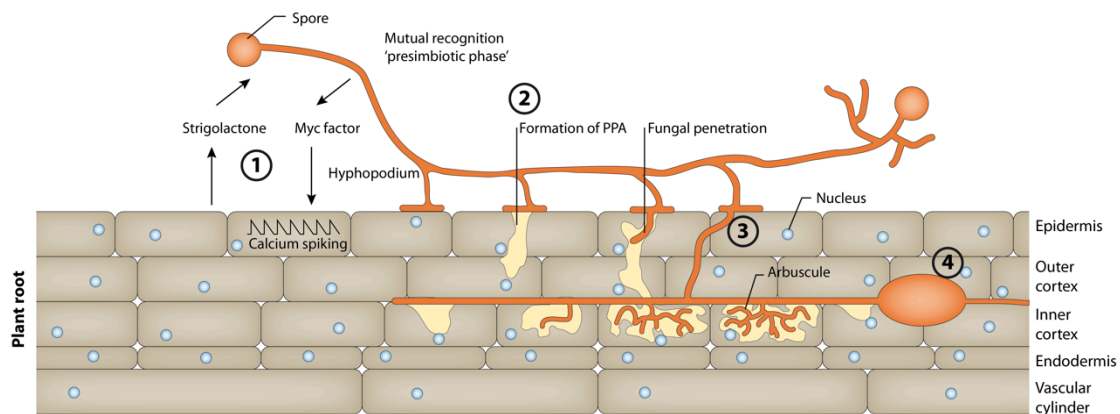


Figure 1: Steps in AM formation. The formation of AM consists of 3 to 4 major steps: (1) the recognition of the symbiotic partner by each other via strigolactones and Myc factors, (2) physical contact between the symbiotic partners (formation of a hyphopodium by the fungus, formation of the pre penetration apparatus by the plant) with successive fungal penetration of the root and (3) colonization of cortical cell layers followed by the establishment of arbuscules. Intracellular steps through and into plant cells are actively guided by the host plant. In most cases the fungus forms vesicles (4) in later stages of the symbiotic interaction which are supposed to be fungal storage organs. PPA = pre penetration apparatus, a tunnel formed by the plant cell to actively guide the fungus through the cells. Figure adopted from Parniske (2008), Genre *et al.* (2008), with permission.

While the formation of AM can be observed microscopically in particular detail (Genre *et al.*, 2005; Genre *et al.*, 2008), the knowledge of events on the molecular level is poor. To date at least nine essential plant genes for AM formation have been found by forward genetic screens and published (for review see Parniske, 2008). Plants without their gene products abort AM formation at different steps, but all of those mutants share a principal disability in establishing functional AM symbiosis. Those genes are so-called “common symbiosis genes” (common sym genes), because they are also essential for the nodule symbiosis of legumes. Nevertheless, the specific roles of their gene products remain unclear (Parniske, 2008). Besides those common sym genes, a phosphate transporter gene (*MtPT4*; Harrison *et al.*, 2002) and two half ABC

transporter genes coding for transporters with unknown substrate (STR1 and STR2; Zhang *et al.*, 2010; Gutjahr *et al.*, 2012) are necessary for the establishment of functional AM symbiosis. Mutant plants are able to guide the fungal hyphae through epidermal cell layers but arbuscules are underdeveloped. In addition to these data, molecular studies in a variety of legumes revealed that a number of plant genes expressed in early steps of nodulation, including *ENOD2*, *ENOD5*, *ENOD11*, *ENOD12*, and *ENOD40*, are also transcribed during root colonization by AM fungi (van Rhijn *et al.*, 1997; Albrecht *et al.*, 1998; Journet *et al.*, 2001), suggesting an evolutionary relationship between both symbioses, but their function in AM is still unknown. Even less – nearly nothing – is known concerning fungal genes and proteins involved in the process of AM formation.

1.1.2 Lifestyle and organization of AMF; cultivation under laboratory conditions

AM fungi are different from most living organisms by their morphological persistence over millions of years, their life-style and genetic organization. They have existed for more than 400 million years morphologically more or less unaltered, thereby describing their perfect adaptation to the ecological niche they are living in (Remy *et al.*, 1994). Although AMF spores are able to germinate (hyphal growth out of the spore or of a hyphal tip) – once or a few times without contact to a host plant – AM fungi are obligate biotrophic organisms, meaning that they are not able to live without being fed by a host plant. They are commonly aseptate and multicaryotic (coenocytic) organized with hundreds or even thousands of nuclei sharing the same cytoplasm. The cumulative occurrence of DNA sequence polymorphisms even in DNA samples of single spores (Stockinger *et al.*, 2009) and their possible explanations – heterogenic nuclei versus high allelic variations inside the nuclei – are still under substantial debate (Pawlowska & Taylor, 2004; Hijri & Sanders, 2005). Recent investigations of the genome size in the model fungus *Rhizophagus irregularis*, however, showed no noticeable differences for the investigated nuclei, thereby pointing into the direction of high allelic variations inside the nuclei (Sedzielewska *et al.*, 2011).

Because of their obligate biotrophy, co-culture with host plants is mandatory for the cultivation of AMF in the lab. Most of them are kept in the soil of pot cultures in association with whole plants (e.g., Gerdemann, 1963). In this culture system, it is not possible to get deeper insights into AM establishment and the infection process, because all the morphological processes take place in the soil. Moreover, the experimental accessibility of the fungus in those cultures is very low. For the investigation of morphological processes during AM establishment a more sophisticated culture method called root organ culture (ROC) has provided a big breakthrough (Figure 2; Declerck *et al.*, 1998; Fortin & Bécard, 2002; Declerck *et al.*, 2005; Ijdo *et al.*, 2011).

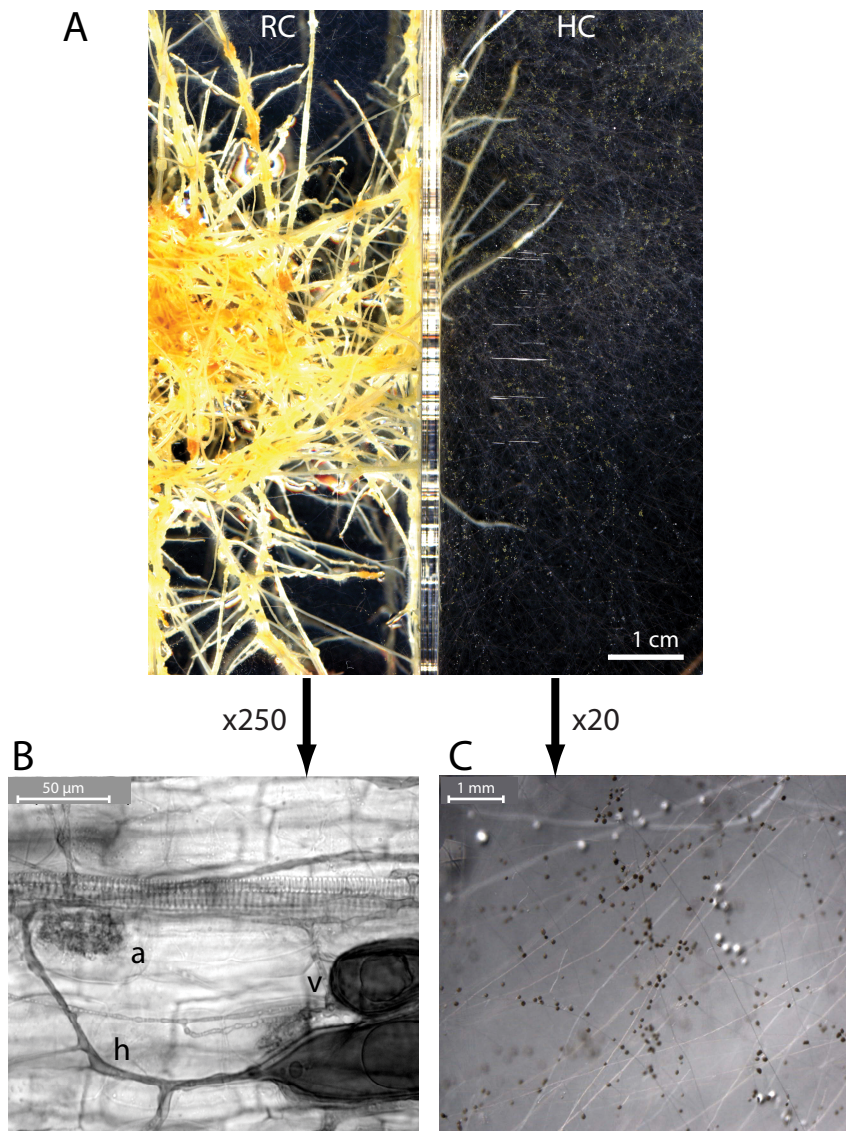


Figure 2: Root organ culture for cultivation of AM fungi. (A) A compartmented petri dish with chicory roots and fungal spores growing in the respective compartments (RC = root compartment, HC = hyphal compartment) is shown. (B) A microscopic picture of stained fungal structures inside a chicory root: arbuscule (a) on the left, storage vesicles (v) on the right, connected by an intercellular hypha (h). (C) A closer look into the fungal compartment (HC) from the above shown Petri dish showing the fungal hyphal network and spores, which are hardly visible in the upper picture.

In ROC *Agrobacterium rhizogenes* transformed roots of carrot (*Daucus carota*) or chicory (*Cichorium intybus*) are growing sterile *in vitro* on solidified, sucrose containing medium in one half of compartmented Petri dishes (split-plates, Figure 2A). On the plates they can be associated with single spores of varying AMF and the downstream processes can be studied. In the second compartment, sugar-free medium is provided and allows only fungal growth (Figure 2C). The development of this culture method was a great advantage for the molecular and biochemical research on AM fungi. Although this method leads to a better accessibility of the fungus than pot cultures, the

propagation of fungal material in reasonable amounts is still time intensive and laborious (see for example Declerck *et al.*, 2005; Campagnac *et al.*, 2009).

For AM research, *R. irregularis* DAOM197198 is the most frequently used member of the *Glomeromycota*. This AMF was erroneously called *Glomus intraradices*, but corresponds to the synonym *Glomus irregulare* (Stockinger *et al.*, 2009), which is now placed in the genus *Rhizophagus* (Krüger *et al.*, 2012). Its wide use in basic research resulted from the easy *in vitro* cultivability in ROC (Bécard & Fortin, 1988; Chabot *et al.*, 1992), providing well characterized biological material for studies in basic research, including a genome sequencing project (Martin *et al.*, 2008; Tisserant *et al.*, 2012) or transient genetic transformation (Helber & Requena, 2008).

ROC of AMF originally was established using *A. rhizogenes* transformed carrot (*D. carota*) roots, and the culturing method has undergone several optimizations in terms of media composition, (re-)association of AMF with host roots and use of multi-compartment systems (for reviews see Fortin & Bécard, 2002; Declerck *et al.*, 2005; Ijdo *et al.*, 2011). The use of transformed chicory (*C. intybus*) roots for ROC was established by Fontaine *et al.*, 2004 (2004). Chicory roots facilitate the handling of many *in vitro* cultured AMF, as colonized roots can be easily transferred to start new cultures, regrow fast, ramify intensely, and even quite old roots readily grow on fresh medium, to name the advantages over the use of carrot roots. While carrot ROCs need regular maintenance (transfer of root tips to new plates to avoid over-ageing of the roots as well as re-association of young roots with fungal infectious units such as spores or colonized old carrot roots) and c. 16-20 weeks to produce sufficient amounts of spores (Bécard & Fortin, 1988; Declerck *et al.*, 1998; Fortin & Bécard, 2002; Ijdo *et al.*, 2011), the chicory based system can be grown in split-plates for up to 6 months without maintenance and produces spores after c. 12 weeks (e.g., see Campagnac *et al.*, 2009). Half a year old chicory roots are still capable of new outgrowth after transfer to fresh plates, while carrot roots lose this capability much earlier.

Despite those developments, there are only a limited number of techniques available for AMF, including only indirect and descriptive techniques on extracted DNA, RNA or protein. To date there is no stable transformation system available and the missing sexual state allows neither genetic nor mutagenesis screens. More sophisticated indirect techniques like immune localization and *in-situ*-PCR had not been extensively tested before.

1.1.4 *Geosiphon pyriformis* symbiosis as a model system for AM symbiosis

During three diploma theses (Dafinger, 2008; Brucker, 2009; Ellerbeck, 2009) and a couple of internships (Brucker, 2008; Ellerbeck, 2008; Loos, 2008), the groups Brachmann and Schübler successfully identified and characterized two putative ammonium transporter (AMT) genes of the Gomeromycotan fungus *Geosiphon pyriformis* (Figure 3). *Geosiphon pyriformis* undergoes a symbiosis with the cyanobacterium *Nostoc punctiforme* (Schübler & Kluge, 2001; Schübler & Wolf, 2005), which is most probably comparable to the classical AM symbiosis of other

Glomeromycota (Figure 3C; Schüßler, 2012). As the bacterial endosymbionts are prokaryotes and do not poly-adenylate their messenger RNAs (mRNAs), a fungal coding DNA (cDNA) expression library of symbiotic active material could be established by RNA extraction from the symbiotic bladders (Figure 3A and B) and subsequent oligo-dT purification. In an additional step, the mRNAs were size fractionated to obtain a full-length library of the respective mRNAs and cloned into the library vector pDR196sfi (Schüßler *et al.*, 2006). The library vector contained origins of replication and selection markers for both *Escherichia coli* and *Saccharomyces cerevisiae*. Claudia Dafinger discovered the first AMT gene of *G. pyriformis* in a yeast complementation screen by coincidence and named it *GpAMT1*. This gene complemented a urea-uptake deficient yeast strain on medium with urea as sole nitrogen source, probably because of urea degradation within the plate medium during autoclaving. Further investigations showed, that *GpAMT1* does not code for a urea transporter (Dafinger, 2008). The same gene was re-isolated in parallel by Matthias Ellerbeck and David Brucker when an ammonium uptake deficient ($\Delta mep1-3$) strain of *S. cerevisiae* (MLY131a/ α ; Lorenz & Heitman, 1998a) was transformed with the cDNA expression library of the symbiotic active bladders of *G. pyriformis* and screened for growth on plate medium containing low ammonium concentrations (100 μ M and 1,000 μ M, respectively) as sole nitrogen source.

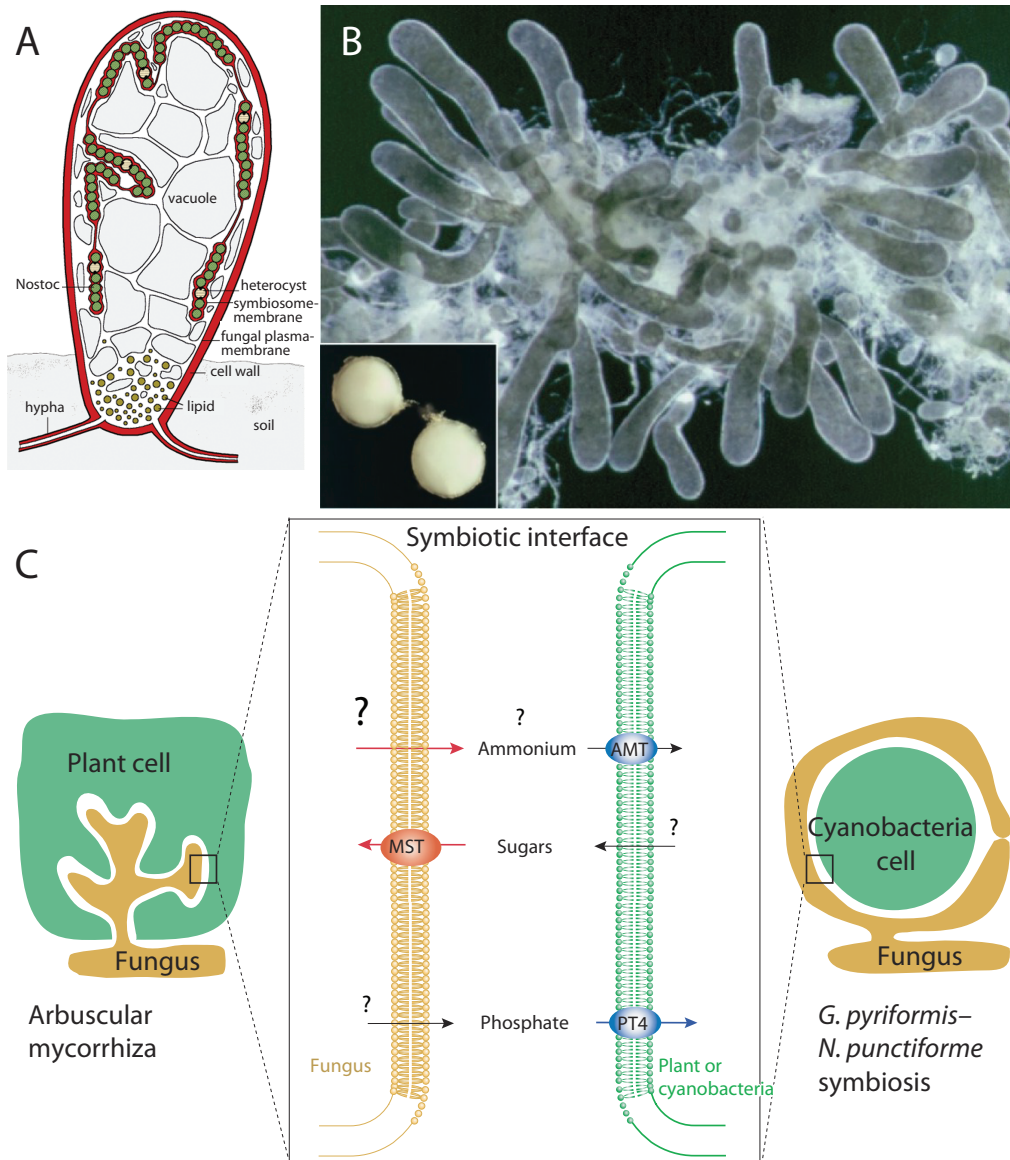


Figure 3: The *G. pyriformis* symbiosis and its comparability to AM. (A) Schematic drawing of a *G. pyriformis* bladder with endosymbiotic bacteria of the species *Nostoc punctiforme* (green spheres, white spheres = heterocysts), surrounded by the symbiosome membrane (red). (B) Pictures of *G. pyriformis* bladders and spores in nature. (C) Schematic comparison of nutrient fluxes in classical AM and *G. pyriformis* symbiosis. Most probably they are comparable. PT = phosphate transporter, MST = monosaccharide transporter, AMT = AMT. Lower panel adopted from Schüßler *et al.*, 2006. Scheme and pictures of the upper panel provided by Arthur Schüßler (Schüßler, 1995).

In a parallel approach, degenerate primers were designed to take advantage of the high conservation levels among AMTs and to pull out AMT coding genes from the cDNA library by PCR directly. For that, *GintAMT1* was compared to either basidiomycotan or ascomycotan sequences at the NCBI webpage (Basic local alignment search tool [BLAST] search; Altschul *et al.*, 1997). The 5 top hits of both BLASTs were aligned together with *GintAMT1* with ClustalW2 (Thompson *et al.*, 1994; Higgins *et al.*, 1996; Larkin *et al.*, 2007) to generate degenerate primers following the CODEHOP strategy (Rose *et al.*, 1998; Rose *et al.*, 2003; Ellerbeck, 2009). Degenerate PCR and subsequent PCR amplification by gene specific and vector

backbone specific primers revealed a second AMT like gene from the cDNA library (Brucker, 2008; Loos, 2008). This gene and the encoded protein share high similarities with already published AMTs, but the gene is not able to complement the $\Delta mep1-3$ yeast mutant (see results). However, it was named *GpAMT2*. Recently, the cDNA library was subject to a next generation sequencing approach (Schüßler *et al.*, unpublished). Blasting of *GpAMT1* and *GpAMT2* sequences against the 454 output data resulted in no hit for *GpAMT1*, three hits for *GpAMT2* and one hit for another closely related AMT coding gene. This gene was named *GpAMT3*. It was – like *GpAMT2* – not able to complement the $\Delta mep1-3$ yeast mutant after amplification and cloning into pDR196sfi (see results). All three genes have been renamed according to the nomenclature proposed for AM fungal genes (Franken, 2002) to *GpyrAMT1*, *GpyrAMT2* and *GpyrAMT3*.

1.1.5 Nutrient fluxes in AM

AM is characterized by massive nutrient fluxes (Figure 4) between the symbiotic partners. As a highly branched structure with enlarged surface the arbuscule is supposed to be the place, where symbiotic nutrient exchange takes place. At the symbiotic interface, the fungus supplies the plant with important growth-limiting inorganic nutrients like phosphate, nitrogen, micro nutrients and water that are transported over the fungal plasma membrane and the plant periarbuscular membrane (Bago *et al.*, 2001; Govindarajulu *et al.*, 2005; Finlay, 2008; Tian *et al.*, 2010). In exchange, the plant provides significant parts of synthetically fixed carbon to the fungus. For all terrestrial plants the summarized amount of carbon fed to AM fungi is calculated to reach 5 billion tons of carbon per year (Bago *et al.*, 2000; Bago *et al.*, 2003). Additionally, the exchange of nutrients is strictly regulated. Govindarajulu and coworkers (2005) discovered that carbon is transported to the fungus without nitrogen – in the form of fatty acids or saccharides and not in the form of amino acids – whereas nitrogen is transported to the plant without carbon – most probably as ammonium and not in the form of amino acids.

While the beneficial effect of AM on plants is known for decades now, the research on the genetic and biochemical determinants that facilitate the massive amounts of nutrient transport still remains in its infancies. On the plant side one phosphate transporter (MtPT4 $\hat{=}$ LjPT4, exclusively expressed in arbusculated cells; Harrison *et al.*, 2002) and one AMT (LjAMT2;1, preferentially expressed in arbusculated cells; Guether *et al.*, 2009) were discovered, which are essential for AM formation. These transporters are supposed to take up AMF derived nutrients from the periarbuscular space (Figure 4). On the fungal side to date there are 7 characterized nutrient transporters published (Figure 4). Two phosphate transporters, two AMTs, one amino acid permease and one zinc ion transporter were found in the extraradical mycelium of different AM fungi (Harrison & van Buuren, 1995; Maldonado-Mendoza *et al.*, 2001; Gonzales-Guerrero, 2005; López-Pedrosa *et al.*, 2006; Cappellazzo *et al.*, 2008; Perez-Tienda *et al.*, 2011). A nitrate transporter is assumed, as cultivation on nitrate is

possible (Govindarajulu *et al.*, 2005; Fellbaum *et al.*, 2012). A fungal monosaccharide transporter, discovered in the symbiotically active bladders of *G. pyriformis*, is supposed to be located in the symbiosome membrane and to take up carbon, which is released by the symbiotic partner (Schüßler *et al.*, 2006), while the other 6 transporters are supposed to take up the respective nutrients from the soil.

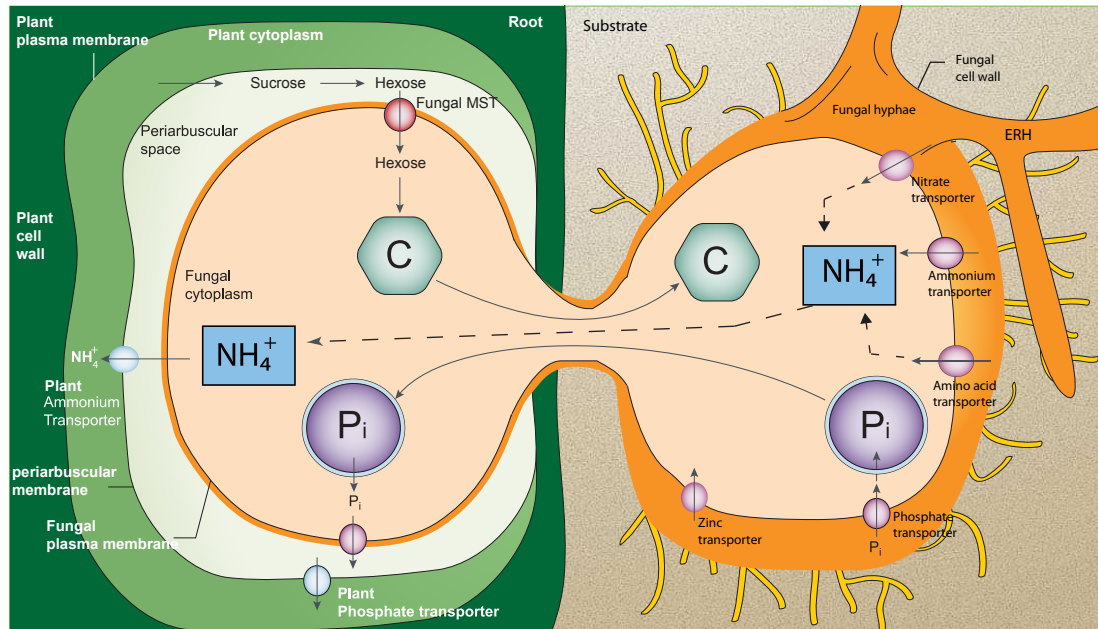


Figure 4: Metabolic fluxes in AM. On the left side a schematic arbuscule is shown, the right side reflects the extraradical mycelium. In the arbuscules plant-derived carbon is transported to the fungus across two membranes. In the first step it is transported into the periarbuscular space, most probably in the form of sucrose, cleaved and taken up by the fungus in the form of hexoses. On the other hand N, P and micronutrients are taken up by the extraradical fungal hyphae (ERH) from the soil. The nitrogen is fixed as arginine (left out for simplicity) and transported (probably) together with the phosphate in polyphosphate bodies to the intraradical hyphae (dashed line). Here the arginine gets metabolized again and N and P are released to the periarbuscular space where they get taken up by plant transport molecules. Figure modified from Bago *et al.*, 2003; Govindarajulu *et al.*, 2005; Jin *et al.*, 2005; Parniske, 2008; Tian *et al.*, 2010, with permission.

The nutrients taken up by the extraradical fungal hyphae get assimilated and partly transported from the extraradical mycelium to the intraradical hyphae, where they are delivered to the host plant. Nitrogen is fixed in the form of arginine, which then most probably is co-transported with negatively charged, membrane enclosed polyphosphate granules towards the intraradical hyphae (Govindarajulu *et al.*, 2005; Tian *et al.*, 2010). There, the arginine is metabolized by an arginase and nitrogen in the form of ammonium is supplied to the plant. On the other hand, the carbon, taken up as hexoses by the intraradical hyphae, gets incorporated into glycogen granules and transported to the extraradical mycelium (Figure 4).

1.2 Ammonium¹ transport

1.2.1 General facts about nitrogen and ammonium

Nitrogen is one of the major components of biological macromolecules such as proteins and nucleic acids and is therefore essential for living organisms. However, around 99% of the existing nitrogen on this planet is present as atmospheric dinitrogen (Rees *et al.*, 2005), which cannot be metabolized by most organisms. Only a specialized subgroup of bacteria contains an enzyme called nitrogenase that is able to break up the very stable triple bond of the dinitrogen molecule and allows the subsequent reduction to ammonium (Rees & Howard, 2000). In the form of ammonium, nitrogen can be incorporated into biological molecules via different pathways (Einsle *et al.*, 1999).

Ammonium usually gets incorporated into glutamine and glutamate (Figure 5) and can be transferred to other amino acids for protein biosynthesis via trans amination. To fit into the nucleotide biogenesis pathways, ammonium needs to be incorporated into carbamoyl-phosphate and then further processed. In all of these enzymatic steps for biosynthesis, ammonium is either the nitrogen source or at least an intermediate metabolite, which underlines directly its biological relevance (Jones, 1963; Stryer "biochemistry" 2003).

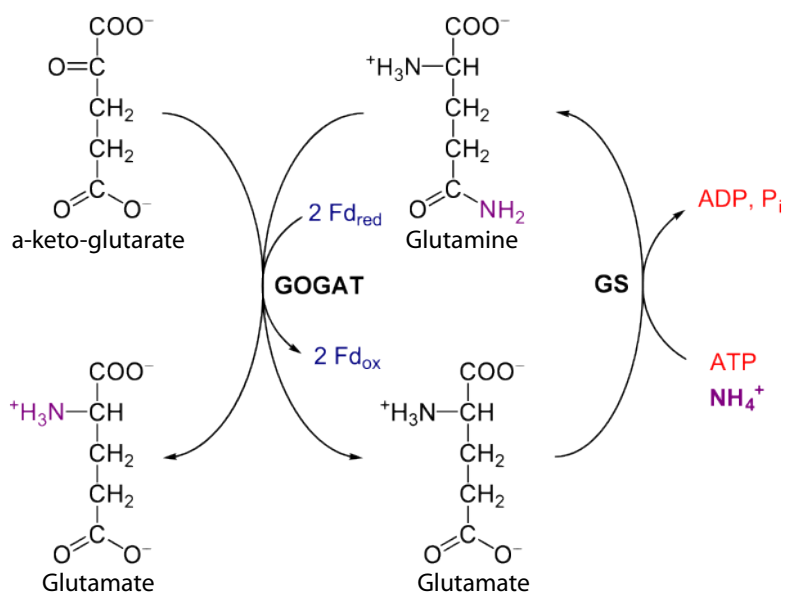


Figure 5: Fixation of Ammonium. Ammonium fixation via the GS/GOGAT pathway (Lea & Mifflin, 1974) is shown. Ammonium is incorporated into glutamine by the glutamine synthetase (GS). The amination of glutamate removes one water molecule. In the next step, the amino group is transferred to an a-keto-glutarate molecule, which gets aminated. In the end two glutamate molecules are formed. Figure adopted from Yikrazuul, de.wikipedia.org, with permission.

¹ The terminus "ammonium" will be used for both, NH_3 and NH_4^+ . If specification is necessary, the chemical formulas will be used.

1.2.2 The Amt/Mep/Rh-family of AMTs

In its free form, ammonia (NH_3) is permeable for biological membranes. The permeability is close to the one of H_2O (Kleiner, 1985). However, NH_3 is in protonation equilibrium with NH_4^+ ($\text{pK}_a = 9.3$) and at physiological pH values, the equilibrium strongly directs to the cationic, membrane-impermeable form. Around 99% of the molecules are protonated at a pH value of 7.3. For more acidic pH values the equilibrium shifts even more into the direction of the protonated form. Because of the NH_3 permeability of biological membranes, initially the predominant opinion in the scientific field doubted the existence of ammonium uptake molecules both as passive channels and as active transporters. But already in the 1970s and early 80s lines of evidence for active ammonium transport mechanisms arose (Hackette *et al.*, 1970; Kleiner, 1981). An increasing amount of publications reported NH_4^+ gradients across microbial plasma membranes and the hints for ammonium uptake systems became obvious (Strenkoski & DeCicco, 1971; Stevenson & Silver, 1977; Kleiner & Fitzke, 1981). To explain these findings, *cyclic retention* was discussed. Cyclic retention means the compensation of nitrogen loss by passive diffusion of NH_3 over the cell membrane in times of nitrogen starvation. Rapid re-uptake (cyclic retention) of the ammonium would be one possibility to counteract this loss. For this, active AMTs would be necessary (Kleiner, 1985).

As most organisms are not able to fix atmospheric nitrogen, they are forced to take up reduced nitrogen in form of ammonium or amino acids from the environment. The first AMT encoding genes – *ScMEP1* and *AtAMT1;1* – were published in 1994. Ninnemann and coworkers cloned the first plant AMT gene – *AtAMT1;1* of *Arabidopsis thaliana* (Ninnemann *et al.*, 1994) while Marini and coworkers cloned the first fungal gene encoding for an AMT – *ScMEP1* from the baker's yeast *Saccharomyces cerevisiae* (Marini *et al.*, 1994). As it was found to enhance sensitivity to the toxic chemical methylammonium (MA, $\text{CH}_3\text{-NH}_3^+ \leftrightarrow \text{CH}_3\text{-NH}_2 + \text{H}^+$; $\text{pK}_a = 10,64$) in yeast, it was named methylammonium permease 1 (MEP1). A few years later, two additional AMT genes of baker's yeast – *ScMEP2* and *ScMEP3* – were discovered and published by the same group (Marini *et al.*, 1997). All three yeast AMTs were able to transport ammonium as well as MA, a toxic derivative of ammonium, which can be radioactively labeled at its carbon atom. Labeled MA was used for biochemical investigations and to determine kinetic variables like K_M and V_{max} . The protein encoded by *AtAMT1;1* was also able to transport ammonium as well as MA.

During the next decade more ammonium transport proteins have been characterized. From the genome sequencing approaches more and more sequences became available that fell into the clade of AMTs. All those gene and their encoded protein sequences are nowadays found to define a specific protein family, the Amt/Mep/Rh-family, that is present in all kingdoms of life – in bacteria, archaea, plants, fungi and animals, even human. For technical reasons, most kinetic measurements and assays have been done with MA and therefore in the fungal field the first transporters were called MEPs. In the plant field AMTs were called AMTs. A few years later, it was

discovered that those two groups share significant amounts of structural and functional conservation. In 1997 the human Rh-antigens, which have already been known for decades in immunology, also were discovered to complement an ammonium transport deficient yeast mutant (Marini *et al.*, 1998; Marini *et al.*, 2000). Therefore the protein family is called Amt/Mep/Rh family for historical reasons. In the following the term AMT proteins will be used to refer to the entire family of Amt/Mep/Rh proteins. In case of MA transport, the family divides into at least two subgroups. The Rh proteins are not able to transport MA, what has been accredited to their low transport capacity. But there is also two plant AMTs – AMT2;1 from *A. thaliana* and LjAMT2;1 from *Lotus japonicus* – that have been reported to transport ammonium but not MA (Sohlenkamp *et al.*, 2000; Sohlenkamp *et al.*, 2002; Simon-Rosin *et al.*, 2003). In a recent publication, all known DNA sequences of AMT coding genes were phylogenetically analyzed. Horizontal gene transfer was suggested and a new classification into MEP-like and AMT-like coding genes was proposed (McDonald *et al.*, 2012).

In contrast to the diverse nomenclature, this family to date consists of nearly 4300 structural and functional highly related members (Pfam database, accession number PF00909, 21st of May 2012). AMT proteins are membrane-spanning proteins consisting of 400 to 500 amino acids and hydropathy analyses predict consistently 10 to 12 (mostly 11) trans membrane domains (e.g. GintAMT1, Figure 6), proven by crystal structures of bacterial and archaeal AMTs (Khademi *et al.*, 2004; Zheng *et al.*, 2004; Andrade *et al.*, 2005a; Andrade *et al.*, 2005b; Andrade & Einsle, 2007; Loqué *et al.*, 2009). Most of the sequences in the database are obtained from sequencing projects. In contrast to the huge number of available sequences only a hand full of the encoded proteins have been investigated further. To date, all of the investigated AMT gene encoded proteins were functional AMTs.

1.2.3 AMTs of fungi

In the fungal field (249 sequences listed in the Pfam database) the studied proteins belong to the ascomycotan fungi *S. cerevisiae* (Marini *et al.*, 1994; Marini *et al.*, 1997), *Schizosaccharomyces pombe* (Mitsuzawa, 2006), *Candida albicans* (Biswas & Morschhauser, 2005) *Aspergillus nidulans* (Monahan *et al.*, 2002; Monahan *et al.*, 2006) and *Fusarium fujikuroi* (Teichert *et al.*, 2008), to the basidiomycotan fungi *Ustilago maydis* (Smith *et al.*, 2003) and *Hebeloma cylindrosporum* (Javelle *et al.*, 2003) and to the glomeromycotan fungus *Rhizophagus irregularis* DAOM 197198 – formerly known as *Glomus intraradices* – (López-Pedrosa *et al.*, 2006).

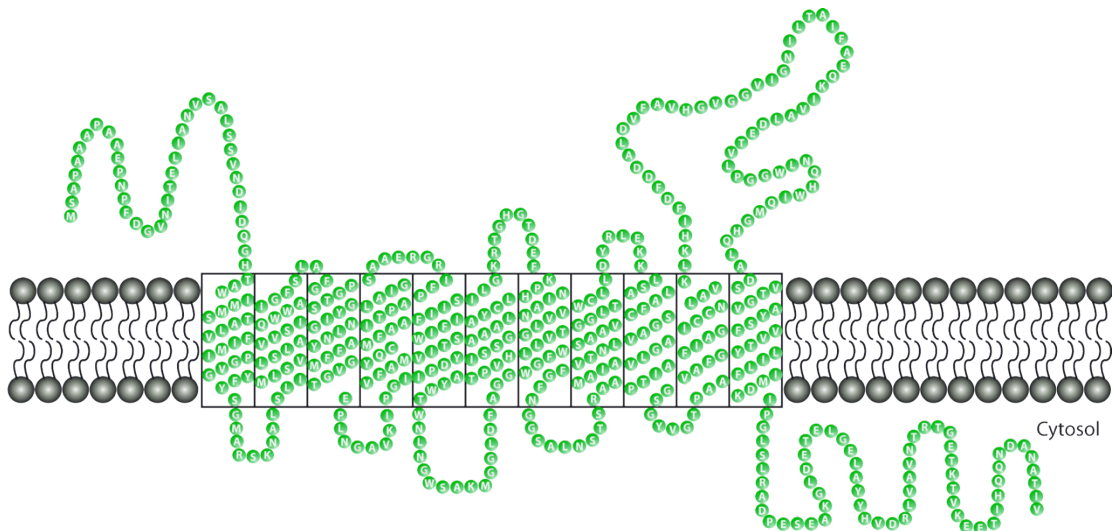


Figure 6: Amino acid sequence and predicted topology of GintAMT1. GintAMT1 probably consists of 11 trans membrane domains (surrounded by rectangles), an extracellular N- and an intracellular C-terminus. Most AMT proteins consist of the same topology. Trans membrane domains were predicted by SOSUI and TMHMM (Krogh *et al.*, 2001; Mitaku *et al.*, 2002).

All of the investigated fungi contain more than one transporter gene in their genomes, coding for at least one high-affinity-low-capacity transporter that is expressed under nitrogen starvation and repressed under high-nitrogen conditions and one low-affinity-high-capacity transporter that is almost constitutively expressed and only down regulated under very high ammonium conditions (see for example Marini *et al.*, 1997). AMTs normally are down regulated under high ammonium conditions to avoid toxic effects. Boeckstaens and coworkers discovered that the exchange of one of the pore amino acids – a histidine residue mutated to a glutamate residue – in ScMEP2 changes its transport properties (Boeckstaens *et al.*, 2008) and suggest an answer to the never solved but highly discussed question for the ammonium transport mechanism. They speculate that the particular histidine residue normally takes over the proton of the NH_4^+ while the glutamate residue in this position is not doing this anymore in ScMEP1 and related proteins. This indicates two distinct transport mechanisms (Figure 7). For MEP1-like proteins (no His in the crucial AA position, like ScMEP1) they suggest transport of the NH_4^+ ion as itself while MEP2-like proteins (with His in the crucial AA position, like ScMEP2 and *E. coli* AmtB) would deprotonate the NH_4^+ ion and either co-transport NH_3 and H^+ or transport only NH_3 while the proton stays outside. The latter possibility, however, seems unlikely, as the yeast MEPs are dependent on the proton motive force of the plasma membrane (Marini *et al.*, 1997; Boeckstaens *et al.*, 2008) and protons that stay extracellular would by itself lead to a higher proton motive force over the plasma membrane by raising the proton concentration outside and consumption of intracellular protons while co-transport of a proton (even if it is the one of the NH_4^+) would use the proton motive force as driving force.

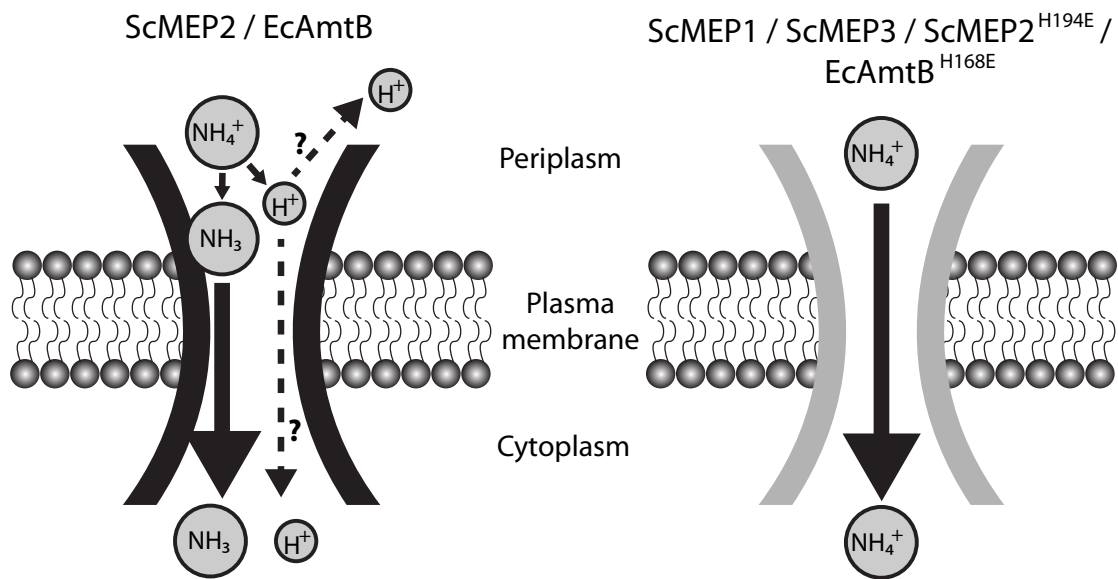


Figure 7: Distinct transport mechanisms for AMT proteins. Dependent on the AA residue in position 168 (*E. coli*) or 194 (*S. cerevisiae*) - either H or E - the transport properties of EcAmtB and ScMEP2 may change. Yeast cells expressing the ScMEP2 H194E mutant protein version lost their ability to grow pseudohyphal. The respective histidine residue is supposed to take over the proton of NH_4^+ , which is abolished, if the histidine is exchanged to an acidic residue. This means, within the AMT protein family two different mechanisms of transporting ammonium over the plasma membrane might exist. Figure adapted from Boeckstaens *et al.* (2008), with permission.

On the other hand, ScMEP2 is strongly connected to a putative sensor function of a subgroup of AMTs since it was published that ScMEP2 is sufficient to abolish the rescue of a phenomenon called pseudohyphal growth (PHG; Lorenz & Heitman, 1998a; Lorenz & Heitman, 1998b; Rutherford *et al.*, 2008). Boeckstaens and coworkers could link the His to Glu exchange to the ability for PHG in their publication. The prerequisites for this sensor function, however, remain unknown.

A more recent publication focusing on the transport mechanism in MEP2-like transporters (with the histidine in the respective position) suggests a more distinct function for the two histidines within the ammonium transduction pore (Figure 8; Wang *et al.*, 2012). They would be directly involved in de- and reprotonation of the transducted NH_4^+ ion.

1.2.4 Bioenergetics of ammonium transport

To date the question, whether AMT proteins act as active transporters or as passive channels, remains unsolved. Originally active transport across the membrane was assumed, as the pH gradient across energized cytoplasmic membranes (acidic outside, neutral to alkaline inside) would rather lead to depletion of ammonium than to accumulation in case of passive diffusion. An active import would be necessary and this import would be dependent on the proton motive force. In fact, this has been proven for the yeast MEPs and a few others (Marini *et al.* 1997, Boeckstaens *et al.*

2008). Successful voltage-clamp measurements of tomato LeAMT1;1 reconstituted in *Xenopus laevis* oocytes support an active, proton-driven transport, but can only exclude passive NH_3 diffusion and not the possibility of ammonium-selective ion channels. The finding of bidirectional bacterial AMTs (Soupene *et al.*, 2002) challenged the active-transport-hypothesis and supported the theory of AMTs being gas channels for NH_3 . Rapid fixation inside the cell would then permanently shift the concentration gradient towards passive influx of ammonium.

Taking into account two different transport mechanisms (see above and figure 7) one could speculate that various possibilities (active transport of NH_3 or NH_4^+ as well as passive diffusion of either the charged or the uncharged version) are realized within the AMT protein family.

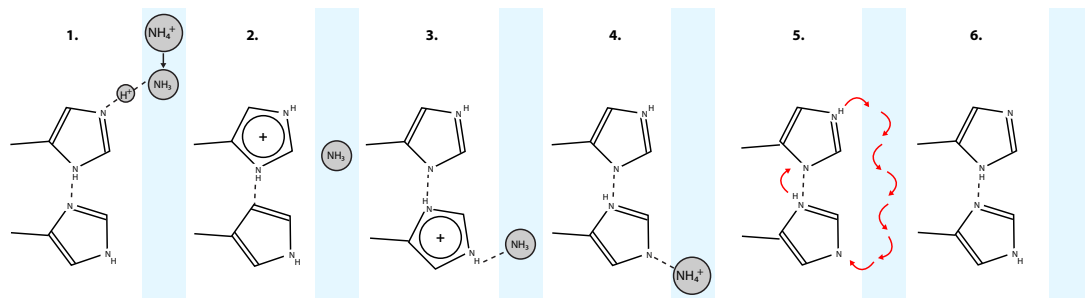


Figure 8: Proposed transport mechanism of MEP2-like AMTs. The NH_4^+ ion reaches the first histidine and transfers its proton, which delocalizes over the histidine dyad (2 and 3). NH_3 slides down the water filled pore (blue) and gets re-protonated either direct (4) or through cytoplasmic solvent. The protonation state of the twin-His can be reset upon formation of a “proton loop” (5) back to initial stage (6). Figure adapted from Lamoureux *et al.*, 2010.

1.2.5 Regulation of AMT proteins

There is limited data about proteins interacting with AMTs. The only class that is known to interact with AMT proteins is the group of so-called P_{II} -proteins (Hsieh *et al.*, 1998; Thomas *et al.*, 2000; Arcondeguy *et al.*, 2001). They are found in bacteria and plants to block the pore whenever the intracellular ammonium concentration is high enough and accumulation to toxic levels must be avoided (Javelle *et al.*, 2004).

From structural data it is known that AMT proteins possibly act as trimers (Andrade *et al.*, 2005a; Andrade *et al.*, 2005b). Furthermore, it was demonstrated that AMT proteins could directly regulate each other in trans (Loqué *et al.*, 2005; Loqué *et al.*, 2007). Against this background, hetero-polymeric complexes of AMT proteins are imaginable. With AMTs acting in trans this would offer another possible level of regulation in response to changing environmental conditions.

1.2.6 Objectives of the study

To get a better insight into nitrogen transport between the symbionts, the targets of this study were the identification and characterization of the AMT complement of the former mentioned two glomeromycotan fungi. Characterization in the heterologous system *S. cerevisiae* and localization studies in *R. irregularis* were performed in order to discover

their functional relevance in AM symbiosis. In theory, two functions for AMTs can be proposed. Either they take up nitrogen from the soil, which subsequently is transported towards and delivered to the host or they are directly involved in ammonium transport towards the host at the symbiotic interface. Although the latter theory sounds unlikely, expression data of our collaborators revealed presence of AMTs inside plant roots. The experiments in this study were meant to further investigate their role at this place.

2. Results

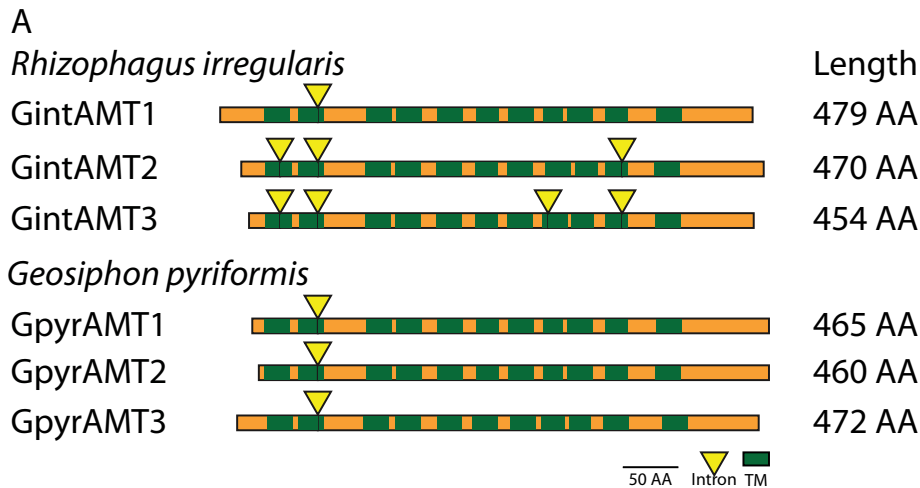
2.1. Identification of glomeromycotan AMTs

2.1.1 *Geosiphon pyriformis* and *Rhizophagus irregularis* each contain 3 AMT-like genes

Three different AMT-like genes were amplified from a cDNA library of *G. pyriformis* that was constructed from symbiotically active material. Those genes could also be amplified from Φ 29 amplified genomic *G. pyriformis* DNA. A comparison between cDNA and genomic sequences revealed one conserved intron for all three AMT genes in the position between a glutamine-coding (CAG or CAA) and a tryptophan-coding (TGG) base triplet lying within the second of 11 predicted trans membrane domains (TMDs, Figure 9A). The intron boundaries are slightly different from formerly known consensus sequences, which is probably a result of the low GC content (roughly 40%) of glomeromycotan coding sequences (Figure 9C).

To get further insights into the symbiotic relevance of AMTs, the fungus *R. irregularis* DAOM 197198 was investigated in parallel. This fungus is a widely used model AM fungus. In its transcriptome (Martin *et al.*, 2008; Tisserant *et al.*, 2012) we found fractions of two yet unknown AMT proteins. By rapid amplification of cDNA ends (RACE) PCR and genome walking we were able to obtain the full-length sequences of those two AMT like genes (*GiAMT2* and *GiAMT3*), amplified and cloned them as well as *GintAMT1*, which was already published (López-Pedrosa *et al.*, 2006), into the SfiI sites of the same expression vector as the *G. pyriformis* cDNA library had been cloned in (pDR196sfi, Schübler *et al.*, 2006). The gene structures of our six AMT coding genes are shown in Figure 9A. After Nuria Ferrols group had published *GiAMT3* as *GintAMT2* (Perez-Tienda *et al.*, 2011), the genes were renamed as follows: *GiAMT2* was renamed to *GintAMT3*; *GiAMT3* was renamed to *GintAMT2*. All results here, including Figure 9, are presented with the changed names.

Comparisons between cDNA and genomic sequences revealed 1, 3 and 4 introns for *GintAMT1*, *GintAMT2* and *GintAMT3*, respectively. Their positions are conserved between the genes, if they are present in more than one gene (Figure 9A). Intron number 2 is even conserved between all six genes of both fungi, suggesting a common ancestral protein before the species split up. This is remarkable as the two fungi are distantly related and divided more than 400 million years ago (Schübler *et al.*, 2001). A comparison with an AMT gene of the basidiomycete *Ustilago maydis*, *UmUMP2*, revealed an intron in a different position, 60 base pairs further downstream between codons for two other highly conserved residues, a glycine and an asparagine residue. Therefore, the position of intron number 2 seems to be highly conserved among glomeromycotan AMT genes but it also seems to be specific for this phylum. The 6 encoded proteins show high levels of amino acid identity and similarity (Figure 9B).



B
Amino Acid identity (similarity)

	GpyrAMT3	GpyrAMT2	GpyrAMT1	GintAMT3	GintAMT2
GintAMT1	65% (81%)	61% (77%)	57% (74%)	60% (75%)	63% (79%)
GintAMT2	65% (81%)	58% (74%)	61% (74%)	65% (80%)	
GintAMT3	60% (77%)	56% (71%)	59% (73%)		
GpyrAMT1	59% (76%)	60% (74%)			
GpyrAMT2	63% (78%)				

C

AA gtaagt /-/ cag TGG	GpyrAMT1
AG gtagaa /-/ cag TGG	GpyrAMT2
AG gtatat /-/ tag TGG	GpyrAMT3
AG gtatgt /-/ aag TGG	GintAMT1
TG gtaatt /-/ cag ATT	GintAMT2 intron 1
AG gtaaag /-/ tag TGG	GintAMT2 intron 2
CG gtaagg /-/ tag GTA	GintAMT2 intron 3
TG gtaatt /-/ aag ATA	GintAMT3 intron 1
AG gtaaaa /-/ tag TGG	GintAMT3 intron 2
TG gtaaat /-/ tag TTC	GintAMT3 intron 3
AG gtaatt /-/ cag GTA	GintAMT3 intron 4

AG GTADDD /-/ HAG D	AMTs	consensus
HG GTWWDI /-/ WAG D	GpMST1	consensus
AG GTATGT /-/ CAG G	yeast	consensus
AG GTRTGT /-/ YAG G	human	consensus



Glomeromycotan AMTs
weblogo representation

Figure 9: Topologies of glomeromycotan AMTs and AMT genes and their relationship. A: Transmembrane domain (TMD) topology and intron localization of the six glomeromycotan AMTs. Green boxes indicate TMD positions, yellow triangles mark intron positions. Both are highly conserved, while N and C termini differ in length and are less conserved. **B:** Reciprocal BLAST (Altschul *et al.*, 1997) analysis (Blosum62 matrix) revealed a high conservation on sequence level between the 6 transporters. They share at least 56% AA identity and 71% AA similarity. Intra species comparisons are marked in dark grey. **C:** Comparison of the exon-intron-boarders. They differ from yeast and human consensus sequences and are closer related to the exon-intron-boarders that were found for the 6 introns of GpMST1 (Schüssler *et al.*, 2006). Conserved nucleotides are shown in blue, unusual nucleotides are shown in red. Weblogo representation (Crooks *et al.*, 2004) of nucleotide conservation of the glomeromycotan AMT intron boarders (bottom) reveals relatively high diversity.

The introns 1 and 4 are conserved between *GintAMT2* and *GintAMT3*, suggesting recent gene duplication. Intron 3 only exists in *GintAMT3*. Also the positions of predicted trans membrane domains (TMDs, green rectangles in Figure 9A) are extremely conserved. The intron boundaries of *R. irregularis* AMT genes are different from human and yeast consensus sequences and shown in Figure 9C.

Further data mining in the 454 sequencing data (*G. pyriformis*) as well as the transcriptome data (*R. irregularis*) discovered no further AMT encoding genes. Degenerate PCRs on the cDNA library of *G. pyriformis* and on cDNA of *R. irregularis* also obtained no further genes. So, together with the fact, that most investigated fungi so far contained 2 or 3 AMT encoding genes in their genomes, it was concluded, that the AMT complement of the two investigated glomeromycotan fungi was completely discovered and defined.

2.1.2 Phylogenetic analysis of glomeromycotan AMTs

To investigate, whether a functional diversification might be encoded in the protein sequences, phylogenetic analysis was performed. DNA sequences of a recent publication suggesting horizontal gene transfer within the AMT family (McDonald *et al.*, 2012) were batch-translated with the ExPASy EMBOSS TRANSEQ tool (Rice *et al.*, 2000). After sorting out untranslatable sequences (due to frame shifts in the DNA sequence), more than 340 AMT protein sequences and the 6 glomeromycotan AMT sequences were taken for alignment (MAFFT, L-INS-i setting, JTT matrix, gap opening cost 1, Katoh *et al.*, 2005) and calculation of a phylogenetic tree (with RAxML via the CIPRES gateway; Miller *et al.*, 2010), using the GAMMA model, JTT matrix and empirical frequencies, with 1000 bootstraps. The glomeromycotan AMTs are divided by species but do not indicate any functional diversification on sequence level (Figure 10), while for example the *S. cerevisiae* transporter ScMEP2 (which is functional distinct) clearly falls apart from the other two yeast transporters ScMEP1 and ScMEP3 (Figure 10). *Geosiphon pyriformis* and *R. irregularis* are only distantly related (Hibbett *et al.*, 2007). More glomeromycotan AMT sequences are probably needed to separate functional diverse AMTs by phylogenetic analyses.

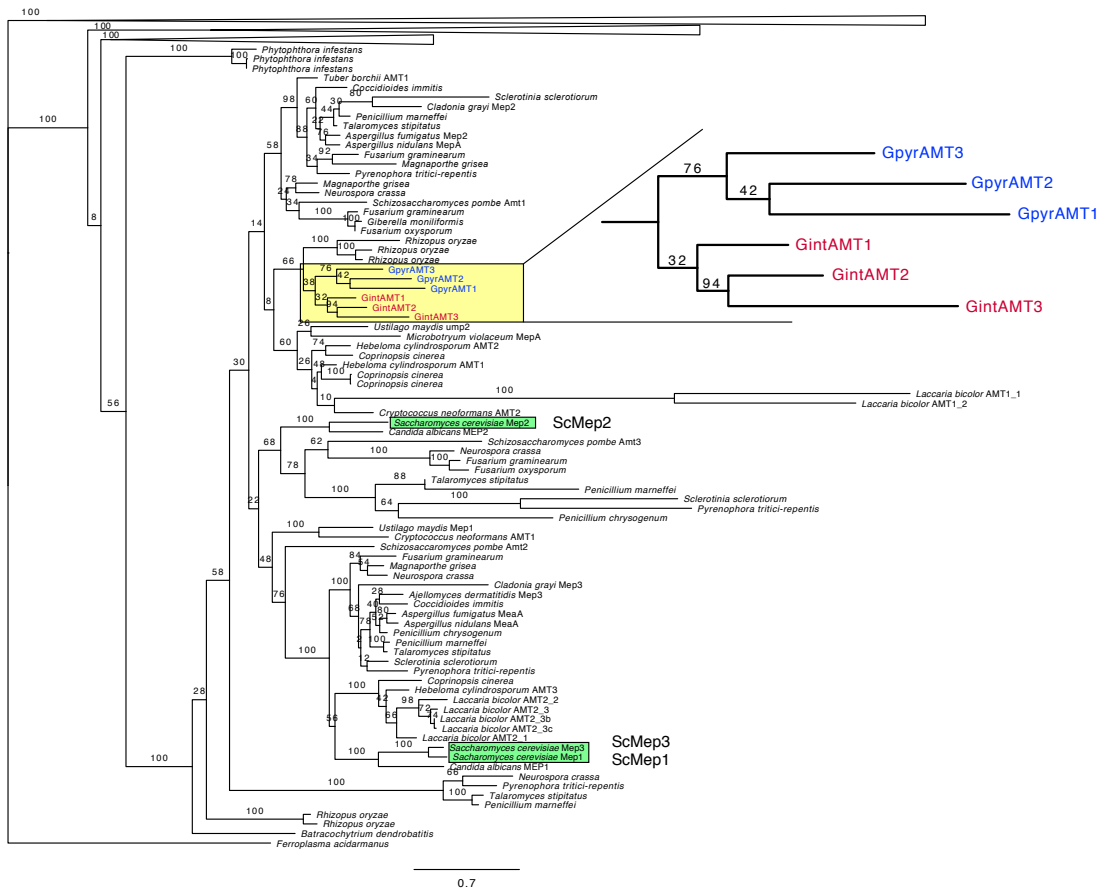


Figure 10: Phylogenetic analysis. More than 340 AMT protein sequences were analyzed. The fungal sequences are shown here. *Geosiphon pyriformis* and *R. irregularis* transporters (yellow box and zoom in) cluster together, but do not split up into different functional groups. *S. cerevisiae* transporters divide into two functional groups (green boxes). Plant and animal clades are collapsed (upper part of the tree). Bootstrap values (n=1000) are written on the branches. Bar indicates substitutions per site.

2.2. Functional characterization

2.2.1 *GpyrAMT2* and *GpyrAMT3* are not able to complement a yeast $\Delta mep1-3$ mutant

The putative transporter genes were tested for complementation of the yeast $\Delta mep1-3$ mutant (strain MLY131a/ α , Lorenz & Heitman, 1998a). Cells were transformed with variants of the plasmid pDR196sfi containing the different AMT genes or a stuffer gene (a part of a human aldolase gene without ORF) cloned into the *Sfi*I sites. The genes were constitutively expressed under the *PMA1* promoter. All three transporter genes of *R. irregularis* at least partly restored the ammonium uptake capability in yeast, what was proven by their capability to restore growth of the $\Delta mep1-3$ mutant on medium containing 50 μ M $(\text{NH}_4)_2\text{SO}_4$ as sole nitrogen source (Figure 11). *GintAMT1* complemented best of the 6 glomeromycotan AMTs, demonstrated by larger colonies in a successive 5x dilution series on medium containing 50 μ M $(\text{NH}_4)_2\text{SO}_4$ as sole nitrogen source (Figure 11).

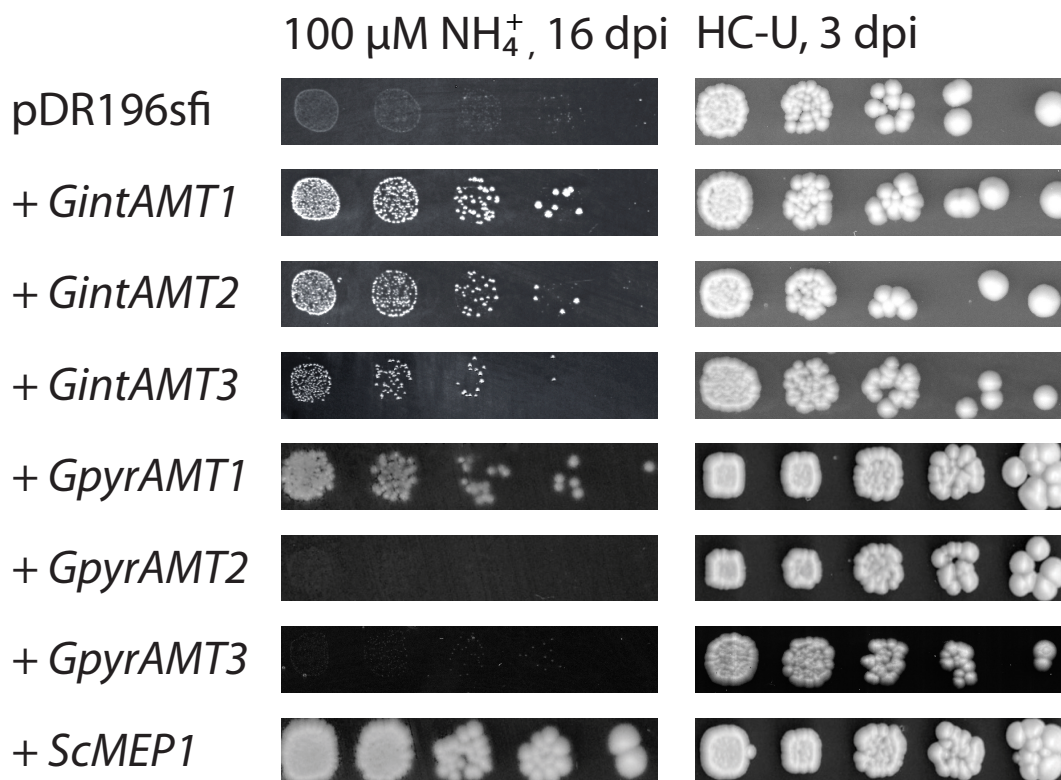


Figure 11: Yeast complementation capability of glomeromycotan AMTs. Ammonium uptake deficient yeast cells ($\Delta mep1-3$) were transformed with an expression vector containing the AMT genes under control of the strong *PMA1* promoter. Five-fold dilution series were incubated either on minimal medium containing 50 μ M $(\text{NH}_4)_2\text{SO}_4$ (= 100 μ M NH_4^+) as sole nitrogen source for 16 days (left panel) or on synthetic complete medium (containing roughly 37.5 mM $(\text{NH}_4)_2\text{SO}_4$), lacking uracil for 3 days (right panel). *Rhizophagus irregularis* AMTs are able to partly complement the growth deficiency of the $\Delta mep1-3$ yeast mutant on low NH_4^+ concentrations (100 μ M, left panel). Of the *GpyrAMT1* genes only *GpyrAMT1* is able to partly complement the mutant phenotype.

Of the three transporter genes found in *G. pyriformis*, however, only *GpyrAMT1* was able to partly complement the growth defect of the yeast mutant (Figure 11). Neither *GpyrAMT2* nor *GpyrAMT3* complemented the mutant phenotype. To exclude the possibility that the proteins might be incorrectly localized or not at all expressed in the heterologous yeast system, we cloned *GintAMT1*, *GintAMT2*, *GintAMT3*, *GpyrAMT1*, *GpyrAMT2* and *GpyrAMT3* 5' of a green fluorescent protein (GFP) coding gene into the expression vector pDR196sfi and transformed these constructs into the yeast $\Delta mep1-3$ mutant, resulting in the expression of C-terminal GFP-tagged AMT fusion proteins in the yeast cells. The localization of these fusion proteins was determined with a Leica SP5 confocal laser-scanning microscope (CLSM, Figure 12). All tagged proteins except *GpyrAMT3* were localized to the plasma membrane in *S. cerevisiae*. Additionally, we saw vacuolar or nuclear membrane localization for some of them, most probably as an overexpression artifact (Figure 12). All tagged transporters behaved like the untagged versions (not shown), either facilitating complementation of the growth defect of the yeast mutant (*GintAMT1*-GFP, *GintAMT2*-GFP, *GintAMT3*-GFP, *GpyrAMT1*-GFP) or not (*GpyrAMT2*-GFP, *GpyrAMT3*-GFP, soluble GFP). *GpyrAMT3*-GFP localized exclusively to the vacuolar membrane. It cannot be excluded that this protein is a functional AMT. Although some vacuolar targeting sequences in yeast are known (Valls *et al.*, 1990; Saalbach *et al.*, 1996), none of them was found in *GpyrAMT3* amino acid sequence. The detection of *GpyrAMT2* and *GpyrAMT3* in the next generation sequencing data, however, suggests a particular function for both encoded proteins, although *GpyrAMT2* seems to be no functional AMT and *GpyrAMT3*'s function cannot be investigated in the heterologous system.

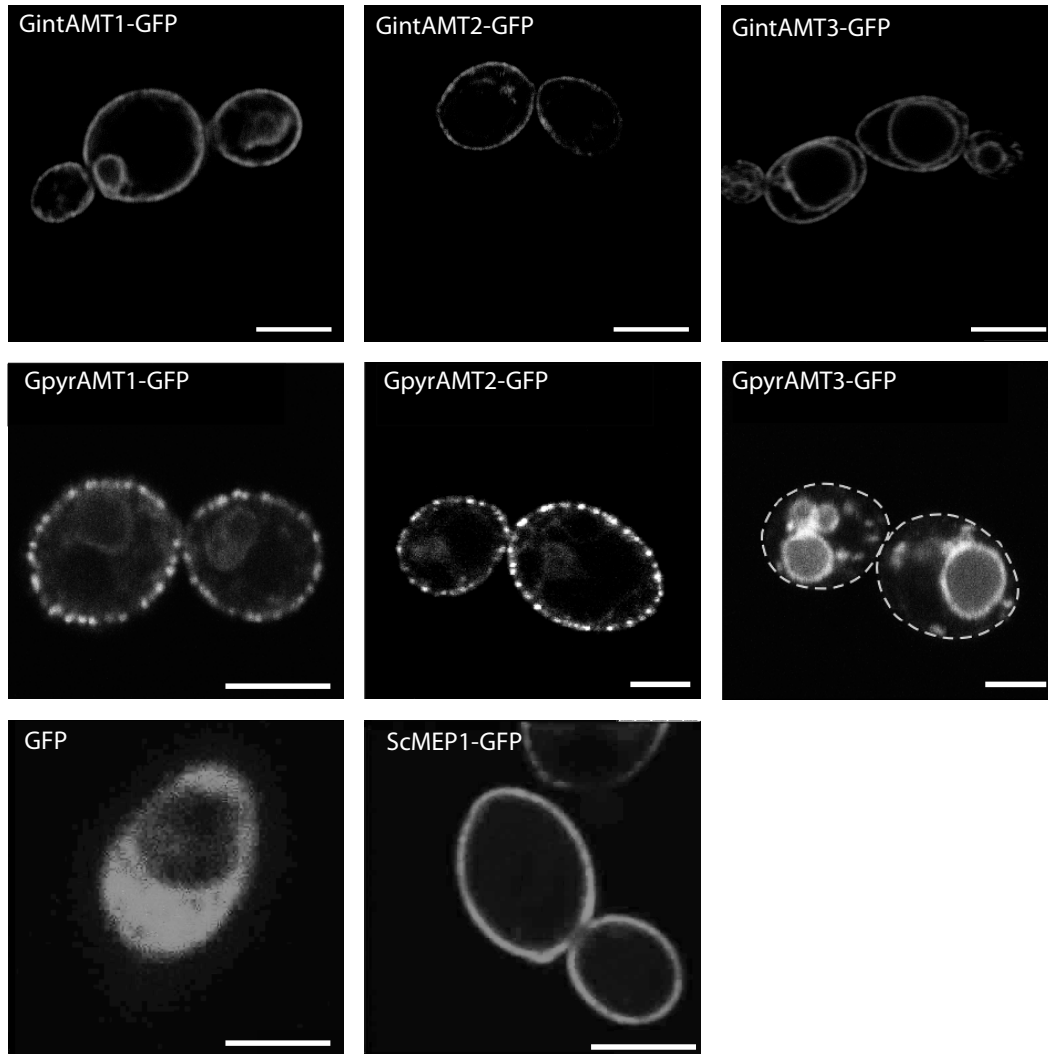


Figure 12: Localization of GFP-tagged AMTs in *S. cerevisiae*. C-terminal GFP-tagged versions of ScMEP1, GintAMT1, GintAMT2, GintAMT3, GpyrAMT1, GpyrAMT2 and GpyrAMT3 as well as soluble GFP were cloned into pDR196sfi and expressed in *S. cerevisiae* under control of the *PMA1* promoter. The cells were grown to logarithmic growth phase and the localization of the fusion proteins was estimated by confocal microscopy. Five of the six glomeromycotan AMTs tagged with GFP are localized at the plasma membrane (PM) like ScMEP1-GFP (lower center panel), the positive control. Soluble GFP is localized to the cytoplasm of *S. cerevisiae* (lower left panel). GpyrAMT1-GFP (center left) and GpyrAMT2-GFP (center right) show spotty localization along the PM while GintAMTs are distributed all over the PM. The spotty localization is not unusual for homologous or heterologous membrane proteins in yeast (Grossmann *et al.*, 2006; Grossmann *et al.*, 2007). Additional vacuolar membrane localization is visible for GintAMT3-GFP (upper right panel). GintAMT1-GFP (upper left panel) and GpyrAMT2-GFP (center) seem to show additional nuclear membrane localization. GpyrAMT3 is not localized at yeast PM but only in the vacuolar membrane (center right). Its functionality cannot be determined in the yeast system. Dashed line in the GpyrAMT3-GFP picture indicates cell borders. GpyrAMT2-GFP, ScMEP1-GFP and soluble GFP pictures taken from Brucker, 2009. Bars are 2.5 μ m.

2.2.2 Only GintAMT1 is capable of methylammonium transport

AMTs are usually biochemically characterized by their methylammonium (MA) transport capability in yeast. As this ammonium analog can be radioactively labeled at its carbon atom and is transported by most AMTs investigated so far, it represents a powerful tool to compare affinity and capacity of AMTs. However, it is not the natural substrate of AMTs. MA uptake assays were performed according to former protocols (Marini *et al.*, 1997; López-Pedrosa *et al.*, 2006). Yeast cells expressing either *ScMEP1* or *GintAMT1* served as positive controls and transported the labeled compound as expected. K_M (40 μ M for ScMEP1 and 11 μ M for GintAMT1) and V_{max} (35 nmol per minute and 100 million cells for ScMEP1 and 13 nmol per minute and 100 million cells for GintAMT1) values for both of them are in the published range (Figure 13B, compare to Marini *et al.*, 1997; López-Pedrosa *et al.*, 2006), although K_M values are slightly higher than expected. Extensive experiments with yeast cells expressing either *GpyrAMT1* or *GpyrAMT2*, however, never lead to measurable active transport (Figure 13 shows the result of an experimental series at pH7, experiments at pH6 showed similar results). *GpyrAMT3* is localized in the vacuolar membrane in *S. cerevisiae* and could therefore not be tested.

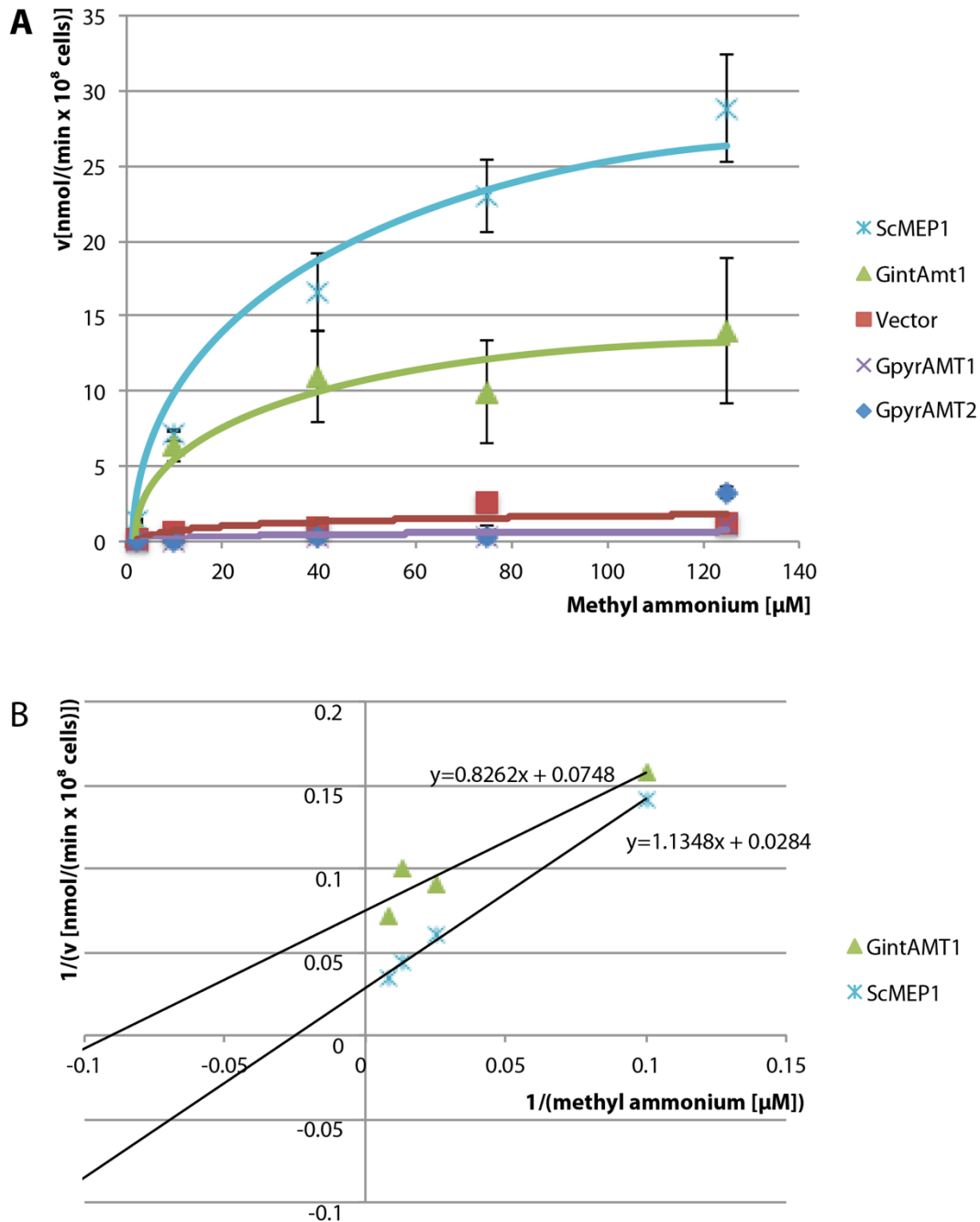


Figure 13: Methylammonium uptake kinetics of ScMEP1, GintAMT1, GpyrAMT1 and GpyrAMT2. (A) Cornish-Bowden plot of respective methylammonium (MA) transport kinetics. Yeast cells were grown to logarithmic growth phase in synthetic dextrose medium containing 0.1% (w/v) proline as sole nitrogen source. The logarithmic growing cells ($OD_{600} = 0.4$ to 0.7) were used for MA uptake measurements. Cells expressing *ScMEP1* or *GintAMT1* served as positive controls. Neither cells expressing *GpyrAMT1* nor cells expressing *GpyrAMT2* showed significant MA uptake compared to cells expressing the empty vector. **(B)** Lineweaver-Burke plot for GintAMT1 and ScMEP1 for the estimation of K_M and V_{max} . Equations of trend lines are given. They lead to K_M and V_{max} in the published range (Marini *et al.*, 1997; López-Pedrosa *et al.*, 2006) for both proteins.

GintAMT2 was the first fungal AMT incapable of MA transport (Perez-Tienda *et al.*, 2011), except for one AMT-like protein of *Aspergillus nidulans*, MepC, which is structural different and only distantly related (31% to 35% AA identity) to other AMTs of *A. nidulans*. Only the human Rh-proteins (Marini *et al.*, 2000) and two plant AMTs (Sohlenkamp *et al.*, 2002; Simon-Rosin *et al.*, 2003) were known members of the protein family lacking MA transport capability.

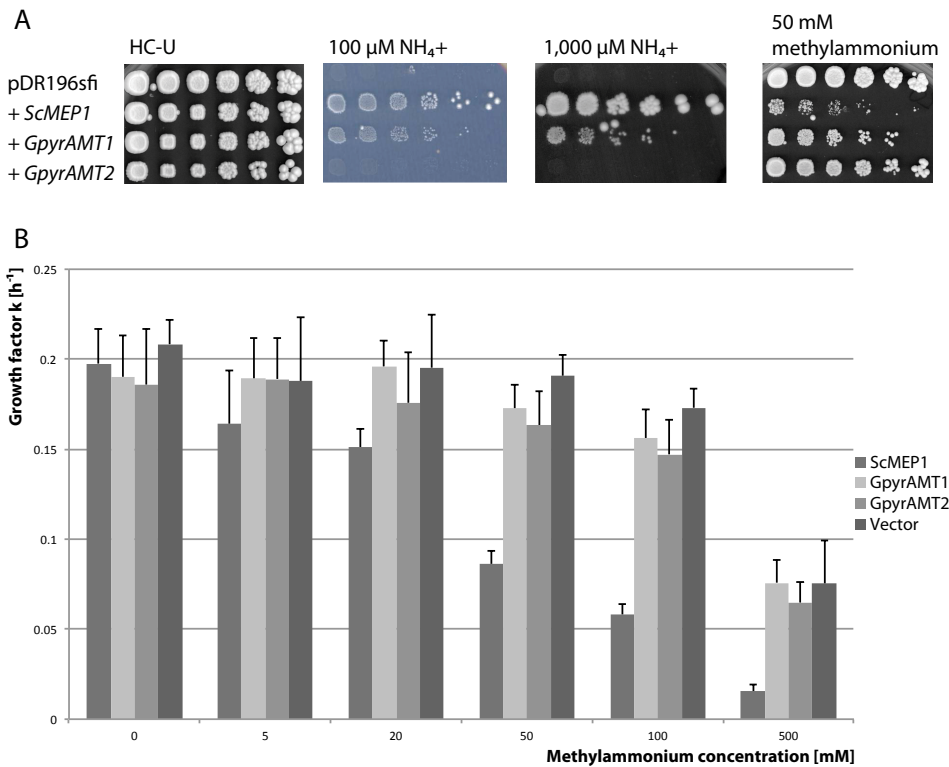


Figure 14: GpyrAMT1 transports ammonium but not methylammonium. (A) *S. cerevisiae* strains carrying the plasmid pDR196sfi with genes coding for different AMTs and the vector control were plated on different media. They were incubated for 3 days on synthetic complete medium lacking uracil (HC-U) or synthetic dextrose medium containing 0.1% (w/v) proline and 50 mM methylammonium (50 mM MA), 16 days on synthetic dextrose medium containing 50 μM $(\text{NH}_4)_2\text{SO}_4$ as sole nitrogen source (100 $\mu\text{M NH}_4^+$) or 6 days on synthetic dextrose medium containing 500 μM $(\text{NH}_4)_2\text{SO}_4$ as sole nitrogen (1,000 $\mu\text{M NH}_4^+$). *ScMEP1*- as well as *GpyrAMT1*-expressing yeast was able to grow on 100 μM and 1,000 μM ammonium as sole nitrogen source. *ScMEP1* expressing yeast moreover shows a severe growth defect on toxic MA. *GpyrAMT1* expressing yeast grows as good on MA containing medium as the vector control and *GpyrAMT2* expressing yeast. **(B)** Yeast strains carrying the same plasmids as in (A) were cultured in liquid synthetic dextrose medium containing varying MA concentrations for 3 days and the growth factor k was calculated from the logarithmic growth phase. *ScMEP1* expressing yeast cells show a severe growth defect compared to the other three strains from 20 mM MA onwards. All strains show reduced growth at 500 mM MA, suggesting passive influx of uncharged methylamine over the plasma membrane. Bars show the average of 6 experiments and standard deviation.

To investigate, whether GpyrAMT1 really is an AMT without MA transport capability, growth assays on plates as well as in liquid medium containing different concentrations of MA were performed (Figure 14). MA is toxic for yeast cells in higher concentrations, if it is transported into the cells. Cells without respective transporters, however, are not affected by MA toxicity (Figure 14). It was clearly demonstrated that only *ScMEP1* expressing yeast cells showed a severe growth defect on plate-medium containing 0.1% (w/v) proline as sole nitrogen source supplemented with 50 mM MA (Figure 14A). When growth curves in liquid medium were recorded and subsequent the growth factor k (which is directly negatively correlated to the doubling time) from the logarithmic growth phase was calculated, we observed the same phenomenon (Figure 14B). A general growth defect for all yeast strains was observed, when 500 mM MA was added to the medium, suggesting passive influx of uncharged methylamine (CH_3NH_3). Even under these conditions, the growth defect for *ScMEP1* expressing cells is stronger than the growth reduction of the other strains (Figure 14).

2.2.3 Ammonium removal assays support ammonium transport capability of GpyrAMT1

To measure the different ammonium transport capacities of the transporters, ammonium removal assays according to Neuhäuser *et al.*, (2011) were performed. In this experimental setup, dense yeast cultures ($\text{OD}_{600} = 2$) are incubated in relatively high ammonium concentrations (1 mM) for several hours and remaining ammonium in the medium is measured at distinct time points (after 10, 30, 60, 120, 180, 240 and 300 minutes). Therefore no kinetics but overall ammonium transport can be measured. The results of the removal assays confirmed the yeast complementation assays. GpyrAMT1 is not able to transport MA (Figure 14), but it transports ammonium - to a lower extent than *ScMEP1* (Figure 15). Neither GpyrAMT2 nor GpyrAMT3 were showing ammonium removal activity in these experiments (Figure 15), supporting thereby the results from the complementation assays on plate, shown in Figure 11.

2.2.4 The ammonium transport capability of GpyrAMT2 can be rescued partly by a single amino acid exchange

To our knowledge, *GpyrAMT2* is the first gene ever encoding a non-functional AMT related protein. Comparison of the amino acid sequence of GpyrAMT2 with characterized and functional AMT sequences revealed, that all the essential amino acids for ammonium transport, known from structural data (Khademi *et al.*, 2004; Andrade *et al.*, 2005a; Javelle *et al.*, 2006; Khademi & Stroud, 2006), are present in GpyrAMT2's protein sequence.

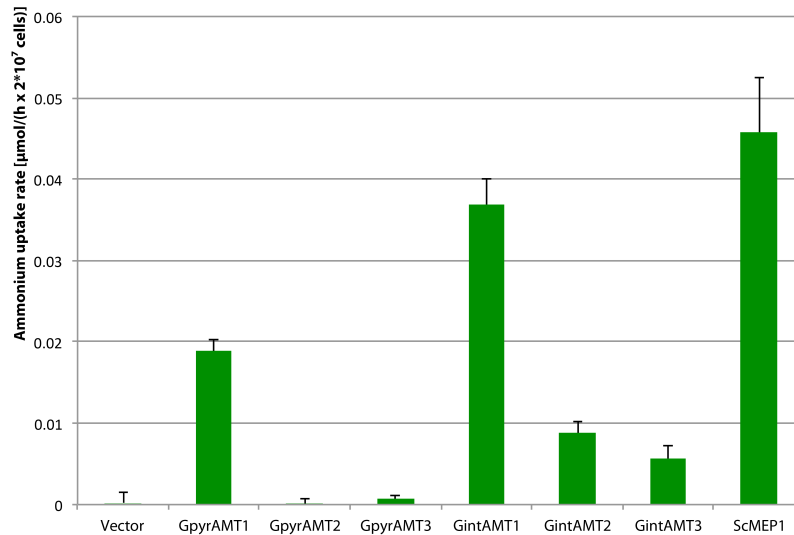


Figure 15: Ammonium removal assays. Yeast cells expressing the stated genes from the plasmid pDR196sfi were grown over night in synthetic complete medium lacking uracil (HC-U), washed and cultured in liquid medium containing a starting concentration of 2 mM ammonium. Samples were taken after 10, 30, 60, 120, 180, 240 and 300 minutes and residual ammonium was determined by a chemical reaction followed by photometric measurement at OD₄₂₀. *ScMEP1* and *GintAMT1* expressing yeast cells were removing ammonium from the medium quite rapidly. *GpyrAMT1*, *GintAMT2* and *GintAMT3* expressing cells imported ammonium slower but above background level ("Vector"). *GpyrAMT2* and *GpyrAMT3* expressing cells were not able to remove ammonium from the medium. Bars show average of 3-4 experiments and standard deviation.

In total, there are at the moment 14 residues suggested to be important for forming the pore and facilitating ammonium transport in *Escherichia coli* AMT EcAmtB (for review see Lamoureux *et al.*, 2010, Pantoja, 2012) and all of them are present in GpyrAMT2. A closer look revealed a difference in the so-called ammonium transporter signature (ATS, Prosite entry PS01219) in trans membrane domain V (von Wirén & Merrick, 2004). A position that usually is occupied by a small residue (serine, alanine or glycine) is replaced by a cysteine in GpyrAMT2 and GpyrAMT3. This residue is located three amino acids downstream from one of the histidines that are supposed to play a crucial role in ammonium conduction through the pore and might influence the proton accepting capability of this histidine by interacting with it. The cysteine was mutated to a serine in GpyrAMT2 and GpyrAMT3 and reciprocally the GpyrAMT1 serine was mutated to a cysteine. Removal assays showed that the ammonium transport capability of GpyrAMT2 C₁₇₃S was partly restored after the mutation while ammonium transport capability of the mutated GpyrAMT1 S₁₇₈C was reduced (Figure 16). The ammonium transport capability of GpyrAMT3, however, was not restored by the mutation C₁₈₉S. This was no surprise, as we did not expect this mutation to relocalize GpyrAMT3 to the PM.

The DNA sequence of the cDNA library for GpyrAMT3 differed in three nucleotides from the sequence amplified from genomic DNA. Most probably they originated from

amplification errors during library construction. One of these nucleotide polymorphisms led to another exchange (A₁₉₂S) in the ATS. Although for the GFP localization the genomic version was taken, we constructed 5 different constructs in total to make sure, that none of those residues was the cause for the vacuolar localization of GpyrAMT3: The cDNA version of GpyrAMT3 (cGpyrAMT3 on plasmid pBL180), the C₁₈₉S version of the cDNA version (cGpyrAMT3_C₁₈₉S on plasmid pBL181), the gDNA version without intron (gGpyrAMT3 on plasmid pBL183), the gDNA version without intron, carrying the C₁₈₉S mutation (gGpyrAMT3_C₁₈₉S on plasmid pBL185) and the gDNA version without intron, carrying the C₁₈₉S and the A₁₉₂S mutations (gGpyrAMT3_C₁₈₉S_A₁₉₂S on plasmid pBL184). However, none of those constructs showed significant ammonium removal from the external medium above vector level, suggesting that there are other critical but not yet identified residues mutated and causative for the vacuolar localization in yeast (Figure 16 and not shown). In parallel we exchanged the respective serine residue of ScMEP2, a yeast ammonium permease known for its signaling function (Lorenz & Heitman, 1998a; Lorenz & Heitman, 1998b).

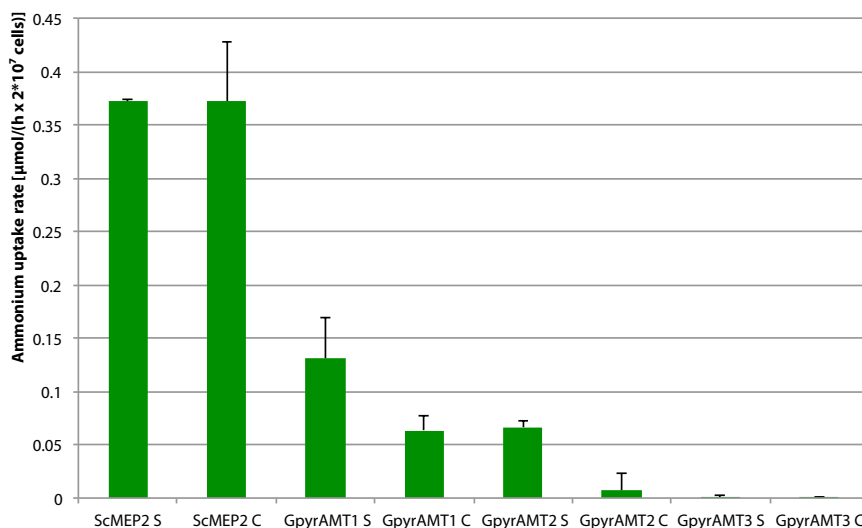


Figure 16: Mutation of cysteine 173 to serine restores transport capacity of GpyrAMT2. After mutation of cysteine 173 of GpyrAMT2 and cysteine 189 of GpyrAMT3 to a serine and the reciprocal mutations in GpyrAMT1 (S₁₇₈C) and ScMEP2 (S₁₉₂C), removal assays of **Figure 15** were repeated. ScMEP2 S₁₉₂C showed no difference in ammonium transport capability while GpyrAMT1 S₁₇₈C and GpyrAMT2 C₁₇₃S showed reduced or restored ammonium transport capability, respectively. For GpyrAMT3, the mutation of C₁₈₉ to a serine did not restore transport capability. Bars show average of 3 experiments and standard deviation.

In this case, the amino acid exchange showed no effect in ammonium removal assays, but in the all over growth rate of the yeast cells (Lott, 2012), suggesting that this residue does not play the same role in all AMTs. In glomeromycotan AMTs, the overall protein structure or the overall transport affinity or capacity, may have additional influence and additive effects may lead to a functional loss.

2.2.5 Summary functional characterization

Six glomeromycotan AMT genes from two glomeromycotan fungi were discovered and their cDNA, gDNA as well as their protein sequences were determined (for sequences see appendix). The phylogenetic analysis revealed no functional information. Five of the 6 encoded proteins, however, behaved different from formerly known AMTs. Although the genes are expressed and 5 of the 6 encoded proteins are correctly localized in the heterologous yeast system, the biochemical characterization in yeast revealed 3 different classes of glomeromycotan AMT-like proteins (see Table 2, discussion). Only one of the 6 proteins transports both ammonium and MA. Three of the proteins are able to transport ammonium but not MA. The remaining two proteins do not even transport ammonium. For one of them, however, ammonium transport capability can be partly restored by a single amino acid exchange while the other one is localized to the vacuolar membrane and cannot restore the growth phenotype of the yeast mutant by physical reasons.

The transcripts of the 3 AMTs of *G. pyriformis* are present in a cDNA library that was obtained from symbiotically active material and therefore expected to play a role in symbiosis. As *G. pyriformis* lives in symbiosis with nitrogen fixing bacteria, the non-functional AMT like protein GpyrAMT2 may have a function in ammonium sensing to either avoid the uptake of toxic amounts of ammonium from the symbiotic bacteria or to determine the nitrogen demand of the bacteria. For GpyrAMT3, we cannot conclude, whether it is a functional AMT as it was localized in the vacuolar membrane in our system. Our collaborators (Nuria Ferrol's group) did expression analyses for the AMTs of *R. irregularis* and detected the transcripts in extraradical as well as intraradical mycelium, again suggesting a role of these transporters in symbiosis.

2.3. Localization of glomeromycotan AMTs

2.3.1 Establishment of specific antibodies

In order to investigate the functional relevance of AMTs in the AM symbiosis, we developed specific antibodies against GintAMT1, GintAMT2 and GintAMT3. To assure their specificity, peptides corresponding to the C-terminal ends of each transporter were synthesized. In particular, the synthesized peptides are listed in Table 1. The peptides were synthesized, injected into 3 rabbits each, and antibodies were harvested after 6 months of immunization (Pineda antibody services, Berlin). Affinity purified antibodies were tested on fungal protein extracts in Western Blot and did not lead to a specific signal (not shown). HA-tagged transporters were expressed in yeast and gave a clear anti-HA-signal but still no signal of the specific antibodies could be detected (not shown). Tests of these antibodies in immune localization on AMT-GFP-construct expressing yeast cells, however, showed a clear signal when the antibodies were detected by a Alexa647 labeled secondary anti-rabbit-IgG antibody. Antibodies were then selected by their amount of colocalization with the GFP signal. For each transporter we got one antibody that was showing the correct localization pattern in yeast (for example see Figure 17). The other 6 antibodies either showed no signal or mislocalized signal (Table 1).

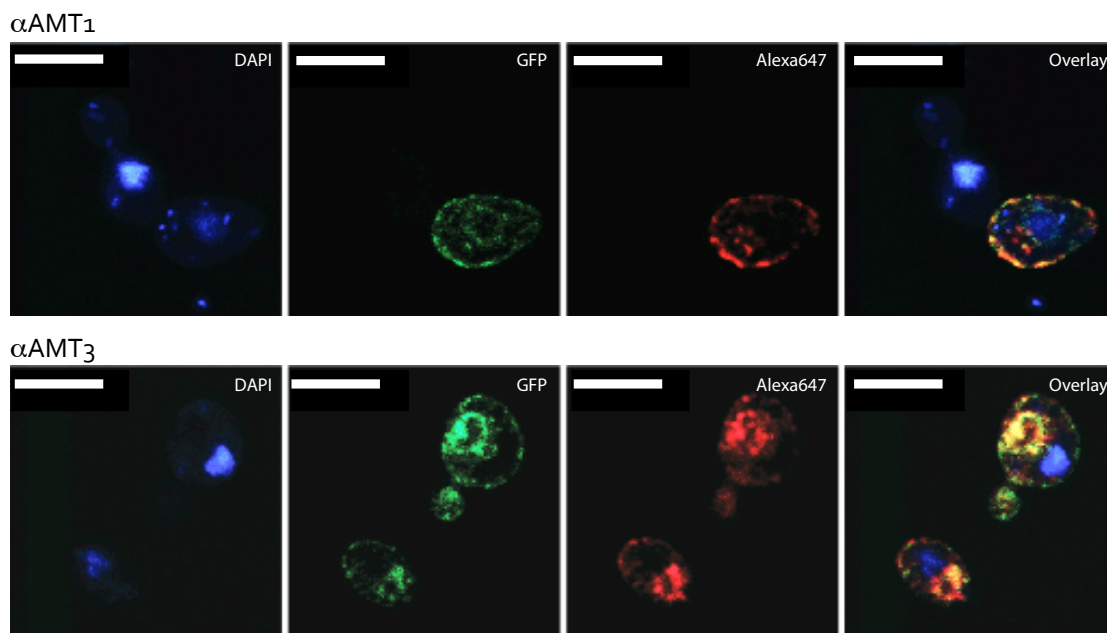
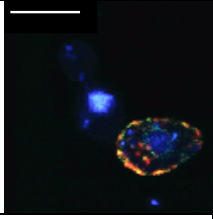
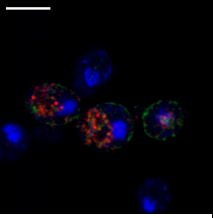
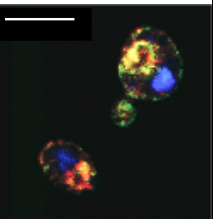
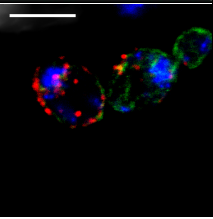


Figure 17: Antibody test on yeast cells expressing AMT-GFP fusion proteins. Antibodies of 9 different rabbits against the 3 GintAMTs were tested on AMT-GFP expressing yeast cells. Yeast cells of the strain MLY131a/α, expressing the different AMT-GFP constructs from the pDR196sfi plasmid were grown over night in HC-U medium, fixed, permeabilized and incubated with the specific primary as well as the fluorescently labeled secondary antibody. Two examples for working antibodies are shown. First column shows DAPI signal, second column shows GFP fluorescence and third column shows antibody signal. In the overlay (fourth column), the colocalization of GFP- and antibody-signal becomes obvious. Bars are 5 μm.

Table 1: Antibody tests on yeast cells expressing AMT-GFP constructs. Yeast cells were grown as in figure 17, fixed, permeabilized and incubated with the specific primary as well as the fluorescently labeled secondary antibody. Antibodies showing no (“no signal”) or wrong (e.g. cytoplasmic or nuclear) localization were excluded from further experiments. Example pictures show either working or non-working antibodies. Rabbit #1 immunized with the GintAMT2 peptide died, so an additional one was immunized (#4). Bars are 5 μm.

Antigen	Rabbit #	Localization	
GintAMT1 (NH ₂ -CKTVKEETIHQQNDANATIV-COOH)	1	No signal	
	2	Plasma membrane	
	3	No signal	
GintAMT2 (NH ₂ -CNINSGKLPQQGTNQYILS-COOH)	2	Cytoplasm, vacuole	
	3	Plasma membrane	
	4	No signal	
GintAMT3 (NH ₂ -CKTMSSPQQTQLQSIDHIHYS-COOH)	1	No signal	
	2	Plasma membrane	
	3	Nucleus, cytoplasm	

2.3.2 Establishment of preparation protocol

The antibodies showing the correct localization in yeast were taken for further experiments on extraradical and intraradical fungal material of *R. irregularis*. Several attempts with embedded and cut fungal material failed, because the fungal material collapsed during cutting. An experiment with a commercial β -tubulin antibody revealed, that not even the fungal cytoskeleton was conserved during this procedure (Figure 18A).

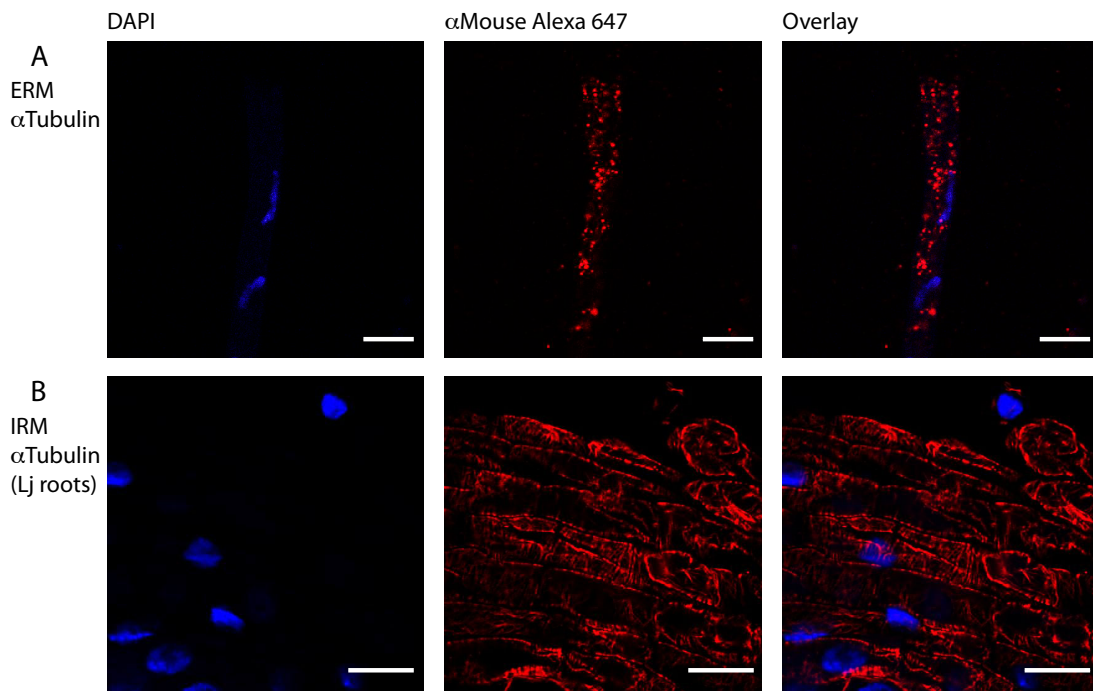


Figure 18: immune localization of beta-tubulin in a fungal hypha and a plant root. (A) *R. irregularis* ERM was harvested from MSR plates, fixed, permeabilized and incubated with a primary mouse anti β -tubulin and a secondary Alexa fluor 647 labeled anti mouse IgG antibody. DAPI staining shows two elongated fungal nuclei. The microtubules seem to be degraded (dotted structures instead of filaments) by the experimental procedure. Bars are 5 μ m. **(B)** *L. japonicus* roots were treated as the fungal mycelium in the upper panel. The microtubules and their filamentous structure are visible. Bars are 25 μ m.

The plant cytoskeleton was conserved when a whole mount protocol was applied. However, fungal structures were not visible (Figure 18B). Our collaboration partners, however, had successfully used a whole mount protocol to localize GintAMT2 in extraradical mycelium (Perez-Tienda *et al.*, 2011). This protocol, finally, was applied for further investigations.

2.3.3 Extraradical localization of fungal AMTs

Fungal material, cultivated on MSR split-plates for 8 to 12 weeks, was harvested by re-solubilizing the solidifying agent, fixed with paraformaldehyde, permeabilized and incubated with the α GintAMT1 antibody that worked best in the yeast experiments (see above). The localization of GintAMT1 in extraradical mycelium was restricted to spores and is shown in Figure 19.

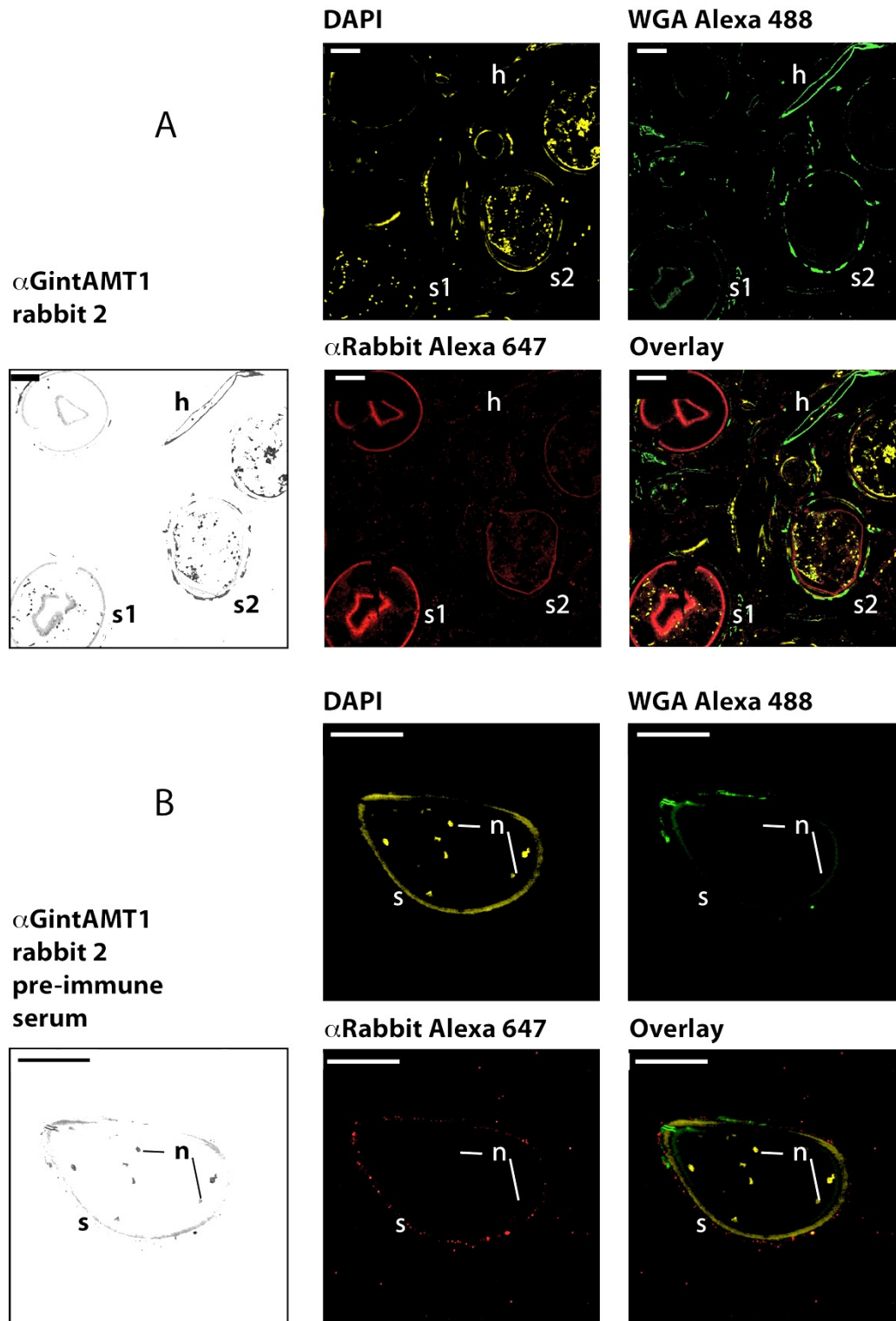


Figure 19 (previous page): Immune localization of GintAMT1 in extraradical mycelium. Gray scale overviews are shown to depict important structures. **(A)** DAPI staining in false yellow shows fungal nuclei. Fungal cell wall is stained with WGA Alexa 488. Chitin containing cell walls that escaped complete degradation during the treatment are stained green. The signal of the specific antibody is shown in red. Spores without residual cell wall (**s1**) show antibody signal located at the plasma membrane and missing signal for spores with residual cell wall (**s2**) confirms that the antibody detects PM components and not cell wall components. Hyphae (**h**) showed no signal. The inner signal in spore 1 (**s1**) derives from the doughnut shape of collapsed spores after drying. This happened to most large spores. **(B)** As a negative control fungal extraradical material was treated with pre-immune serum of the respective rabbit that was taken before immunization and then incubated with the Alexa 647 labeled secondary antibody. In this experiment no specific antibody signal is visible. Bars are 25 μm .

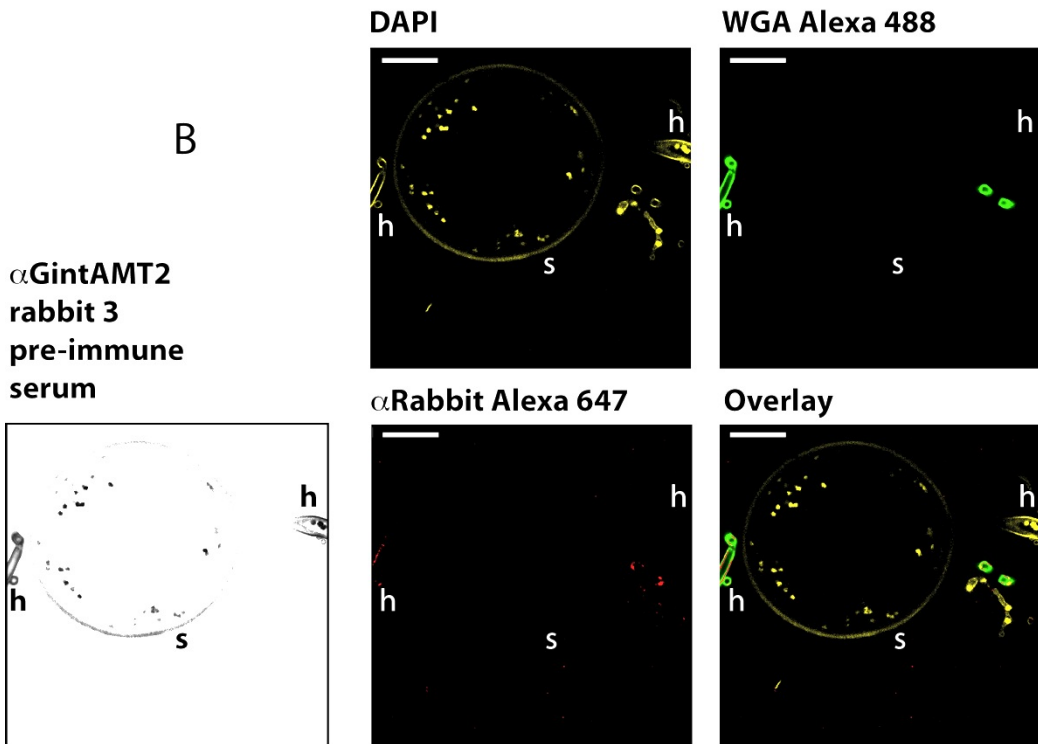
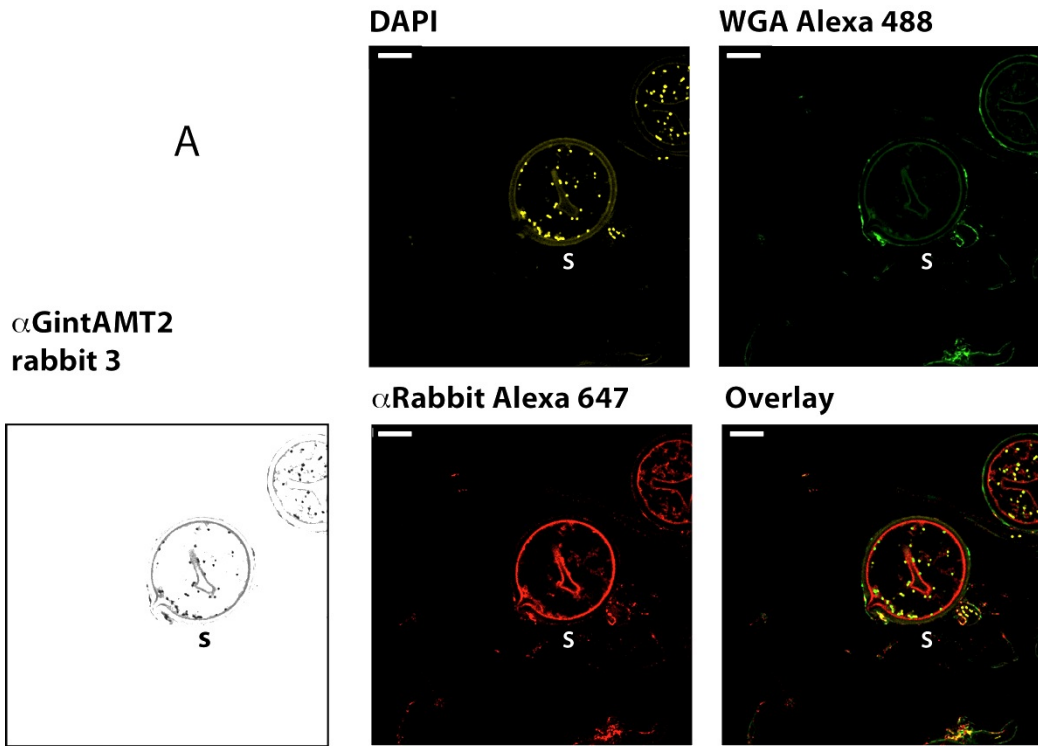
GintAMT1 was expected to be present in extraradical mycelium. However, as an uptake transporter, which plays a role in nitrogen intake, it would be expected in the extraradical hyphal network instead of extraradical spores.

GintAMT2 was published previously to be localized in extraradical spores and hyphae although its expression is increased in intraradical mycelium (Perez-Tienda *et al.*, 2011).

Following the same procedure as for GintAMT1, GintAMT2 was detected and also exclusively localized to extraradical spores (Figure 20).

GintAMT3 was newly discovered and no knowledge about its specific localization was given. Immune localization on extraradical mycelium showed that it is also localized in extraradical spores (Figure 21). Figure 21 also shows the specificity of the localization pattern. A hypha (**h**) deriving from a clearly labeled spore (**s1**) shows no signal, although the cytoplasm is continuous - indicating that the localization of GintAMTs to spores is very distinct and tightly regulated.

Figure 20 (next page): Immune localization of GintAMT2 in extraradical mycelium. Gray scale overviews are shown to depict important structures. **(A)** DAPI staining in false yellow shows fungal nuclei. Fungal cell wall is stained with WGA Alexa 488. Chitin containing cell walls that escaped complete degradation during the treatment are stained green. The signal of the specific antibody is shown in red. Spores without residual cell wall (**s**) show antibody signal located at the plasma membrane, but hyphae (**h**) do not. The inner signal inside the spore (**s**) derives from the doughnut shape of collapsed spores after drying. This happened to most large spores. **(B)** As a negative control fungal extraradical material was treated with pre-immune serum of the respective rabbit that was taken before immunization and then incubated with the Alexa 647 labeled secondary antibody. In this experiment no specific antibody signal is visible. Bars are 25 μm .



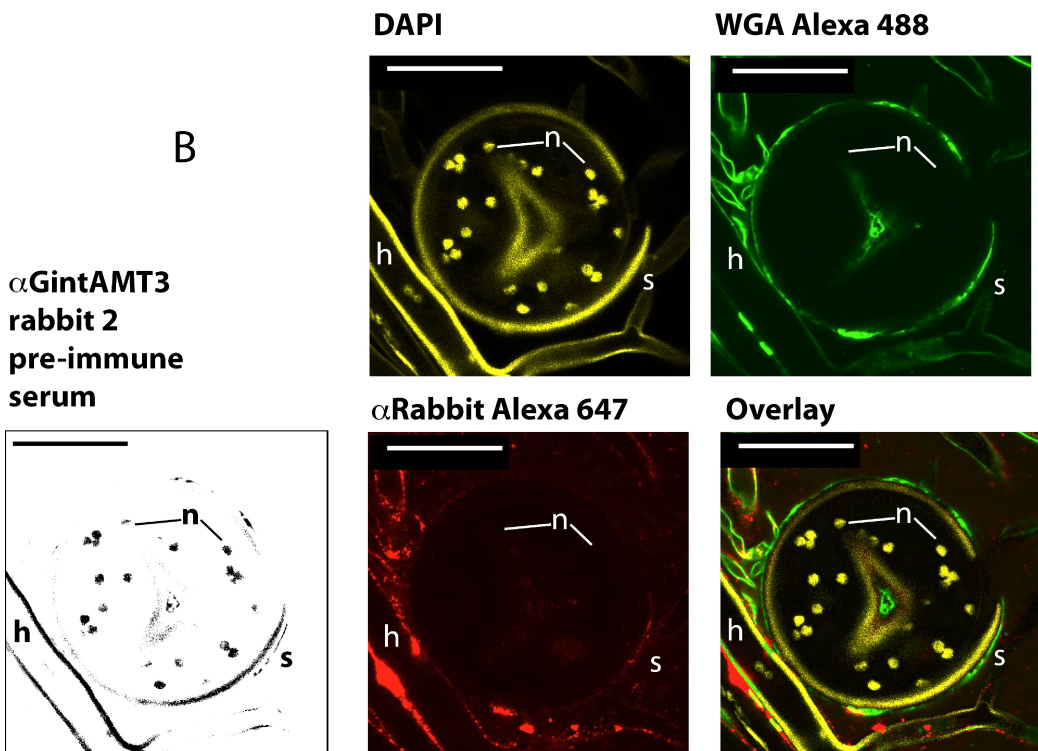
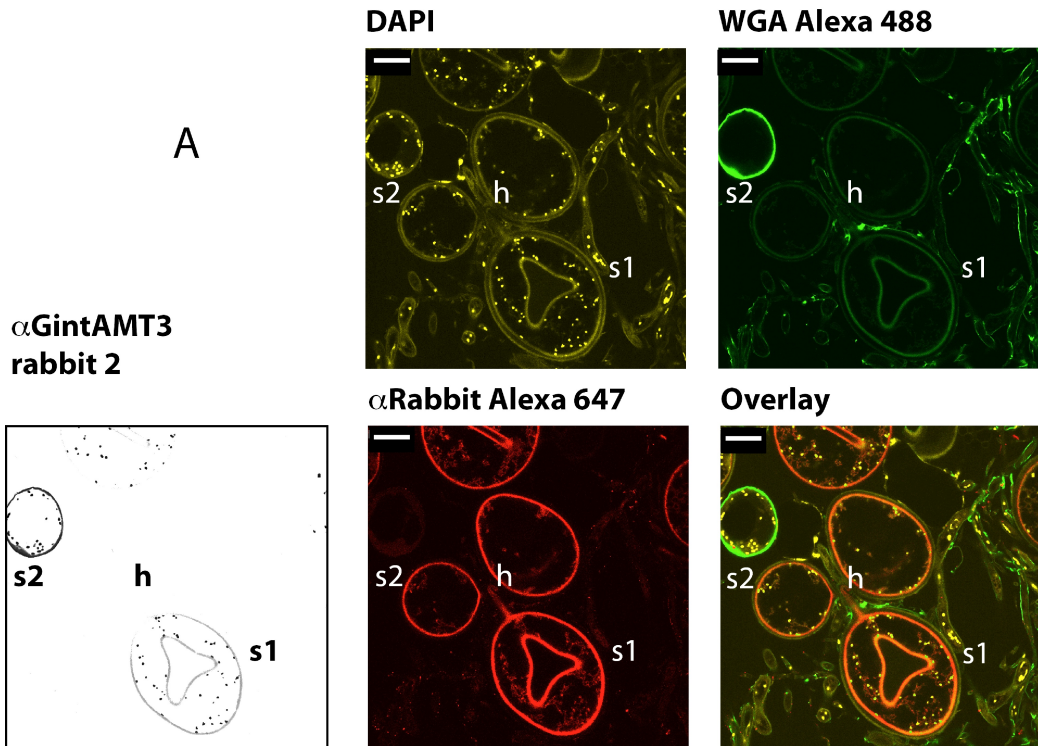


Figure 21 (previous page): Immune localization of GintAMT3 in extraradical mycelium. Gray scale overviews are shown to depict important structures. **(A)** DAPI staining in false yellow shows fungal nuclei. Fungal cell wall is stained with WGA Alexa 488. Chitin containing cell walls that escaped complete degradation during the treatment (spore **s2**) are stained green. The signal of the specific antibody is shown in red. Spores without residual cell wall (**s1**) show antibody signal located at the plasma membrane. Here it is obvious that not even hyphae (**h**) originating from a clearly labeled spore show an antibody signal. Spores with residual cell wall (**s2**) also do not show antibody signal. The inner signal inside the spore **s1** derives from the doughnut shape of collapsed spores after drying. This happened to most large spores. **(B)** As a negative control fungal extraradical material was treated with pre-immune serum of the respective rabbit that was taken before immunization and then incubated with the Alexa 647 labeled secondary antibody. In this experiment no specific antibody signal is visible. Bars are 25 μm .

All *R. irregularis* transporters were detected in extraradical growing mycelium (Figures 19-21). The signal, however, was restricted to spores in this setup. Fungal mycelium was grown on plate medium containing 300 μM ammonium. The experiment was repeated on plates containing no ammonium (M medium) and under those circumstances, in a small proportion of hyphae the AMTs could be detected (see Figure 22, Figure 23).

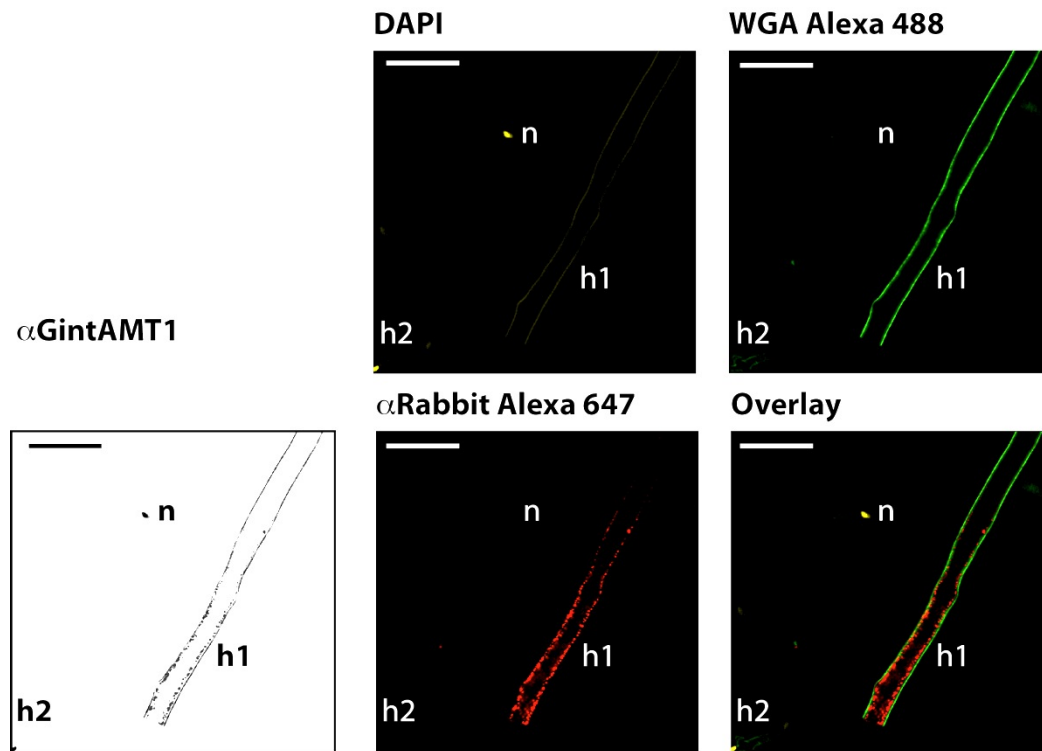


Figure 22: Immune localization of GintAMT1 in extraradical mycelium on medium lacking NH_4^+ . Gray scale overview is shown to depict important structures. DAPI staining in false yellow shows a fungal nucleus (**n**). Fungal cell wall is stained with WGA Alexa 488. Chitin containing cell walls that escaped complete degradation during the treatment are stained green. The signal of the specific antibody is shown in red. Extraradical mycelium (ERM) was harvested, fixed, permeabilized and incubated with the $\alpha\text{GintAMT1}$ antibody and a secondary, Alexa 647 labeled $\alpha\text{Rabbit IgG}$ antibody. WGA Alexa 488 staining was performed to check fungal cell wall digestion. A subpopulation of hyphae (**h1**) shows antibody signal located at the plasma membrane, clearly distinct from cell wall signal. Bars are 25 μm .

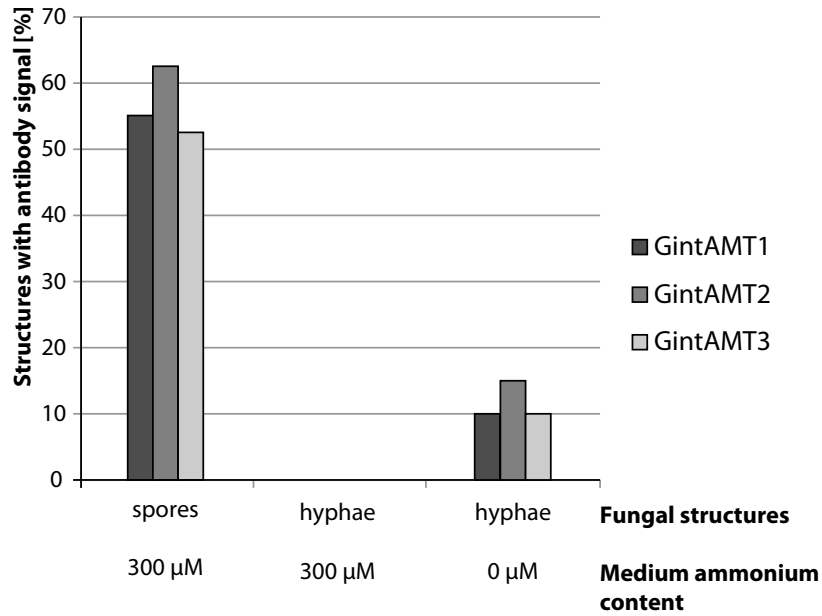


Figure 23: Summary of immune localization data in varying extraradical fungal structures. ERM fungal structures were examined. Structures giving a clear antibody signal were scored positive and the percentage from all observed structures is given. Extraradical structures (spores, extraradical hyphae in medium containing 300 μ M ammonium, extraradical hyphae in medium containing no ammonium) were analyzed. When ERM was harvested from plates containing 300 μ M of ammonium, only in spores signal could be observed. When there was no ammonium in the medium, a low percentage of extraradical hyphae also showed antibody signal. N = 40 for spores and extraradical hyphae.

For quantification, 40 spores and 40 hyphae were checked for antibody signal of each AMT. The percentage of spores and hyphae containing the respective AMT is shown in Figure 23.

2.3.4 Intraradical Localization of fungal AMTs

In order to obtain information about the functional role of the three AMTs during AM symbiosis, their localization in intraradical structures was the next step. Nuria Ferrol's group was not successful in establishing this technique for immune localization of fungal proteins on intraradical material because of cross reactivity of their antibodies with plant structures.

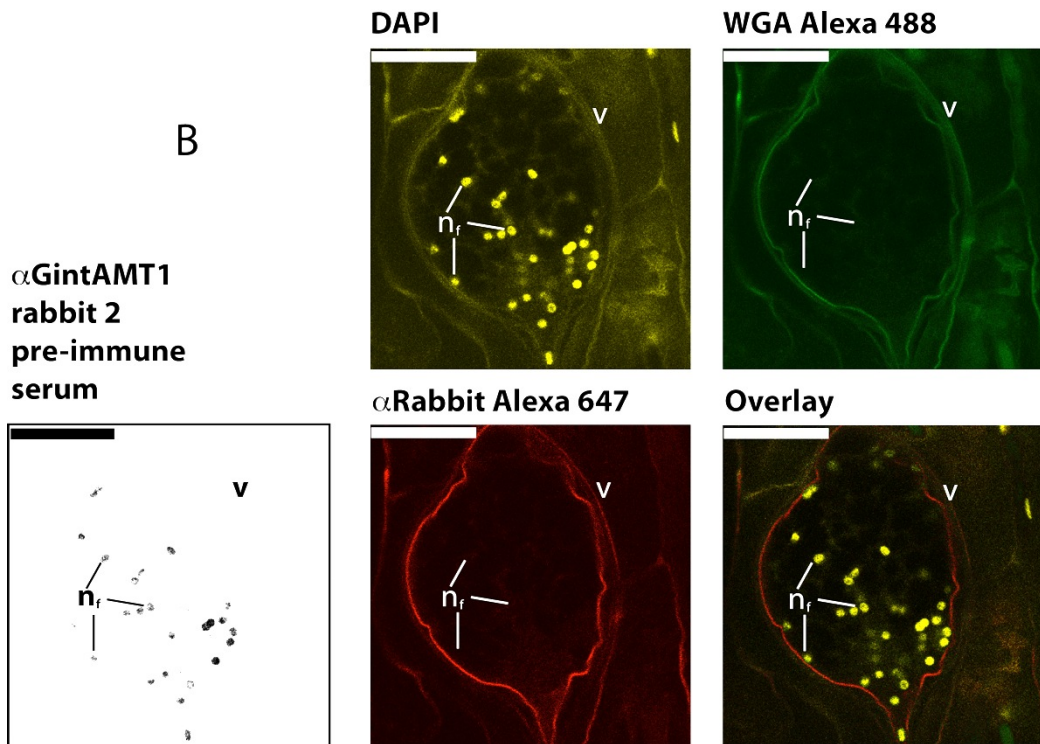
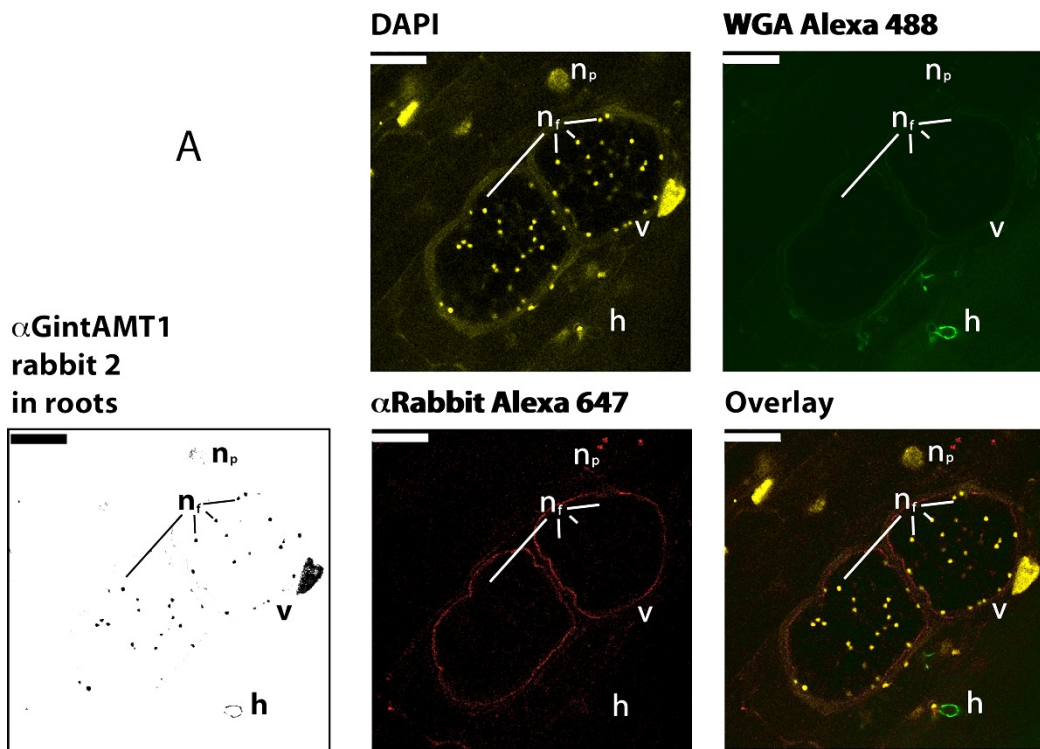
Our new, affinity purified antibodies were tested on *Daucus carota* and *Lotus japonicus* roots. On *D. carota* roots no signal was obtained, meaning that the antibodies most probably could not penetrate the permeabilized roots. On *L. japonicus* roots, however, they showed specific signals for GintAMT2 and GintAMT3.

GintAMT1 signal could not be discriminated from the negative control (Figure 24). One explanation could be that GintAMT1 is not at all expressed in intraradical structures. Expression data of GintAMT1 shows a higher abundance of transcripts in extraradical mycelium. However, the possibility that the antibody was not able to penetrate the permeabilized roots or just the background fluorescence was too high cannot be excluded.

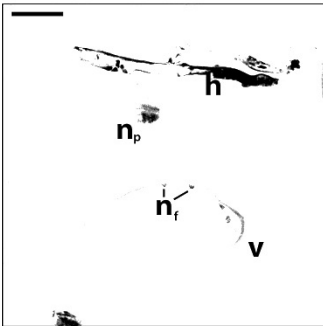
GintAMT2 signal was expected in colonized roots because of the published expression data (Perez-Tienda *et al.*, 2011). As a putative ammonium exporter, it was supposed to be localized in arbuscules. This hypothesis, however, had to be rejected. In Figure 25 the obtained localization data is shown. GintAMT2 localizes to vesicles in mycorrhized roots.

For GintAMT3 there was again nothing known about its putative localization in colonized roots. Experiments were performed as for the other two transporters and showed that GintAMT3 is – like GintAMT2 – localized in fungal vesicles inside colonized roots (Figure 26).

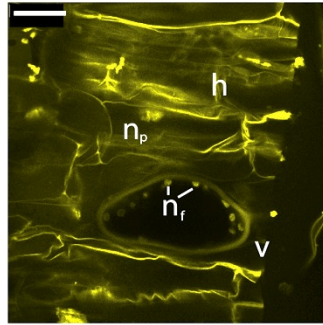
Figure 24 (next page): Immune localization of GintAMT1 in colonized roots. Gray scale overviews are shown to depict important structures. **(A)** DAPI staining in false yellow shows fungal nuclei (n_f) and plant nuclei (n_p). Fungal cell wall is stained with WGA Alexa 488. Chitin containing cell walls that escaped complete degradation during the treatment are stained green. The signal of the specific antibody is shown in red. No specific signal was observed in vesicles (v), hyphae (h) or arbuscules (not shown). **(B)** As a negative control colonized root material was treated with pre-immune serum of the respective rabbit that was taken before immunization and then incubated with the Alexa 647 labeled secondary antibody. In this experiment also no specific antibody signal is visible. Bars are 25 μm .



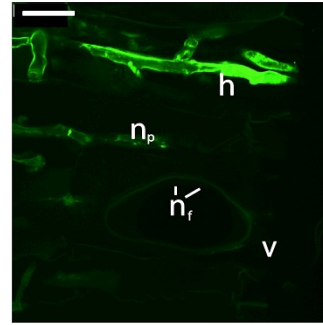
**α GintAMT2
rabbit 3
in roots**



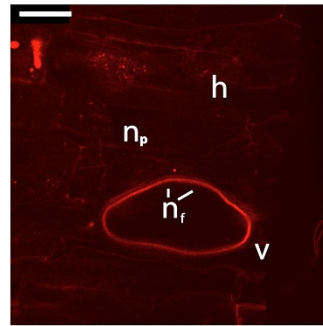
DAPI



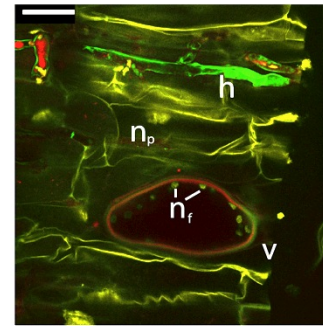
WGA Alexa 488



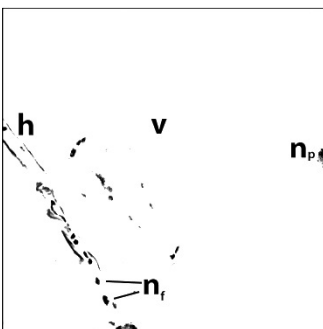
α Rabbit Alexa 647



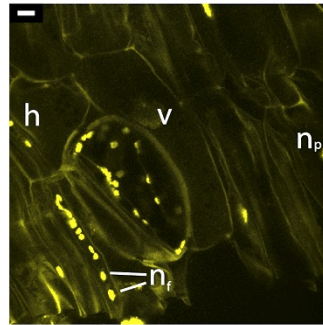
Overlay



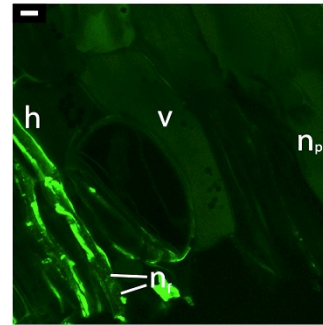
**α GintAMT2
rabbit 3
pre-immune
serum**



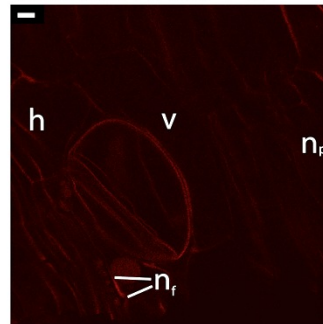
DAPI



WGA Alexa 488



α Rabbit Alexa 647



Overlay

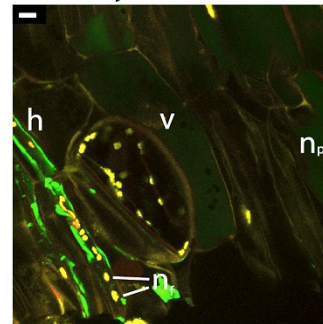


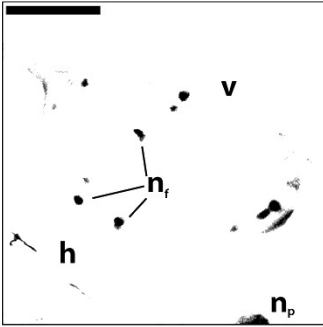
Figure 25 (previous page): Immune localization of GintAMT2 in colonized roots. Gray scale overviews are shown to depict important structures. **(A)** DAPI staining in false yellow shows fungal nuclei (n_f) and plant nuclei (n_p). Fungal cell wall is stained with WGA Alexa 488. Chitin containing cell walls that escaped complete degradation (hyphae, h) during the treatment are stained green. The signal of the specific antibody is shown in red. No specific signal was observed in hyphae (h) or arbuscules (not shown). However, specific signal was obtained from vesicular plasma membrane (v). **(B)** As a negative control colonized root material was treated with pre-immune serum of the respective rabbit that was taken before immunization and then incubated with the Alexa 647 labeled secondary antibody. In this experiment no specific antibody signal is visible. Bars are 25 μ m.

Summarizing the results, the glomeromycotan AMTs could be localized in plant roots colonized with *R. irregularis*. GintAMT2 and GintAMT3 localized to intraradical vesicles (Figure 25, Figure 26) while GintAMT1 could not be detected (Figure 24). This was not expected from the expression data, so it was concluded that the respective GintAMT1 antibody was not working in this system, probably because of too high background fluorescence.

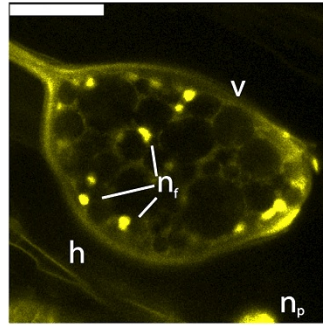
Although several arbuscules were observed, they never showed an AMT specific antibody signal. As an example, Figure 27 shows an arbusculated stretch of a *L. japonicus* root. Fungal nuclei as well as plant nuclei can be observed, but no antibody signal was visible.

Figure 26 (next page): Immune localization of GintAMT3 in colonized roots. Gray scale overviews are shown to depict important structures. **(A)** DAPI staining in false yellow shows fungal nuclei (n_f) and plant nuclei (n_p). Fungal cell wall is stained with WGA Alexa 488. Chitin containing cell walls that escaped complete degradation (hyphae, h) during the treatment are stained green. The signal of the specific antibody is shown in red. No specific signal was observed in hyphae (h) or arbuscules (not shown). However, specific signal was obtained from vesicular plasma membrane (v). **(B)** As a negative control colonized root material was treated with pre-immune serum of the respective rabbit that was taken before immunization and then incubated with the Alexa 647 labeled secondary antibody. In this experiment no specific antibody signal is visible. Bars are 25 μ m.

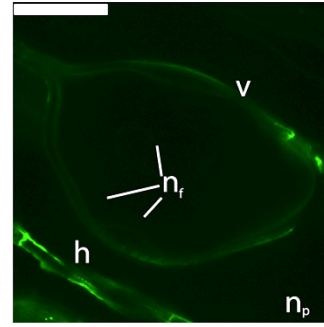
**α GintAMT3
rabbit 2
in roots**



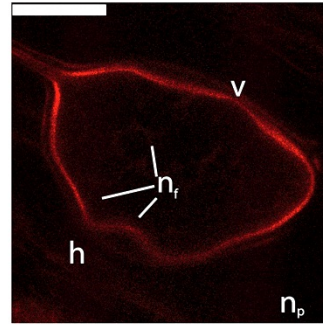
DAPI



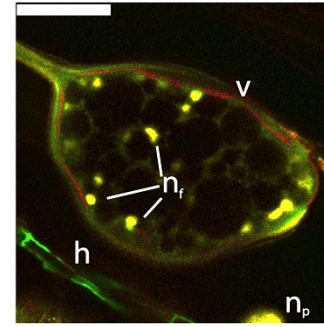
WGA Alexa 488



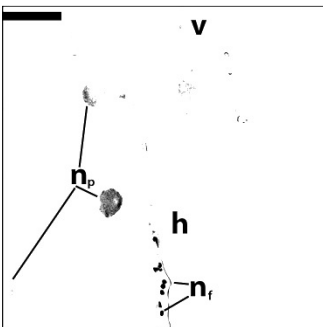
α Rabbit Alexa 647



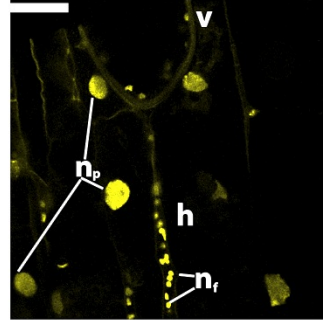
Overlay



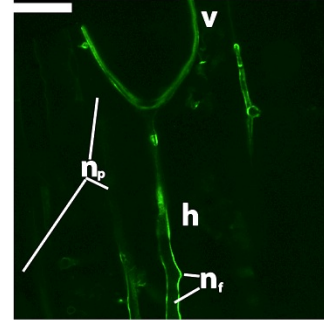
**α GintAMT3
rabbit 2
pre-immune
serum**



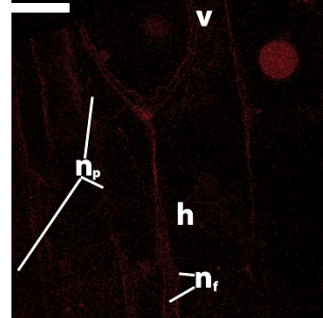
DAPI



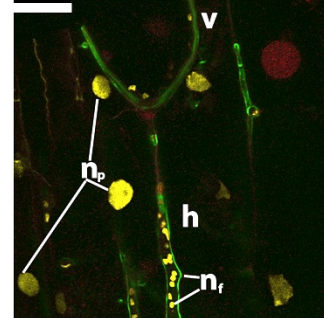
WGA Alexa 488



α Rabbit Alexa 647



Overlay



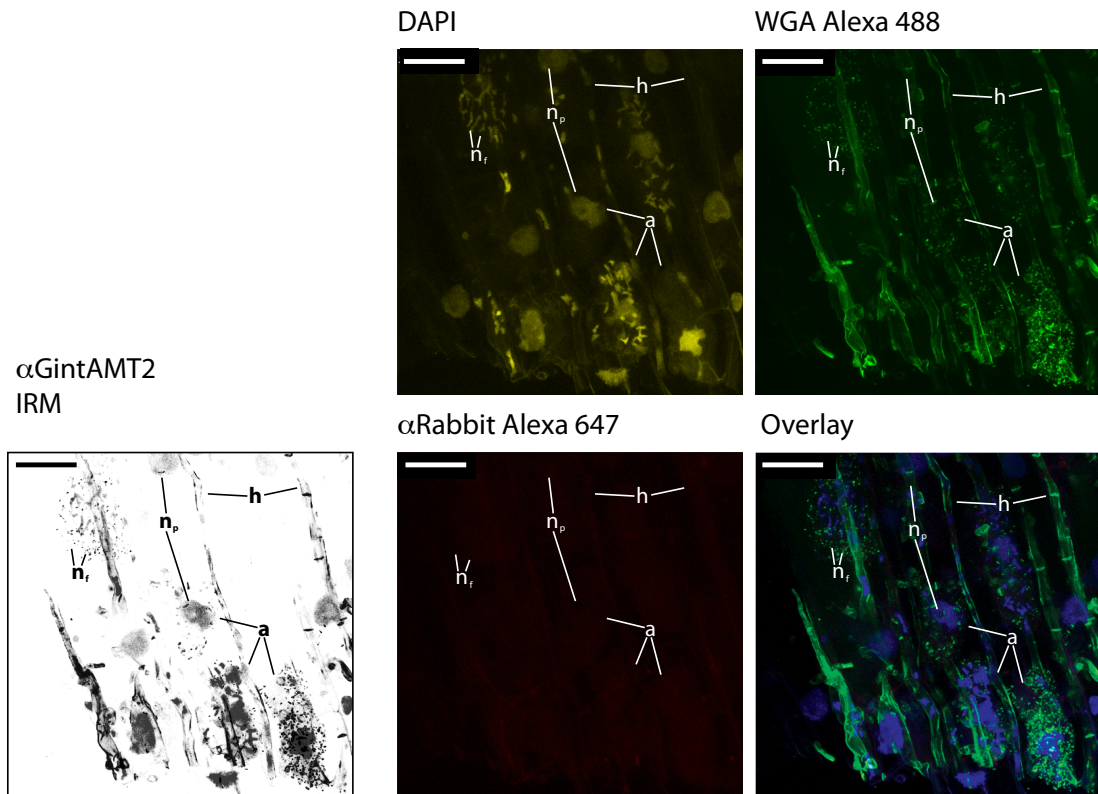


Figure 27: GintAMTs are not located to arbuscules. Mycorrhizal *L. japonicus* roots were harvested, fixed, permeabilized and incubated with the aGintAMT2 antibody and a secondary, Alexa 647 labeled aRabbit IGG antibody. First column shows DAPI staining in false yellow. Fungal (n_f) and plant (n_p) nuclei are visible. Second column shows fungal cell wall staining. Chitin containing cell walls that escaped complete degradation during the treatment are stained green. Third column shows the signal of the specific antibody, fourth column shows the overlay of the first three columns. Intraradical hyphae (h) and arbuscules (a) are visible by nuclear arrangement and residual cell wall staining, but no GintAMT could be detected in and around arbuscules under our experimental conditions. Bars are 25 μ m.

Again, localization data on colonized roots was quantified by observing several intraradical hyphae, vesicles and arbuscules for each transporter. The quantitative analysis of AMT specific signals in varying intraradical fungal structures is shown in Figure 28.

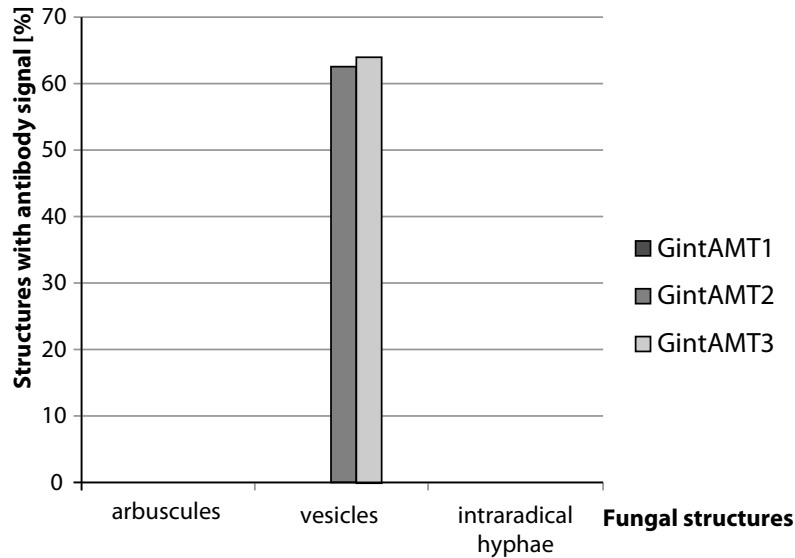


Figure 28: Summary of immune localization data in varying intraradical fungal structures. IRM fungal structures were examined. Structures giving a clear antibody signal were scored positive and the percentage from all observed structures is given. Intraradical structures (arbuscules, vesicles, intraradical hyphae) were analyzed. No AMT was present in arbuscules or intraradical hyphae. GintAMT2 and GintAMT3 can be detected only in vesicles, while GintAMT1 is not detectable at all. N = 12-14 for arbuscules, 8-12 for vesicles, 17-21 for intraradical hyphae.

Summary of immune localization data:

Figures 19-23 are showing the localization patterns of *R. irregularis* AMTs in extraradical mycelium, which was fixed, permeabilized with chitinase, incubated with the specific first antibody and finally incubated with an Alexa647 labeled secondary antibody. Detection was performed with a Leica SP5 confocal laser-scanning microscope. All three transporters were detected in the PM of fungal spores, when the fungus was cultivated on MSR medium containing 300 μ M ammonium. For a second experiment the fungus was cultivated on M medium, which lacks ammonium completely. In this case, AMTs were also localized to a sub population of hyphae (Figure 22, Figure 23). It was concluded that the main function of the AMTs is the minimization of ammonium loss by passive diffusion of NH_3 across the PM. This explains, why AMTs are always localized in spore PM (storage organs with potentially high ammonium concentrations) and it also explains their localization in hyphae in an environment lacking ammonium (concentration gradient is then pointing towards outside all over the hyphal network).

Figures 24-28 show localization pattern of GintAMTs in colonized roots (*L. japonicus*), which were fixed, permeabilized with cellulase, pectinase and chitinase, incubated with the specific first antibody and finally incubated with an Alexa647 labeled secondary antibody. Detection was performed with a Leica SP5 confocal laser-scanning microscope. GintAMT2 and GintAMT3, but not GintAMT1 could be detected in colonized roots. The visible signal for GintAMT2 and GintAMT3 was restricted to

vesicles. Figure 27 shows arbusculated cortical cells of a *L. japonicus* root, incubated with the α GintAMT2 antibody. The structure of the arbuscules is already obvious by the arrangement of the fungal nuclei and becomes more obvious by the residual fungal cell wall, but there was no antibody signal detectable. There was no AMT detected in arbuscules in any of the experiments (Figure 27, Figure 28). It was concluded that again AMTs are only needed to re-uptake passively lost NH_3 . This would on the one hand explain, why the transporters are again localized to the storage organs (vesicles) with potentially higher ammonium concentrations and on the other hand would provide a powerful tool for the fungus to control how much nitrogen is released to the plant host. The host is actively removing ammonium from the periarbuscular space and the fungus is not localizing its AMTs to the arbuscules, meaning that it actively feeds its host by passive diffusion.

2.3.5 Localization of fungal AMT transcripts

To verify the results of the immune localization experimentation, *in-situ*-RT-PCR was performed (Figure 29, Figure 30) in collaboration with Daniel Wipf's group. Colonized *Medicago truncatula* roots were fixed and permeabilized with pectinase and chitinase. Genomic DNA was degraded with Dnase and gene specific reverse transcription was carried out. Afterwards, PCR with texas-red-labeled primers was performed and the signal was detected with the Leica SP5 CLSM.

For negative control, samples were treated with Rnase before reverse transcription. For positive control, the large ribosomal sub unit (LSU) encoding gene was chosen. No signal was detected in the Rnase control. LSU transcripts were detected in arbuscules and vesicles (Figure 29).

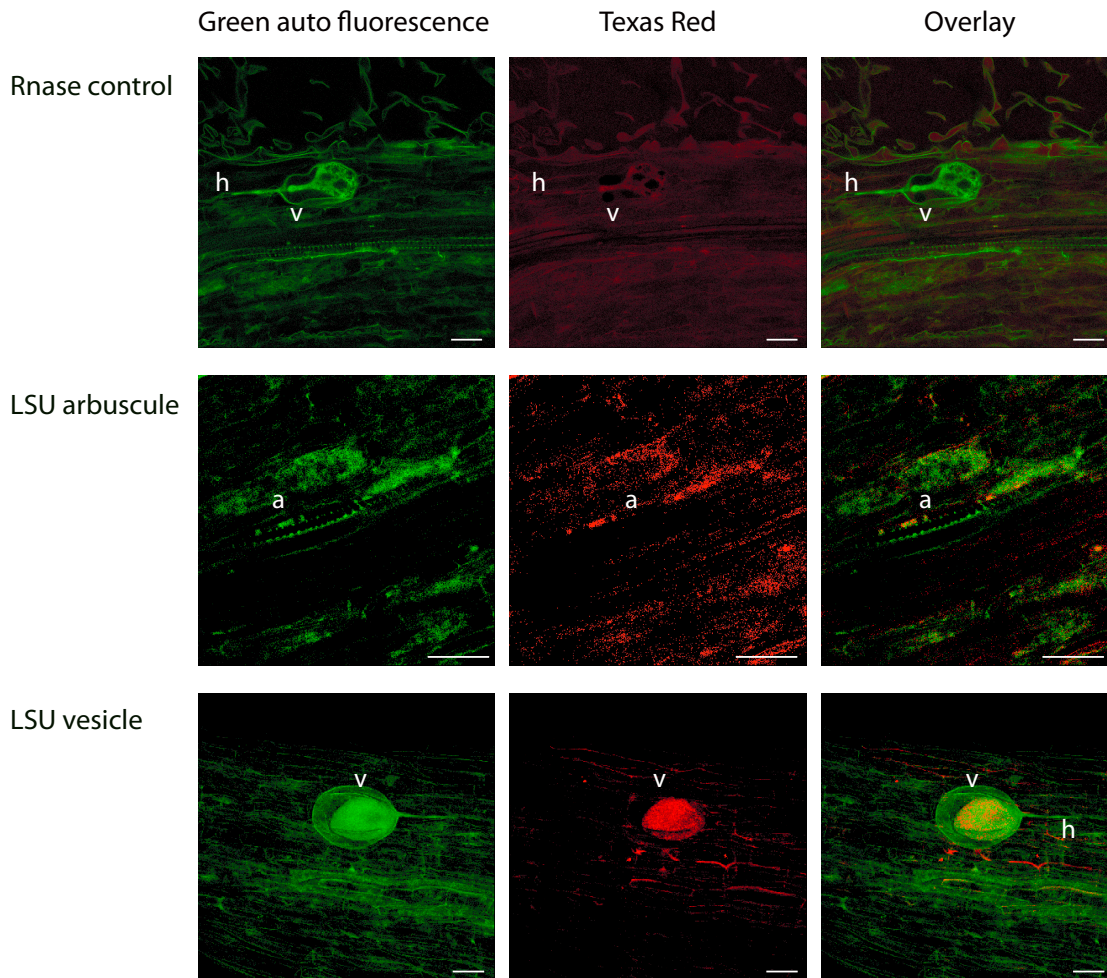


Figure 29: *In-situ*-RT-PCR controls on colonized *M. truncatula* roots. Roots were fixed, permeabilized and Dnase treated before gene specific reverse transcription was carried out. PCR with Texas-Red-labeled primers was performed and samples were analyzed using a Leica SP5 CLSM. Fungal structures were visualized by their green auto fluorescence (first column), Texas Red fluorescence was visualized using the 633-nm-laser (detection from 640 to 700 nm, second column). The third column shows the overlay of the first two columns. If samples were treated with Rnase before reverse transcription or if reverse transcription was not performed (not shown), no transcripts were detectable in the red channel, indicating that no residual genomic DNA was present. Weak ribosomal large sub unit (LSU) transcripts could be detected in arbuscules (a) and strong LSU signal was visible in vesicles (v), but not in hyphae (h). Bars are 25 μ m.

As the controls were working, transcripts of AMTs were examined. For *GintAMT1* no signal was expected as the encoded transport protein was not detected in immune localization experiments. However, a very strong signal was detected in vesicles (Figure 30). This indicates technical problems during the immune localization procedure for this protein. *GintAMT2* and *GintAMT3* transcripts were – as expected – detected in vesicles but not in arbuscules or hyphae (Figure 30).

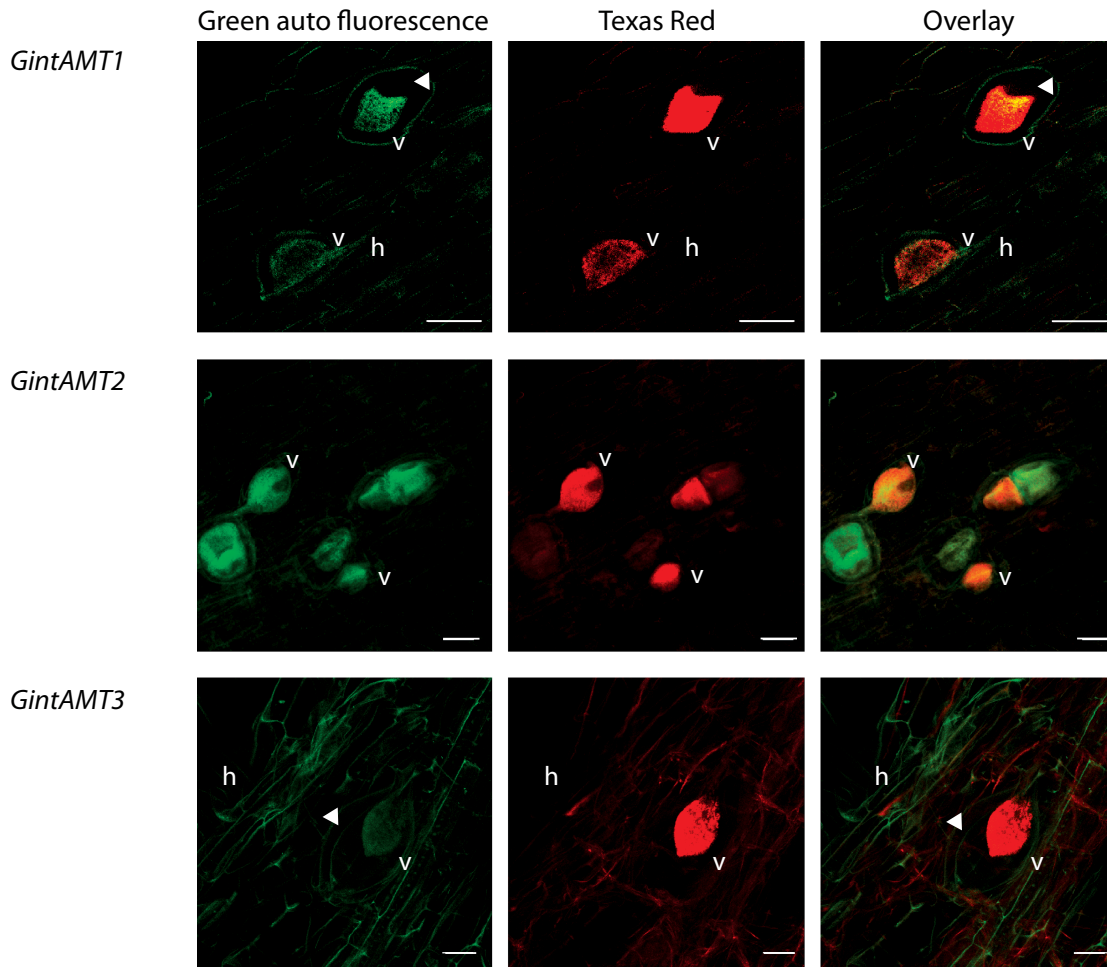


Figure 30: *In-situ*-RT-PCR on colonized *M. truncatula* roots. Roots were fixed, permeabilized and Dnase treated before gene specific reverse transcription was carried out. PCR with Texas-Red-labeled primers was performed and samples were analyzed using a Leica SP5 CLSM. Fungal structures were visualized by their green auto fluorescence (first column), Texas Red fluorescence was visualized using the 633-nm-laser (detection from 640 to 700 nm, second column). The third column shows the overlay of the first two columns. Transcripts of *GintAMT1*, *GintAMT2*, and *GintAMT3* were detected in vesicles (v), but not in intraradical hyphae (h) or arbuscules (not shown). During PCR reaction the cytoplasm shrank and became clearly distinct from vesicle cell wall (arrow heads). Bars are 25 μ m.

Surprisingly, all three *AMT* transcripts were detected by very bright signals. The positive controls showed weaker signals and probably need optimization of the oligonucleotides.

The localization data of *AMTs* in the model AMF *R. irregularis* show that the *AMTs* are most prominently expressed in fungal storage organs like extraradical spores and intraradical vesicles. However, if the fungus is grown on medium without any ammonium, the transporters are also expressed in a small portion of the extraradical hyphae. These data strongly suggest, that *AMTs* are only expressed to counteract the loss of ammonium but not for active uptake of ammonium from the outside. For active uptake, nitrate or amino acids might be the preferred nitrogen sources.

2.3.6 Summary localization of glomeromycotan AMTs

The three AMTs and their transcripts were localized *in situ* in structures of *R. irregularis*. A protocol giving rise to reliable *in situ* localization data was setup. AMTs were localized in ERM as well as in IRM. In ERM, they were preferentially located in fungal spores and only under no-ammonium-conditions they were detected in a subpopulation of fungal hyphae. In IRM they were not at all localized in fungal hyphae or arbuscules, but exclusively in vesicles. As this was unexpected, a second technique for *in situ* detection of the respective mRNA transcripts in the IRM was setup. AMT transcripts accumulated in vesicles and could not be detected in arbuscules or hyphae. For GintAMT2 and GintAMT3 *in situ* PCR confirmed the results of the immune detection. GintAMT1, however, was only detected in IRM on mRNA level, but not by immune detection. Immune localization was not possible because of slightly higher background in the pre-immune-serum-samples. A lower protein content taken together with higher background might be the reason for the lacking signal in this experiment.

2.4. Optimization of the fungal *in-vitro*-culturing system

For the studies on *R. irregularis* AMTs, sterile fungal material, produced in root organ culture (ROC), was a prerequisite. ROC is a laborious system with low efficiency. To improve this system, we added a step of liquid culture in our culture cycles. We could prove that this system works better and produces higher amounts of spores faster than previous used systems.

2.4.1 ROC success rate (RSR) can be used to determine root colonization of mother-culture

During initial Root organ liquid culture (ROL) experimentation, it was tested whether the potential of root material as successful starting material for new ROCs can be used as a measure for % root colonization. The ROC success rate (RSR) was defined as the percentage of well colonized fungal compartments in the newly setup split-plates. Three cultures from a batch of ROLs were randomly chosen. From each ROL, 2 g root material was used to inoculate 10 new split-plates with c. 0.2 g root material, each, and a part of the residual 2 g of roots were stained for measuring the root-length colonization. Colonization for the three samples was 23%, 15%, and 1% and the RSR of the newly established split plates was 70, 30, and 20% after 8 weeks, respectively (Figure 31). This indicates that the RSR follows, and can probably be used as a measure for, the percentage of root colonization of the mother-culture.

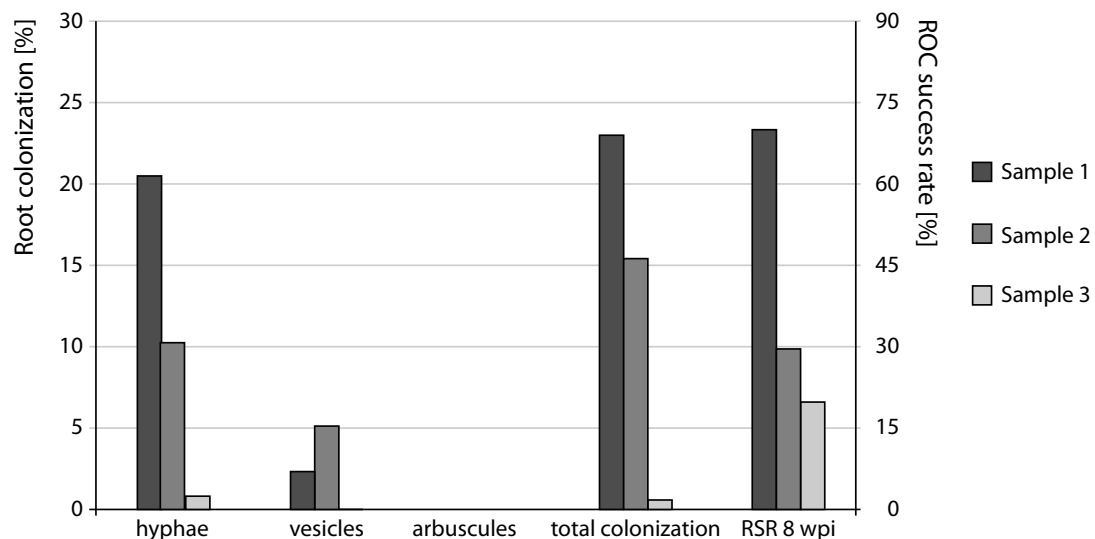


Figure 31: Comparison of mycorrhization level and ROC success rate. Three randomly chosen ROCs (different grey shades) were taken either for direct estimation of mycorrhization (internal hyphae, vesicles, arbuscules and total) by methyl blue staining or for indirect estimation by inoculation of ROCs and estimation of ROC success rate (RSR) 8 weeks later (right bars). The success rate of newly inoculated ROCs follows the mycorrhization level of the mother-culture.

2.4.2 Reduction of phosphate content in liquid MSR improves stable root colonization

After 5 to 6 succeeding cycles of ROL, with *c.* 1.5 g root material used to start new ROLs, we noticed a significant drop in ROC success rate, indicating that the colonization of the chicory roots in ROL decreased over the duration of culturing. Because chicory roots grow very fast in the liquid MSR medium, fungal colonization might be too slow for efficient root colonization. It was tested, whether the root growth and fungal colonization rate could be balanced, by reducing the phosphate concentration. Five flasks containing 30 μM (high-P), five flasks containing 3 μM (low-P), and five flasks containing 0 μM (no-P) KH_2PO_4 were inoculated with 1.5 g of roots and incubated in the dark for 12 weeks. The root biomass was measured every second week. For the low-P concentrations root growth was significantly reduced; after 4-6 weeks 1.5-2 g of new root material were produced, meaning a root biomass doubling in *c.* 4 weeks (Figure 32).

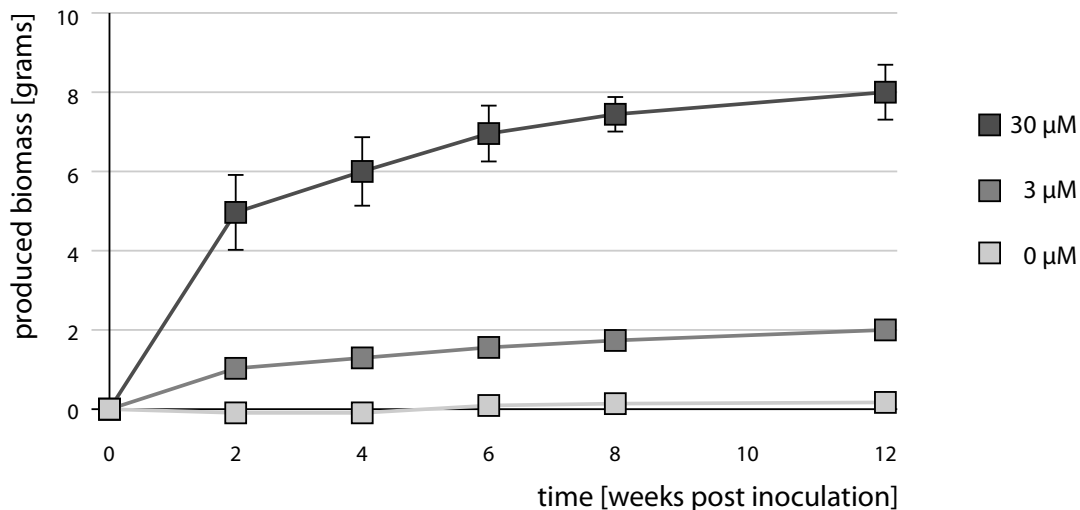


Figure 32: Biomass production of mycorrhizal chicory roots in ROL with different phosphate concentrations. Roots were grown in 30 μM (high-P, dark grey), 3 μM (low-P, medium grey) or without any phosphate in the medium (light grey). Root fresh weight was measured every second week. Average fresh weight of 5 root systems and standard deviations are shown.

Based on the results shown in Figure 32, we decided to use the root material from 6 weeks old ROLs for continuous intervening culturing using ROC and ROL. The root material was split and used to inoculate one new ROL with one half and 10 new ROCs (*c.* 0.15 g each) with the other half of the material. This was done for 9 high-P and low-P ROLs, each, and for 3 ROLs with no-P medium. After *c.* 6 weeks the high- and low-P ROLs were harvested and used to inoculate 10 split-plate ROCs, each. The three no-P ROLs were harvested after 6 months. The ROC success rate was estimated 8 weeks later. For the ROCs inoculated with material from low-P ROLs the RSR increased at least two-fold, compared with plates inoculated with material from high-P ROLs (Figure 33). For material from the three no-P ROLs, a 100% RSR was obtained, demonstrating

that the roots were still alive and became very well colonized by the AMF over time. The no-P ROLs stood for 4 of the 6 months without shaking, indicating that there is no problem with oxygen shortage in liquid medium even without shaking.

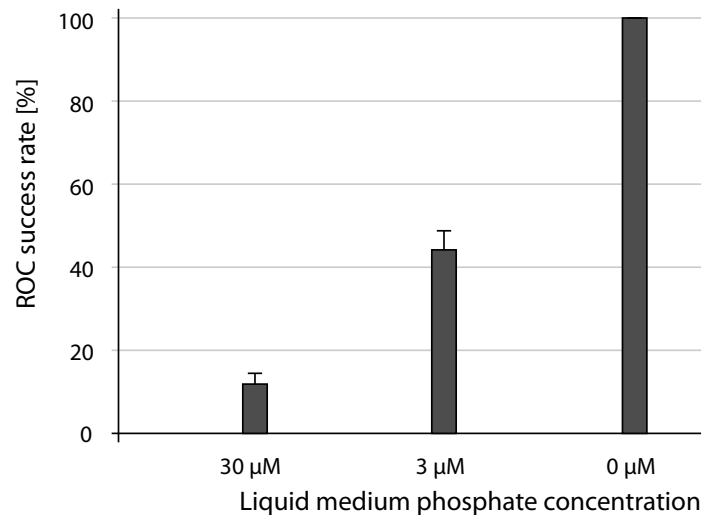


Figure 33: Comparison of high-P and low-P ROLs. Nine ROL flasks containing MSR medium with high phosphate content (30 μM) and 9 flasks containing MSR medium with low phosphate content (3 μM) as well as 3 flasks containing MSR medium without phosphate were incubated at room temperature in the dark. Flasks were distributed on ROC plates and RSR was determined after 8 weeks. Low-P ROLs revealed the more efficient ROCs and higher RSR. Average of 9 experiments with 10 plates, each (30 μM and 3 μM) and standard deviation are shown. Three no-P flasks were distributed on ROC plates after 26 weeks, resulting in 100% RSR (0 μM).

2.4.3 A continuous liquid culture method of mycorrhizal chicory roots

To investigate, whether low-P ROL can be used to inoculate new ROLs continuously, without losing fungal root colonization, 9 flasks with low-P medium were inoculated with low-P ROL root material and grown for 6 weeks. This was repeated successively, always using 1.5 g root material (about half of the root material in a flask) as inoculum. The other half was used to start 10 ROCs to determine RSR after 8 weeks. As shown in Figure 34, the system results in stable ROC success rates of 40-60%.

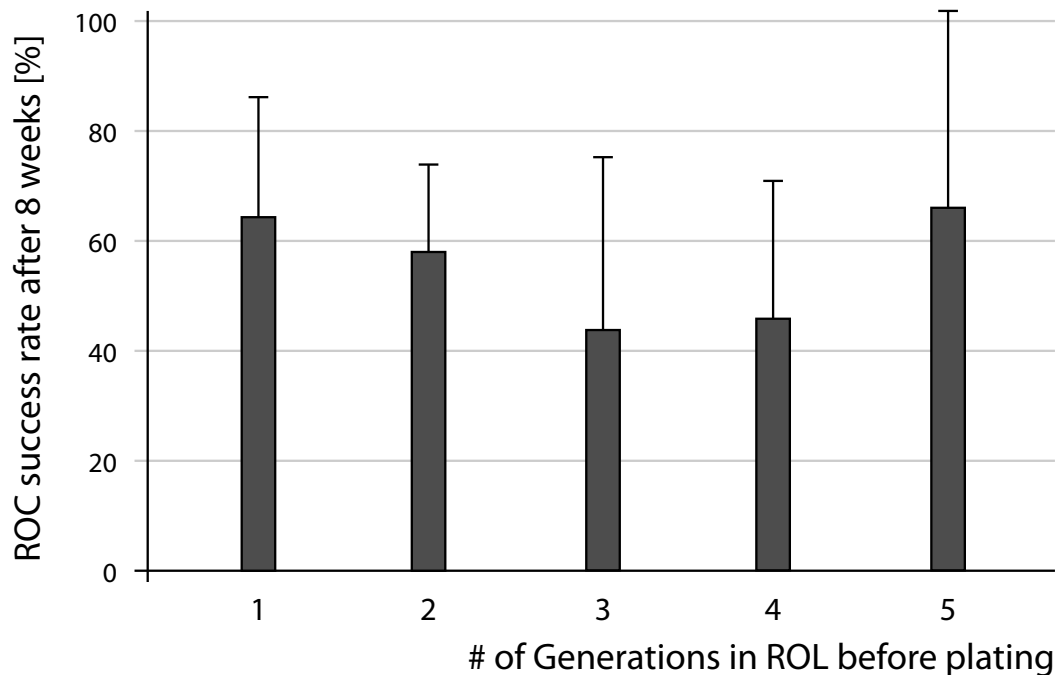


Figure 34: Continuous ROL cycles are stable. Low-P ROLs were directly incubated from ROLs for 1, 2, 3, 4 or 5 generations. Half of the root system was used to estimate the RSR after 8 weeks. Bars show average RSR of 9 replicates (10 plates each) after 8 weeks. Error bars depict standard deviation.

2.4.4 Effect of sucrose and gellan gum concentration on fungal root colonization and RSR

To perform molecular investigations on AMF (e.g. RNA or protein extraction), it is necessary to extract fungal material from the culture plates as fast as possible. To enhance the harvest of the fungus and fasten the dissolvability of the plate medium, we tried plates with lower content of solidifying agent. Surprisingly, we discovered, that the gellan gum concentration in the fungal compartment was considerably influencing the successful colonization of the fungal compartment. While for the lower gellan gum concentration (0.05% and 0.1% w/v) 40-70% of the fungal compartments were colonized after 60 days (Figure 35), the usually used gellan gum concentration of 0.3% (w/v) resulted in only 20% RSR after 60 days (not shown). Highest colonization rates were seen with the combination 0.05% or 0.1% gellan gum and 1.0% sucrose (Figure 35) and 0.05% gellan gum was chosen for further experiments.

In the root compartment, the standard concentration of 0.3% gellan gum was used, because a test with 60 split-plates that contained 0.05% gellan gum in the root compartment did not result in higher RSR. In addition, it was difficult to harvest the fungal material from such plates, because it was no longer possible to pour out the medium from the fungal compartment without getting root contamination.

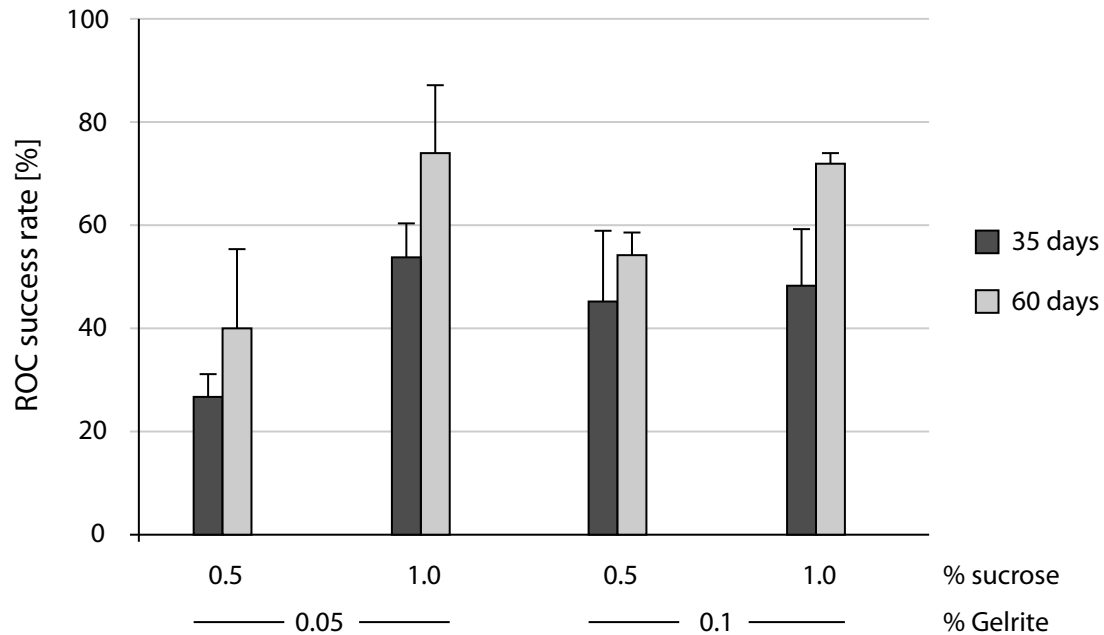


Figure 35: Influence of gellan gum and sucrose concentration on ROC success rate. ROL grown roots were used to inoculate split-plates. Three replicates with 60 plates each were setup, with fungal compartments containing either 0.1 or 0.05% Gelrite and root compartments (0.3% Gelrite) containing either 0.5% or 1.0% sucrose. RSR was estimated after 35 and 60 days. Bars show average colonized plates of 3 replicates à 60 plates after 35 and 60 days. Error bars depict standard deviation.

2.4.5 ROL of mycorrhizal chicory positively affects the fungal growth in successive ROCs

We realized a strong positive effect on *R. irregularis* sporulation and hyphal growth in ROC, when the mycorrhizal roots used for inoculation were taken from ROL and not from ROC. When inoculated with ROC material, it took at least 2 months until mycorrhizal roots from the newly setup ROCs could be efficiently used for inoculation of new plates and another two months until the fungal compartment was well colonized. Additionally, only in *c.* 20% of the ROCs the fungal compartment became colonized with the formerly used standard procedure. When using ROL (cultures were setup in parallel to the ROCs used for comparison) produced material for inoculation we were able to shorten the time until spores can be harvested to 6-8 weeks (Figure 36). This is a great advantage over both, the carrot root system (see for example Ijdo *et al.*, 2011) and the previously published chicory root system (see for example Campagnac *et al.*, 2009).

Three different shaking conditions (0 rpm, 30 rpm and 60 rpm) were tested, whereby shaking of ROLs with 30 rpm resulted in the highest RSR. The first generations of ROLs took about 2 months until the roots used for inoculation had colonized the whole volume of liquid medium. From these starting ROLs we inoculated new two-compartment Petri dishes, which could be used for new liquid cultures as soon as fungal growth was observed (after 3-4 weeks, dependent on the desired fungal stage).

It took 5 weeks until a RSR of *c.* 50% was reached (Figure 35). The fungal biomass harvested per plate in average was *c.* 100 mg/plate (MW=98, N=10, SD=47.16) after 8 weeks. This corresponds to about 10,000 spores per 9 cm split-plate, what is roughly in the range of the carrot root system after 16 weeks (Ijdo *et al.*, 2011). The harvested fungal material was used in our laboratory for RNA extraction, germination tests, or protein extraction, inoculation of plants, and other approaches.

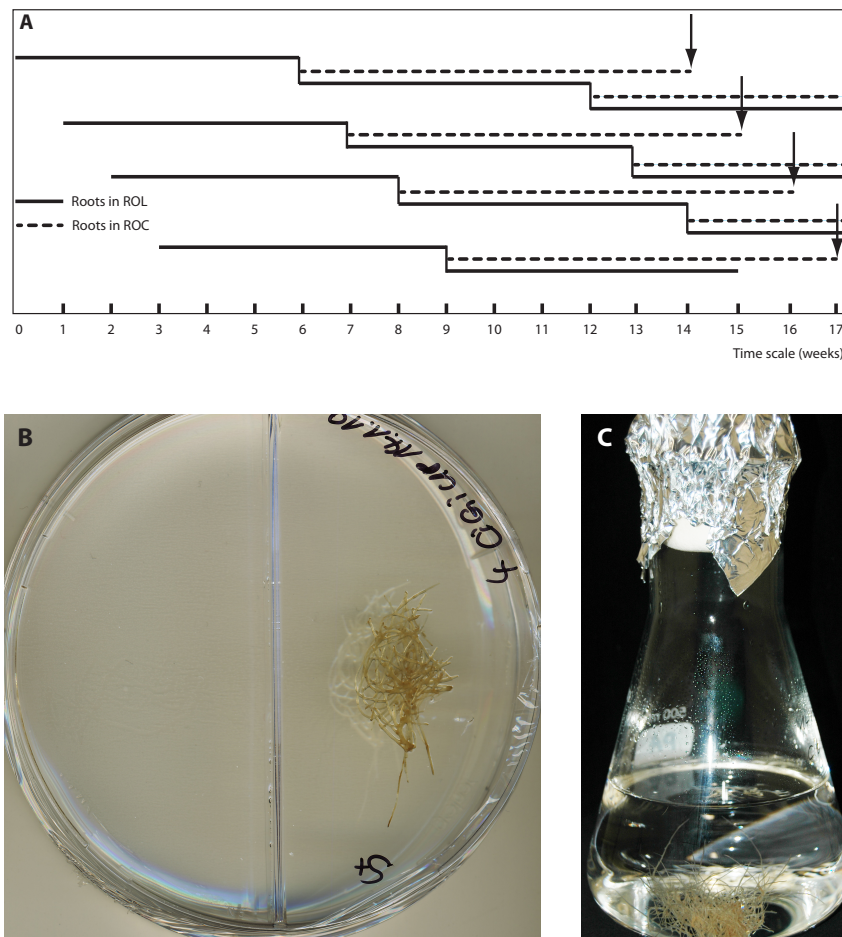


Figure 36: Experimental setup and time management. (A) Time scale of the experimental setup. Continuous black lines indicate incubation of colonized roots in ROL, dashed lines in ROC. Black arrows indicate the time points when fungal material was ready to harvest. We harvested this material every week after the starting period of 10-14 weeks. Here we show the timeframe, if ROLs are transferred to ROC after 6 weeks and ROCs are harvested after 8 weeks. (B,C) Representative pictures of a newly inoculated Petri-dish and Erlenmeyer flask, respectively. About 0.2 grams of roots were used for inoculation of split-plates and about 1.5 grams were used for inoculation of Erlenmeyer flasks.

2.5. Establishment of a transformation system for *R. irregularis*

To date there is no stable transformation system for any AM fungus available. Taken together with the lack of mutants due to the coenocytic nature of AMF and the lacking sexual phase, this is a major drawback slowing down the research on AMF and AM symbiosis. There is no possibility to create knockout mutants or to localize proteins by GFP fusion without a working transformation system. Recently, a transient system has been published for *R. irregularis* (Helber & Requena, 2008). The establishment of this transient system is the first step to develop a stable transformation system. Therefore, the experiment from 2008 was repeated with two different plasmids.

One hundred colonized split-plates were grown and the fungal compartments (in total ~200,000 to 1,000,000 spores) were harvested, washed and distributed on 10 water agar plates (~20,000 to 100,000 spores/plate). Biolistic transformation with a BioRad particle gun was performed under varying conditions (900, 1100 PSI; 5, 7 cm distance) with 2 different plasmids. Half of the plates was bombarded with a plasmid (pBL157) carrying the GintAMT1-GFP construct under control of the yeast *PMA1* promoter; the other half was bombarded with the plasmid pIG1783 (Pöggeler *et al.*, 2003), carrying a cytoplasmic EGFP construct under control of the *GPD* promoter of *Aspergillus nidulans*. Only spores bombarded with pIG1783 showed green fluorescence two days after bombardment (Figure 37).

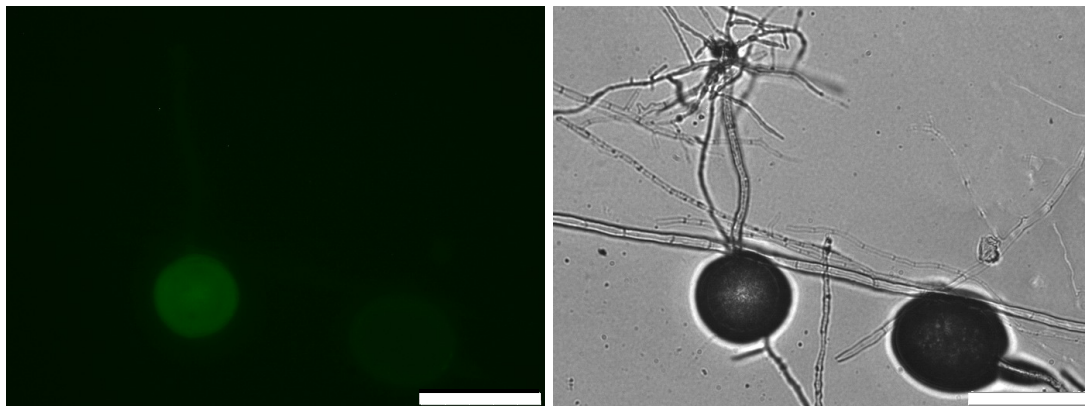


Figure 37: Transformed *R. irregularis* spore expressing GFP. Left: GFP signal, right: bright field. Biolistic transformation following the protocol of Helber & Requena, was carried out. More than 200,000 spores were grown on MSR plates, harvested, washed and placed on water agar plates for biolistic bombardment. Of more than 100,000 spores bombarded with pIG1783, 50,000 spores were investigated and about 50 were showing cytoplasmic GFP signal (see spore on the left side). Only slight background fluorescence (see spore on the right side) was visible. Spores bombarded with pBL157 (GintAMT1-GFP) were not fluorescent at all. Bars are 100 μ m.

The pBL157 bombarded spores showed no fluorescence after 2, 3 and 4 days. In total, ~50 spores (out of ~50,000 investigated ones), bombarded with pIG1783 were green fluorescent and still alive (a time series of respective spores was recorded to check for cytoplasmic streaming). An empty vector control, however, was not included in the experiment. No differences in transformation efficiency were observed for the different particle gun adjustments.

3. Discussion

Arbuscular mycorrhiza symbiosis is the symbiosis between plant roots and fungi of the phylum *Glomeromycota* (Parniske, 2008; Smith & Read, 2008). Characteristically, it comprises advantages for both partners. The plant benefits from the enlarged surface of the hyphal network as well as from the smallness of individual fungal hyphae, whereby the fungus can access smaller nutrient and water reservoirs in the soil and make them available for both partners. Respective nutrients like phosphorous, nitrogen, metal ions, other micronutrients and water are then transported along the fungal hyphae towards the host plant and released. In change, the host plant supplies the fungus with photosynthetically fixed carbon in the form of monosaccharides (Schüßler *et al.*, 2006; Helber *et al.*, 2011). Because of its agricultural relevance, the main research so far was concentrating on the role of phosphate in AM.

To investigate the role of nitrogen in the AM symbiosis, fungal AMTs were chosen as the principal research target. AMTs are most probably acting as nitrogen uptake machinery from the soil, but might also be involved in nitrogen release to the plant at the symbiotic interface. Two glomeromycotan fungi were chosen for investigation of their AMTs. One of them, *Rhizophagus irregularis*, had become a widely used model AMF after it was demonstrated to be cultivable *in vitro* in so-called root organ culture (ROC) together with *Agrobacterium rhizogenes* transformed host plant roots (Bécard & Fortin, 1988; Chabot *et al.*, 1992; Declerck *et al.*, 1998) and therefore became available for academic research. The second fungus, *Geosiphon pyriformis*, has been used as a model fungus for AM symbiosis because of its special symbiotic interference with cyanobacteria of the species *Nostoc punctiforme* (Gehrig *et al.*, 1996; Redecker *et al.*, 2000; Schüßler & Kluge, 2001) and their prokaryotic nature. It had already been used to identify the first glomeromycotan sugar transporter (GpMST1; Schüßler *et al.*, 2006). The goal of our research was the identification, characterization and functional investigation of these two fungi's ammonium transporter complements.

3.1 Definition of the AMT complements of two glomeromycotan fungi

Both investigated fungi, *R. irregularis* and *G. pyriformis*, each contain 3 AMT encoding genes. The genes are expressed under symbiotic conditions – shown by RACE-PCR (for both fungi), 454-sequencing (for *G. pyriformis*) and qRT-PCR (for *R. irregularis*; lab rotation practicum by Markus Grundmann, also shown in published data of Nuria Ferrol and co-workers: López-Pedrosa *et al.*, 2006; Perez-Tienda *et al.*, 2011) – as well as in non-symbiotic extraradical mycelium – shown for *R. irregularis* by RACE-PCR and qRT-PCR. Bioinformatic investigations revealed the common features for AMTs for all six glomeromycotan AMT encoding genes and the encoded transport proteins. The conserved trans membrane domain (TMD) structure as well as the presence of highly conserved residues, which are suggested to assure ammonium conduction through the pore (Khademi *et al.*, 2004; Andrade *et al.*, 2005a; Khademi & Stroud, 2006; Marini *et al.*, 2006; Andrade & Einsle, 2007; Boeckstaens *et al.*, 2007; Boeckstaens *et al.*, 2008; Loqué *et al.*, 2009; Lamoureux *et al.*, 2010; Pantoja, 2012; Wang *et al.*, 2012) were

characteristic for common (fungal) AMTs. Nearly every fungal AMT up to now is transporting methylammonium (MA). We discovered that this is not true for *GpyrAMT1*, which encodes a functional AMT but the protein is not able to transport MA (see results and Brucker, 2009; Ellerbeck, 2009). Until recently, *MepC* of *Aspergillus nidulans*, which is only distantly related (31% to 35% identity) to the other AMTs of *A. nidulans* (Monahan *et al.*, 2006), was the only fungal AMT lacking MA transport capability. The second one, *GintAMT2*, was recently described from an AMF (Perez-Tienda *et al.*, 2011). An additional experiment with only two different MA concentrations showed the same negative result for yeast cells expressing *GintAMT3* (not shown). Thus, interestingly, of the four glomeromycotan AMTs functionally active in yeast (*GintAMT1*, *GintAMT2*, *GintAMT3* and *GpyrAMT1*), only one (*GintAMT1*) transports MA. For *GpyrAMT3*, this experiment was not performed, because the encoded transporter is due to its vacuolar localization not expected to transport MA. Biochemical characterization in the heterologous yeast system, therefore, revealed at least three differential functional classes in terms of ammonium transport on the one hand and MA transport on the other hand for the six transporters (Table 2). Interestingly, one of those classes (group III in Table 2) includes AMT like proteins, which are not able to transport ammonium in yeast. The transport capacity of one of them (*GpyrAMT2*) could be partly restored by a single amino acid exchange from cysteine to serine. The respective amino acid is located in the AMT signature (ATS, von Wirén & Merrick, 2004) three residues downstream of one of the two conserved histidines, which are probably involved in de- and reprotonating the ammonium ion during the transduction through the pore (Figure 38; Lamoureux *et al.*, 2010; Wang *et al.*, 2012).

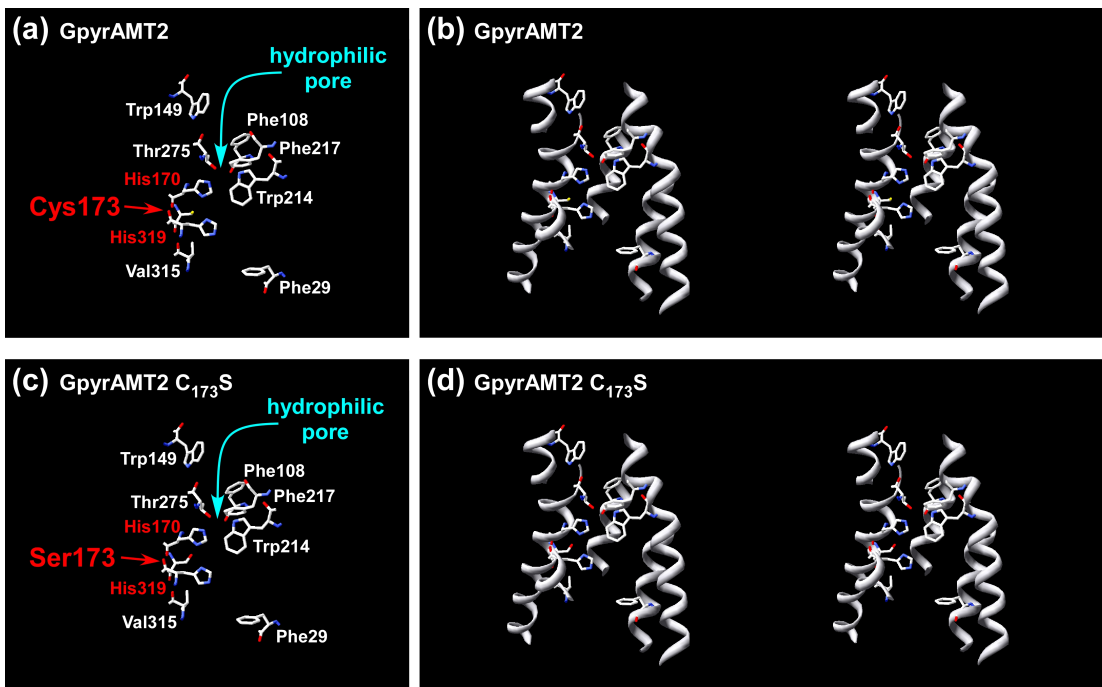


Figure 38: Structural model of the hydrophilic pore in GpyrAMT2. (a,c) Representation of the conserved and functionally important residues inside the hydrophilic pore for ammonium transduction and of cysteine/serine 173. (b,d) Stereo images of the 3D structure of the pore region. Cysteine/serine 173 is located in close proximity to the histidine dyad. Structures of GpyrAMT2 and GpyrAMT2 C₁₇₃S were generated using SWISS-MODEL and the PDB template 2b2h of *Archaeoglobus fulgidus* amt-1.

In most fungal AMTs serine is located in this position while there are also transporters known with an alanine or glycine in this position (von Wirén & Merrick, 2004). The cysteine of GpyrAMT2 (C₁₇₃) and GpyrAMT3 (C₁₈₉) can be deprotonated ($pK_S = 8.1$) while serine ($pK_S \sim 15$, in aqueous solutions not able to be deprotonated), alanine and glycine cannot. The respective proton of GpyrAMT2 C₁₇₃ might interfere directly with the histidines and therefore inhibit ammonium transduction or indirectly interfere via H-bonds with the protein backbone and thereby change the electro negativity of the histidine or another residue in its range. By protein modeling, we observed that the thiole group of the cysteine is in close proximity to the imidazole group of this histidine (Figure 38; Lott, 2011). The exchanged serine, however, was not investigated further, so far, meaning that its involvement in ammonium transduction could be illustrated for the first time.

A further investigation of this residue in yeast AMTs will be performed in the near future. If this residue plays a role in the yeast transporters, a slightly reduced ammonium transport capacity should be measurable. First investigations with yeast cells expressing ScMEP2 or the respective mutated protein ScMEP2_S₁₉₇C in liquid cultures point into the direction of slightly reduced growth performance of the cells expressing the mutated ScMEP2 version (Lott, 2011). ScMEP2 was chosen because of

its putative role in pseudohyphal growth and its predicted role in ammonium sensing. Our prior results with the three yeast AMTs (Ellerbeck, 2009) suggest that the discrimination between MEP1/3-like and MEP2-like AMTs might be an artificial discrimination. Experiments showed that ScMEP1 and ScMEP3 are able to restore pseudohyphal growth, too. Those results might be caused by using a different promoter (the *PMA1* promoter) and are under further investigation under the original promoters in a bachelor project. If this particular serine residue, however, plays an essential role in ammonium sensing, one might expect limited pseudohyphal growth in addition or independent of reduced ammonium transport capacity. If the residue would play a role only in glomeromycotan AMTs, there should be no difference in transport capacity or pseudohyphal growth detectable for the yeast transporters. In this case, it would be necessary to crystallize the respective proteins to get further information about the structural differences between glomeromycotan and other (fungal) AMTs by X-ray diffraction analysis. Mutations of the respective serine residues of the GintAMTs to cysteine and subsequent removal assays are also still missing. For GpyrAMT3, the exchange of the respective cysteine (C₁₈₉) showed no rescue of ammonium transport capability. This was expected due to its vacuolar localization in yeast. For further investigations of GpyrAMT2 to its new or abolished substrate specificity and its putative ammonium sensing capability, it would be necessary to purify the protein and do either interaction studies with ammonium (-like compounds) or electrophysiological studies with a number of imaginable transport substrates like choline and other small amines.

The localization in yeast via C-terminal GFP-tags and subsequent CLSM microscopy revealed vacuolar localization for GpyrAMT3. The classification of this transporter into group III might therefore be misleading. However, it is not a functional AMT in *S. cerevisiae*. *Geosiphon pyriformis* forms a symbiosis with *N. punctiforme* cyanobacteria that form heterocysts (also in the symbiosis) and are capable of atmospheric N₂ fixation (Schübler & Kluge, 2001). The three AMTs characterized here could play a role in ammonium uptake from the environment or of ammonium released by the cyanobacterial symbiont into the symbiosome space. GpyrAMT3 could be responsible for the transport of ammonium into or from the vacuole (or both) in the homologous system. Due to its vacuolar localization in yeast, GpyrAMT3 was not further characterized by the approaches used in this study. However, its localization is interesting. Large amounts of arginine are cleaved in the arbuscules within the plant root cells to provide the plant with ammonium (Tian *et al.*, 2010). The expression of respective arginine anabolism genes was also identified in the symbiotic bladder cDNA library (Schübler *et al.*, unpublished), meaning that similar mechanisms also exist in *Geosiphon*. GpyrAMT3-like transporter types could therefore be responsible for ammonium release from vacuoles or for pumping ammonium into vacuoles.

The vacuolar localization of GpyrAMT3 in yeast is also interesting with regard to the fact that no fungal vacuolar AMTs are known; Amt/Mep/Rh proteins are usually plasma membrane located. To our knowledge, only for *Dictyostelium discoideum* a vacuolar AMT, AmtB, was characterized (Kirsten *et al.*, 2008), which is specifically located at the

contractile vacuole and exports excess ammonium. However, it is unknown whether this transporter localizes in the vacuolar membrane in the yeast system. One should also note that the contractile vacuole is not a typical vacuolar membrane and partly continuous with the plasma membrane. Similar characteristics are present for the perisymbiotic membrane in the *Geosiphon* symbiosis, which is derived from an invaginated plasma membrane. Probably homologous to this membrane is the arbuscular plasma membrane, which also must have a very specific protein complement different from the 'normal' hyphal plasma membrane. It is entirely speculative, but one may hypothesize that GpyrAMT1 is responsible for ammonium uptake from the environment while GpyrAMT2 performs uptake or sensing at the symbiotic membrane. The role of GpyrAMT3 might be the export of ammonium from the fungal cytoplasm, perhaps to deliver ammonium to the photoautotrophic symbiosis partners in glomeromycotan symbioses, for vacuolar ammonium transport, or for detoxification of high ammonium concentrations. It will be very interesting to study such speculative questions in future.

Table 2: Glomeromycotan AMTs can be classified into three functional groups. From our biochemical characterizations, we can divide the investigated transporters in a normal behaving (GintAMT1), a transport capacity restricted (GintAMT2, GintAMT3, GpyrAMT1) and a non-functional (GpyrAMT2, GpyrAMT3) AMT group. The asterisk indicates that lacking transport capability in GpyrAMT3 is caused by its vacuolar localization in yeast.

Name	NH ₄ ⁺ transport	CH ₃ -NH ₄ ⁺ transport	Functional group
GintAMT1	+++	+++	I
GintAMT2	+	-	II
GintAMT3	+	-	II
GpyrAMT1	+	-	II
GpyrAMT2	-	-	III
GpyrAMT3	-*	-*	III*

3.2 The functional relevance of glomeromycotan AMTs in arbuscular mycorrhiza symbiosis

Lacking a stable transformation system for *Glomeromycota*, a direct approach for the determination of the functional relevance of AMTs during symbiotic interaction with the plant host is not possible. Immune localization was only used once before to localize a distinct protein in fungal mycelium (Perez-Tienda *et al.*, 2011) and had never been successfully used for localization of fungal proteins in mycorrhizal roots before. *In-situ*-RT-PCR had been used before, but only for control genes to proof the technique (Seddas *et al.*, 2008). By immune detection of the proteins and detection of their transcripts by *in situ* RT-PCR, the transporters were successfully localized in various fungal structures. Both techniques were established for *Glomeromycota*. However, in

both extraradical and intraradical fungal mycelium, the transporters and their transcripts could only be detected in storage organs, either spores or vesicles, respectively. In the culture medium, not ammonium but nitrate was the major nitrogen source, while in natural environments amino acids are supposed to be the predominant nitrogen source (~99.5% of N in soils in organic form; Woodmansee *et al.*, 1978). Therefore, the AMTs might not be the major machinery to assure the fungal nitrogen feeding. Only under very low ammonium concentrations in the culture medium, the transporters could rarely be detected in extraradical hyphae (Figure 23). Their transcripts were enriched in extraradical mycelium after a phase of nitrogen starvation on ROC plates (López-Pedrosa *et al.*, 2006; Perez-Tienda *et al.*, 2011 and unpublished data).

Ammonium transport systems had been discussed to play a role in cyclic retention (Kleiner, 1981; Kleiner & Fitzke, 1981; Kleiner, 1985) before the first transporter genes were cloned (Marini *et al.*, 1994; Ninnemann *et al.*, 1994), suggesting them to re-uptake effectively and with high affinity ammonium, which was lost over the plasma membrane as plasma membrane permeable ammonia (NH₃) and rapidly protonated to plasma membrane impermeable ammonium (NH₄⁺) in the acidic extracellular environment.

In extraradical mycelium, the AMTs localized exclusively to spores as long as the medium contained ammonium (300 μM). Spores are supposed to be storage organs and might contain a lot of ammonium or other nitrogen storage forms, which can be spontaneously deaminated. As soon as ammonium was removed from the medium, a subpopulation of the hyphae also contained AMTs (Figure 23). A lower ammonium concentration on the outside may be suitable to drive ammonium loss over the plasma membrane with the concentration gradient to an extent that re-uptake is also necessary in extraradical hyphae.

Taking into account the intraradical localization data of glomeromycotan AMTs and their mRNAs in vesicles, but not in arbuscules, they might be involved in plant nitrogen feeding by the following mechanism: *glomeromycotan* AMTs might assure the minimization of passive ammonium loss as well as constitute a tool to indirectly regulate the nitrogen flux towards the host plant by fine-tuning the amount of nitrogen that is passively released over the fungal plasma membrane. One could imagine that the fungal AMTs are down regulated in intraradical mycelium (arbuscules) if the fungus is fed with carbon. This would lead to higher ammonium “loss” and therefore indirectly feed the host plant with nitrogen. This alternative model fits to current models, because the nutrient exchange interface would then be characterized by the highly branched arbuscules and intraradical hyphae. Quantitative measurements, however, are very limited with the used tools. Deeper insights into the mechanism depend on a working transformation and gene knockout system.

Investigations on plant phosphate transporters as well as AMTs revealed the importance of the periarbuscular membrane for nutrient exchange. The highest up-regulated genes in *Lotus japonicus* when plants were inoculated with *Gigaspora margarita* turned out to be an AMT, which is only expressed in mycorrhized roots, but

not expressed in nodules (Guether *et al.*, 2009). Transcripts have been preferentially detected in arbusculated cells in a laser micro dissection approach and subsequent semi quantitative RT-PCR (Guether *et al.*, 2009). However, a visible signal in non-colonized cells of mycorrhizal roots was obtained after 37 as well as 40 PCR cycles. This indicates already, that the arbuscule at least is not the only site of fungal ammonium release, but also intraradical hyphae might play a role.

AM specific plant phosphate transporters, however, were exclusively localized to the periarbuscular membrane – the part of the plant plasma membrane surrounding the arbuscule (Harrison *et al.*, 2002; Javot *et al.*, 2007; Pumplin *et al.*, 2012). By investigating MtPT4 localization under varying promoters, it was demonstrated, that the correct localization of this transporter to the periarbuscular membrane depends on precise temporal expression of the protein (Pumplin *et al.*, 2012). A knockout of MtPT4 leads to formation of degenerate arbuscules, giving hereby strong evidence, that the arbuscule is the phosphate exchange interface.

The knock-down of a fungal monosaccharide transporter (GintMST2) by trans kingdom silencing also leads to reduced expression of PT4. The monosaccharide transporter is not only expressed in arbuscules but also in intercellular hyphae under normal conditions (Helber *et al.*, 2011), indicating again that different sites might serve as symbiotic nutrient exchange interface.

Recent studies on a MtPT4 mutant revealed that N transport alone might be sufficient for the establishment of functional AM (Javot *et al.*, 2011). This result provides further evidence for the strict regulation of nutrient exchange between AM symbiotic partners in order to preserve an evolutionary stable mutualism.

Such particular investigations have not yet been performed for either plant or fungal AMTs. However, labeling experiments demonstrated, that nitrogen is released to the plant without additional carbon (Govindarajulu *et al.*, 2005), suggesting, that ammonium is the form of nitrogen released by the fungus. This model was supported by expression studies of the putatively involved enzymes (Tian *et al.*, 2010). An additional possibility instead of ammonium release would be the release of urea to the periarbuscular space and successive degradation. The formed carbon dioxide would have escaped the labeling studies.

For further investigations of nutrient fluxes, a transformation system for *Glomeromycota* is indispensable. Direct tagging of proteins with fluorophores could enhance the research velocity in this field considerably. A next step would then be the generation of fungal knock-out-lines as a reverse genetics tool to study different mutants. The coenocytic nature of those organisms, however, is a major drawback in such experiments. It was possible to reproduce the transformation by following an earlier protocol (Helber & Requena, 2008). However, this is only a transient method and improvements are essential for further research in this direction.

3.3 Optimization of the culturing system of *R. irregularis*

We developed an efficient method for the *in vitro* production of *R. irregularis* material (hyphae and spores) by using root organ liquid culture (ROL) with chicory roots as host. High amounts of mycorrhizal root material can easily be produced in ROL. For fungal spore and hyphae production we used the chicory-based ROC system (Fontaine *et al.*, 2004), which has advantages, when compared to the formerly often used carrot system. Using chicory, it is not necessary to re-associate fresh host roots with spores or infected roots to start cultures. Colonized roots can be very efficiently used directly to setup new cultures. Furthermore, chicory roots grow faster and are easier to handle. By reducing the phosphate content of the liquid medium or by extending culturing time in ROL we could avoid the loss of AMF colonization over successive ROL cycles. It turned out that stable ROLs could be obtained not only by reducing the phosphate content, but also by extending culturing cycles or keeping cultures at a static growth phase. The use of further developed compartments for ROL, e.g. including gassing instead of shaking, will most likely improve fungal growth even more, although some of the experiments point into the direction, that oxygen is not a limiting factor in the liquid cultures (Figure 33).

By parallelization of ROL and ROC steps it is possible to produce a large amount of ROC split-plates, which are ready for harvest at the periodic time intervals used to setup the cultures 8 weeks after inoculation on plates. For example, the continuous production of 40 split-plates with well colonized hyphal compartments (HCs; 40 plates means about 4 grams fresh weight of fungal material or ~200,000 spores) per week would require the inoculation of 8 Erlenmeyer flasks (ROLs) per week, harvesting the ROLs after 6 weeks and using half of the produced material as inoculum for 80 split-plate ROCs and the other half to again set up a ROL, and harvest the ROCs after another 8 weeks. An inoculation of 20 flasks every day would yield more than 100 colonized plates and more than 10 grams of fungal material or 500,000 spores every day, after the initial lack phase of 14 weeks in total, culturing a total of 840 flasks in parallel. This method could be up-scaled by using other culture vessels, and shaking will probably not be necessary when using gassing, which also allows the use of high liquid media volumes per vessel. A preliminary experiment with (closed) 1 litre Schott bottles containing 400 ml of medium is running and the roots seem to grow as good as in Erlenmeyer flasks, confirming that gas exchange might not be limiting for root growth. The colonization rate, however, could not yet been determined. Also, when ROL cycles are extended to 26-52 weeks, even for high-P ROL the use of 0.15 g root material to setup new ROCs leads to 100% RSR. Such “long cultured” ROLs can be easily kept for more than 10 months and used for extremely efficient ROC inoculation whenever needed. In a recent experiment 120 plates were inoculated with such material and all of the HCs were colonized 6 weeks after inoculation.

Although it is necessary for clean separation of fungal material from the roots to use intermediate split-plate based ROCs, one may produce large amounts of mixed (root fragment, spores and hyphae containing) inoculum by just performing ROL. A

disruption of 10 grams root material into 1 mm pieces (~1.6 µg/piece) should yield at least 6 million fungal propagation units, in case of 100% mycorrhizal roots. For carrot roots we were not able to establish an efficient liquid culture system. However, one could imagine to try other *A. rhizogenes* transformed host roots like potato, strawberry or *plantago* roots in order to further optimize the system by finding the optimal host-fungus combination.

The mass production of fungal propagules for agricultural or similar application to date is usually carried out by unsterile production methods. These systems rely on different host plants and usually apply a mixture of fungi to the respective host plants. These methods are easy to handle and produce a lot of fungal material within a few months. However, for the research on AM fungi they are not suitable as the fungi have to be recovered from the soil, the identity of the included fungi often is unclear and the cultures are not sterile. Under lab conditions, pot cultures can be kept sterile under huge effort, but still the fungus has to be recovered from the soil. On the other hand, a lot of AM fungi cannot be cultivated in ROC to date. For those, the cultivation in pot cultures is the only possibility. In order to further optimize the ROC and ROL culturing system, varying fungi could be applied to blank chicory roots and might establish the symbiosis under the liquid conditions better than on plates. By applying antibiotics to the medium, bacterial contaminations should be kept in reasonable limits.

By using the ROL-ROC succession culturing we realized a much more efficient colonization of fungal compartments in comparison to the “standard” system, in which roots are transferred from ROC to ROC. Additionally the colonization was faster and the produced biomass was higher with the new system. For inoculation of plants with *R. irregularis*, one may use the spores, or the ROL grown roots.

The low concentration of solidifying agent in the fungal compartment was tested to save time while harvesting extraradical mycelium. Additional to the fact, that this provided lower costs, we realized that the fungal hyphae grew faster, colonizing the fungal compartment within 3-4 weeks. This faster colonization also means a more synchronized development compared to standard ROC systems, for example allowing harvesting of well colonized fungal compartments before sporulation. Gene expression studies, protein or metabolite extractions often depend on non-degraded and metabolically active hyphae. With the system presented, it is easy to obtain ROCs with large amounts of growing hyphae, but not yet sporulating.

The roots in ROLs became well colonized and are efficient to rapidly establish fast growing ROCs, also after 40 weeks in ROL. Mycorrhizal chicory roots from 12 weeks old ROC plates usually show a few weeks lag phase before they grow vigorously. As a trial, we cultured three ROLs without added phosphorous in the medium for 6 months and two high-P ROLs for 10 months. Although for the no-P conditions no root growth could be measured in the ROL, the roots were still alive after 6 months as demonstrated by plating 0.15 gram aliquots on 30 split-plate ROCs, which lead to 100% RSR. This indicates that the roots, although not growing, became highly colonized by the AMF in the no-P medium. Such cultures can be utilized to store

material under sterile conditions over longer periods, and directly use it to setup new cultures, needing even less maintenance than the chicory ROCs. For the high-P ROLs, the roots rapidly colonized the liquid medium and after c. 10 weeks had stopped growth. This material was used after 10 months to inoculate 120 new ROCs, again resulting in a RSR of 100%. This clearly demonstrates that chicory roots become highly colonized after prolonged ROL time also under high-P conditions.

A promising system allowing massive spore production and being useful for gene expression studies is described in Voets *et al.*, (2009), based on *in vitro* whole plant culture (WPC) systems. In this system, plant seedlings are placed on a well colonized HC for a few days, and then used as inoculated plant to establish a WPC for fast production of mycelium, which in turn can then be used to inoculate other plants, like potato (Gallou *et al.*, 2010), in an experimental system. The time schedule is similar to that of our system, as the newly setup cultures produced up to c. 7000 spores per plate, after 4 weeks. However, for production of fungal material this whole plant culture system is much more difficult to set up and the risk of contamination is much higher than in ROLs, as the plants have to be transferred between different culture vessels and the shoot of the seedlings has to be exposed to air and therefore to grow outside of the plates.

4. Material and methods

4.1 Material

4.1.1 Equipment

96 well plate reader	Tecan Sunrise Plate Reader, Tecan Trading AG, Crailsheim
ABI 3730 48 capillary sequencer	Applied Biosystems, Darmstadt
Ampicillin	Sigma-Aldrich, Taufkirchen
Autoclave	Varioklav 135 S steam sterilizer, Thermo Scientific, Schwerte
BioAnalyzer 2100	Agilent, Waldbronn
Biofuge 15 (table top centrifuge)	Heraeus Sepatech GmbH, Osterode
Centrifuge 5417R	Eppendorf, Hamburg
Chloramphenicol	Sigma-Aldrich, Taufkirchen
CLSM Leica DMI 6000 TCS SP5	Leica Micro systems, Wetzlar
DNA Engine Tetrad 2 (thermo cycler)	Bio-Rad, München
Filter unit	Filtration unit for 6 probes (41406) Hölzel, Wörth/Hörlkofen
French® Press	SIM-Aminco Spectronic Instruments, Rochester
Heraeus Inkubator	Heraeus Sepatech GmbH, Osterode
iCycler iQ5 (thermo cycler for quantitative real time PCR)	Bio-Rad, München
IKA combimag RCT (magnetic stirrer)	Janke & Kunkel, Staufen
Inverted microscope Leica DMI6000 B	Leica Mikrosysteme, Wetzlar
Leica MZ 16 FA (stereo microscope)	Leica Mikrosysteme, Wetzlar
Magnetic 80 (magnetic stirrer)	Edwards Kniese & Co. Hochvakkum GmbH, Marburg
Micro dismembrator S	Braun Biotech, Melsungen
Micro centrifuge SD	Roth, Karlsruhe
Multifuge 3 L-R (centrifuge)	Heraeus Sepatech GmbH, Osterode
Multitron V2 (incubation shaker)	Infors, Einsbach
Multiwave (Micro wave oven)	LG, Willich
Nanodrop ND-1000 spectro photometer	Labtech International, Burkhardtsdorf
Odyssey Infrared Imaging System	Li-cor Biosciences, Bad Homburg
Optima TLX Ultracentrifuge	Beckmann, München
Pipettes (P10, P20, P200, P1000)	Gilson, Middleton (USA)
Powerpac 300 (power supply)	Biorad, München
PTFE beaker, 3 ml	Sartorius, Göttingen
Sartorius universal (balance)	Sartorius, Göttingen

SBC31 (balance)	Scaltec Instruments GmbH, Göttingen
Baffled flasks, varying sizes	Schott, Regensburg
Scintillation counter	LS500TD, Beckmann Instruments, USA-Fullerton
Sorvall RC50 plus	DuPont Sorvall, Bad Homburg
Steam sterilizer	Memmert, Schwabach
Sterile bench, type KS12	Thermo Scientific, Schwerte
Thermo mixer comfort	Eppendorf, Hamburg
Thermo mixer compact	Eppendorf, Hamburg
Tissue lyser (bead mill)	Qiagen, Hilden
TProfessional (thermo cycler)	Biometra, Göttingen
Ultrospec 3000pro (UV spectrophotometer)	Amersham Biosciences, Freiburg
Univapo 100 H (vacuum pump)	Uniequip, Martinsried
Ultra Clear UV plus (ultra pure water supply)	SG GmbH, Barsbüttel
Universal 30 RF (table top cooling centrifuge)	Hettich, Tuttlingen
Varifuge 3.0R (centrifuge)	Heraeus Sepatech GmbH, Osterode
2016 Vacugene Vacuum Blotting Pump	LKB, S-Bromma
Vortex Genie 2	Bender & Hobein AG, CH-Zürich
Tungsten beads, varying sizes	Sartorius, Göttingen

4.1.2 Chemicals and consumables

Ammonium sulphate ((NH ₄) ₂ SO ₄)	Roth, Karlsruhe
Ampicillin sodium salt	Roth, Karlsruhe
β-mercapto ethanol	Sigma-Aldrich, Taufkirchen
Bacto agar	Becton Dickinson, Heidelberg
Bacto peptone	Becton Dickinson, Heidelberg
Bacto yeast extract	Becton Dickinson, Heidelberg
Boric acid	Roth, Karlsruhe
Bromo chloro propane (BCP)	Ambion, Austin (USA)
Bromphenole blue	Roth, Karlsruhe
BSA (Bovine serum albumin)	New England Biolabs, Frankfurt a. M.
Chloroform	Roth, Karlsruhe
Complete protease inhibitor cocktail without EDTA	Roche, Penzberg
Coomassie brilliant blue R250	Serva Electrophoresis, Heidelberg
Dithiothreitol (DTT)	Roche, Penzberg
DNeasy plant mini kit	Qiagen, Hilden
dNTP-Mix	New England Biolabs
EDTA	Merck, Darmstadt
Ethanol	Merck, Darmstadt
Ethidium bromid solution (1%)	Fluka, Sigma-Aldrich, Taufkirchen
Acetic acid	Merck, Darmstadt
Falcon tubes (15 and 50 ml)	Greiner bio-one, Essen

Fluoresceine	Invitrogen, Karlsruhe
Gel Rite	Roth, Karlsruhe
Glucose	Roth, Karlsruhe
Glycerin 99,5%	Roth, Karlsruhe
Glycine	Applichem, Darmstadt
HEPES	Roth, Karlsruhe
Hybond N+ membrane	Amersham Biosciences, Freiburg
Imidazole	Sigma-Aldrich, Taufkirchen
Isopropanol	Mallinckrodt Baker, Griesheim
KCl	Merck, Darmstadt
KH ₂ PO ₄	Merck, Darmstadt
KOH	Mallinckrodt Baker, Griesheim
Lithium acetate	Roth, Karlsruhe
Methanol	J.T. Baker, Deventer Holland
[¹⁴ C]-Methylamine hydrochlorid	Hartmann Analytic GmbH, Braunschweig
Methylamine hydrochlorid	Sigma-Aldrich, Taufkirchen
Milk powder	Roth, Karlsruhe
NaCl	Mallinckrodt Baker, Griesheim
Na ₂ HPO ₄	Merck, Darmstadt
NaH ₂ PO ₄	Mallinckrodt Baker, Griesheim
dNTPs	NEB, Frankfurt a. M.
NucleoBond Maxi®	Macherey-Nagel, Düren
NucleoBond Midi®	Macherey-Nagel, Düren
NucleoSpin ExtractII®	Macherey-Nagel, Düren
NucleoSpin Plasmid®	Macherey-Nagel, Düren
Orange G	Sigma-Aldrich, Taufkirchen
Parafilm	Rechiney, Menasha
Petri dishes	Greiner bio-one, Essen
Phenole	Roth, Karlsruhe
Phusion Mastermix	New England Biolabs, Frankfurt a.M.
Plant DNeasy Kit	Qiagen, Hilden
Platinum SYBR Green qPCR SuperMixUDG	Invitrogen, Karlsruhe
PMSF	Roth, Karlsruhe
Poly ethylene glycol (PEG 3350)	Roth, Karlsruhe
Poly vinyl pyrrolidon (PVP)	Roth, Karlsruhe
Restriction enzym buffer (NEB1 bis 4)	New England Biolabs, Frankfurt a. M.
RNAse Zap	Ambion, Austin (USA)
Rotiphorese Gel 30 (acryl amid)	Roth, Karlsruhe
Sucrose	Sigma-Aldrich, Taufkirchen
SDS	Roth, Karlsruhe
Seakem LE Agarose	Biozym, Oldendorf
Sorbitol	Sigma-Aldrich, Taufkirchen
Steritop filter unit, 0.22 µM	Millipore GmbH, Schwalbach
Talon metal affinity granules	ClonTech, Mountain View (USA)
TriReagent	Ambion, Austin (USA)
Tris	Applichem, Darmstadt
Yeast nitrogen base without amino acids	Difco, USA-Detroit
Yeast nitrogen base without amino acids and ammonium sulphate	Difco, USA-Detroit

4.1.3 Enzymes

Big Dye Terminator Sequencing Mix v3.1	Applied Biosystems, Darmstadt
DNase I	New England Biolabs, Frankfurt a. M.
Phusion Polymerase	New England Biolabs, Frankfurt a. M.
Primary α GFP antibody, monoclonal, mouse	Roche, Penzberg
Proteinase K	Invitrogen, Karlsruhe
Restriction endonucleases	New England Biolabs, Frankfurt a. M.
RNase A	Sigma-Aldrich, Taufkirchen
Sekundary antibody α mouseIRDye800	Biomol, Hamburg
Secondary antibody α rabbit IgG HRP	Biomol, Hamburg
Secondary antibody α rabbit IgG Alexa 647	Biomol, Hamburg
T4 DNA Quick Ligase	New England Biolabs, Frankfurt a. M.
Taq Polymerase	New England Biolabs, Frankfurt a. M.

4.1.4 Buffers and solutions

All buffers were prepared with ultra pure water from the Ultra Clear UV plus water supply. Buffers and solutions were autoclaved or sterile filtered and listed in Table 3.

Table 3: For this work prepared and used buffers and solutions

Description	Components	Amount/Concentration
Adenine solution	Adenine sulphate H ₂ O	1 g Ad 1l
Agarose gel Loading buffer (10x)	Glycerin 99.5% TE buffer (pH8.0) Orange G	5 ml 5 ml 20 mg
Ammonium sulphate solution 1M	Ammonium sulphate H ₂ O	132 g Ad 1l
Basic medium (pH6.1) for BA medium	Magnesium sulphate Potassium dihydrogen phosphate Calcium chloride Sodium chloride Potassium sulphate Citrate Potassium hydroxide H ₂ O	0.7 g 1.0 g 0.4 g 0.5 g 1.0 g 10.5 g 9.03 g Ad 1l

Bradford solution	Biorad solution diluted 1:5 and filtered, store at 4°C	
Blocking solution (Western)	TBS-T Milk powder	100 ml 5 g
Citrate solution (1M)	Citric acid H ₂ O	192.4 g Ad 1l
Citrate buffer pH6 (10 mM)	1M Citrate solution 1M Na Citrate solution H ₂ O	0.9 ml 4.1 ml Ad 500 ml
Coomassie staining solution	Ethanol Acetic acid Coomassie brilliant blue R-250 powder H ₂ O Stirred over night and filtered	100 ml 100 ml 10 g Ad 1l
Coomassie destaining solution	Ethanol Acetic acid H ₂ O	100 ml 100 ml Ad 1l
Elution buffer pH7,5 for protein expression	NaH ₂ PO ₄ NaCl Imidazole Glycerin H ₂ O	0.3 g (50 mM) 0.43 g (150 mM) 0.85 g (250 mM) 10% (v/v) Ad 50 ml
Gel drying solution	Ethanol Glycerin H ₂ O	200 ml 20 ml Ad 1l
Glucose solution (50%)	Glucose H ₂ O	500 g Ad 1l
HC dropout mix (10x)	Methionine Tyrosine Isoleucine Phenylalanine Glutamate Lysine Threonine Aspartate Serine Arginine H ₂ O	0.8 g 2.4 g 3.2 g 2.0 g 4.0 g 9.6 g 8.0 g 4.0 g 16.0 g 0.8 g Ad 4l

Histidine solution	Histidine H ₂ O	10 g Ad 1l
KH ₂ PO ₄ solution (1M)	KH ₂ PO ₄ H ₂ O	136.1 g Ad 1l
Leucine solution	Leucine H ₂ O	20 g Ad 1l
Lysis buffer pH7.5 for protein extraction	NaH ₂ PO ₄ NaCl Glycerin H ₂ O	1.49 g (50 mM) 4.38 g (300 mM) 10% (v/v) Ad 250 ml
Micro elements solution for BA medium (1000x)	Stock solutions (100 ml): S1: 50 mg H ₃ BO ₃ S2: 100 mg CuCl S3: 100 mg KI S4: 100 mg Na ₂ MoO ₄ 2H ₂ O S5: 1,4 g ZnSO ₄ 7H ₂ O Citrate MnSO ₄ H ₂ O FeCl ₃ 6H ₂ O H ₂ O	1 ml 0.1 ml 0.2 ml 0.4 ml 0.1 ml 0.1 g 0.04 g 0.5 g Ad 100 ml
[¹⁴ C]-Methylamine-Hydrochlorid in water		0,75 mM
NaOH (0.2 M)	NaOH H ₂ O	8 g Ad 1l
Na ₂ HPO ₄ solution	Na ₂ HPO ₄ H ₂ O	142 g Ad 1l
Na citrate solution (1M)	(Na) ₃ Citrate H ₂ O	258.1 g Ad 1l
PEG solution (50%)	PEG 3350 H ₂ O	50 g Ad 100 ml
Phosphate buffer pH 6 (10 mM)	1M KH ₂ PO ₄ solution 1M Na ₂ HPO ₄ solution H ₂ O	8.77 ml 1.23 ml Ad 1l
Proline solution	Proline H ₂ O	10 g Ad 1l
Lithium acetate solution	Lithium acetate dihydrate H ₂ O	10.2 g Ad 100 ml
SB-Puffer (20x) Brody & Kern, 2004	NaOH H ₃ BO ₃ ddH ₂ O	8 g 45 g Ad 1l

SDS electrophoresis buffer (10x)	Tris Glycine SDS H ₂ O	25 mM 190 mM 10 g Ad 1l
SDS loading buffer	Tris-Hcl (pH6.8) Glycerin SDS β-mercapto ethanol Bromphenole blue	60 mM 25 % (m/v) 2 % (m/v) 14.4 mM In H ₂ O
Solution 1 for MSR medium	MgSO ₄ 7H ₂ O KNO ₃ KCl KH ₂ PO ₄ H ₂ O	73.9 g 7.6 g 6.5 g 0.41 g Ad 1l
Solution 1a including (NH ₄) ₂ SO ₄ for MSR medium (with 300 μM (NH ₄) ₂ SO ₄)	MgSO ₄ 7H ₂ O KNO ₃ KCl KH ₂ PO ₄ (NH ₄) ₂ SO ₄ H ₂ O	73.9 g 7.6 g 6.5 g 0.41 g 4 g Ad 1l
Solution 1b without nitrogen for MSR medium (with nitrate as sole nitrogen source)	MgSO ₄ 7H ₂ O KNO ₃ KCl KH ₂ PO ₄ (NH ₄) ₂ SO ₄ H ₂ O	73.9 g 0 g 6.5 g 0.41 g 0 g Ad 1l
Solution 1c with more (NH ₄) ₂ SO ₄ for MSR médium (with (NH ₄) ₂ SO ₄ as sole nitrogen source)	MgSO ₄ 7H ₂ O KNO ₃ KCl KH ₂ PO ₄ (NH ₄) ₂ SO ₄ H ₂ O	73.9 g 0 g 6.5 g 0.41 g 13 g Ad 1l
Solution 2 for MSR medium	Ca(NO ₃) ₂ x 4H ₂ O H ₂ O	35.9 g Ad 1l
Solution 2a with reduced nitrate for MSR medium	Ca(NO ₃) ₂ x 4H ₂ O H ₂ O	12 g Ad 1l
Solution 2b without nitrate for MSR medium	CaSO ₄ H ₂ O	2g Ad 1l

Solution 3 for MSR medium	Calcium panthotenate Biotin Nicotinic acid Pyridoxine Thiamine Cyano cobalamine H ₂ O	0.09 g 0.0001 g 0.1 g 0.09 g 0.1 g 0.04 g Ad 500 ml
Solution 4 for MSR medium	NaFeEDTA H ₂ O	0.16 g Ad 500 ml
Solution 5 for MSR medium	MnSO ₄ x 4H ₂ O ZnSO ₄ x 7H ₂ O H ₃ BO ₃ CuSO ₄ x 5H ₂ O Na ₂ MoO ₄ x 2H ₂ O (NH ₄) ₆ Mo ₇ O ₂₄ x 4H ₂ O ddH ₂ O	1.225 g 0.14 g 0.925 g 0.11 g 0.0012 g 0.017 g Ad 500 ml
Storage buffer pH7.5 for purified proteins	NaH ₂ PO ₄ NaCl DTT H ₂ O	1.49 g (50 mM) 4.38 g (300 mM) 0.037 g (1 mM) Ad 250 ml
Transfer buffer (Western)	Tris Glycine Ethanol	25 mM 190 mM 20 % (v/v) In H ₂ O
TBS buffer (Western)	Tris-HCl (pH7.5) NaCl	50 mM 150 mM In H ₂ O
TBS-T buffer (Western)	TBS buffer Tween20	99.9% (v/v) 0.1% (v/v)
TE buffer pH8	Tris Na ₂ -EDTA in H ₂ O pH8.0 adjusted with HCl	10 mM 1 mM In H ₂ O
Tris buffer pH6.8	Tris-HCl pH6.8 adjusted with HCl	1 M In ddH ₂ O
Tris buffer pH8.8	Tris-HCl pH 8,8 adjusted with HCl	1.5 M In ddH ₂ O
Tryptophan solution	Tryptophan H ₂ O Store in the dark	10 g Ad 1 l

Uracil solution	Uracil H ₂ O	1 g Ad 1l
Vitamin solution for BA medium (1000x)	Thiamin Calcium pantothenate Biotin Pyridoxine Inositol H ₂ O	100 mg 200 mg 250 µg 100 mg 1 g Ad 100 ml
YNB solution (without AA, 10x)	Bacto Yeast nitrogen base without amino acids	67 g In 1l H ₂ O
YNB solution (without AA and ammonium sulphate = YNB-N, 10x)	Bacto yeast nitrogen base without amino acids and ammonium sulphate	17 g In 1l H ₂ O

4.1.5 Media

Media usually were prepared from their single components and sterile filtered. They are listed in Table 4. For bacterial and yeast plate medium water was autoclaved together with agar and solutions were added later. For bacterial plates 1.4% agar and for yeast plates 2% agar were used. For MSR medium plates all components were added and autoclaved with the respective amount of Gel Rite.

Table 4: Media used in this study (end concentration in parentheses)

Medium	Rezept
YPAD (Amberg <i>et al.</i> , 2005)	10 g Bacto yeast extract (1%) 20 g Bacto peptone (2%) 20 g Glucose (2% m/v) 40 mg Adenine sulphate (0.004%) In 1l H ₂ O
HC-U medium (Amberg <i>et al.</i> , 2005)	40 ml Glucose solution (2%) 100 ml YNB-(without AA) solution (0.67% m/v) 100 ml 10x HC dropout solution 20 ml Adenine solution 8 ml Tryptophan solution 4 ml Leucine solution 2 ml Histidine solution H ₂ O ad 1l
SD-Medium (Amberg <i>et al.</i> , 2005)	100 ml YNB solution (without AA) (0.67% m/v) 40 ml Glucose solution (2 % m/v) H ₂ O ad 1l

SD-Medium without N (= Minimal medium, MM)	100 ml YNB solution (without AA and $(\text{NH}_4)_2\text{SO}_4$) (0.17% m/v) 40 ml Glucose solution (2% m/v) H ₂ O ad 1 l Complemented with respective amounts of 1 M $(\text{NH}_4)_2\text{SO}_4$ solution to the desired ammonium concentration
SD-Medium without N + 0,1% (m/v) proline + 50 mM methylamine	100 ml 10x YNB-N solution (0.17% m/v) 100 ml proline solution (0.1% m/v) 50 mM methylamine 40 ml Glucose solution (2% m/v) H ₂ O ad 1 l
BA medium (Jacobs <i>et al.</i> , 1980)	938 ml BA basic medium 1 ml mikco elements solution 1 ml vitamin solution 60 ml Glucose solution (3% m/v) nitrogen source as desired
LB medium (Sambrook & Russell, 2001)	5 g Bacto yeast extract 10 g Bacto tryptone 10 g NaCl H ₂ O ad 1l
dYT medium (Sambrook & Russell, 2001)	16 g Bacto tryptone 10 g Bacto yeast extract 5 g NaCl H ₂ O ad 1l
dYT/glycerin cryo medium (Sambrook & Russell, 2001)	16 g Bacto tryptone 10 g Bacto yeast extract 5 g NaCl 800 ml 87% glycerin H ₂ O ad 1l
MSR Medium (Fortin & Bécard, 2002; Declerck <i>et al.</i> , 2005) For the hyphal compartment sucrose was left out	10 ml solution 1 10 ml solution 2 5 ml solution 3 5 ml solution 4 1 ml solution 5 10 g sucrose 3 g Gel Rite H ₂ O ad 1l

The classical MSR medium was modified for different purposes and different nitrogen sources and amounts in the following way. Media called MSR a, MSR b and MSR c with the nutrient compositions of Table 5 were developed. They were setup as shown in Table 6.

Table 5: Nutrient compositions of MSR medium variants. Concentrations in μM are given.

	MSR	MSR a	MSR b	MSR c
NO ₃	3800	3800	1000	0
NH ₄	0.18	300	0.18	1000
P	30	30	30	30
K	1650	1650	900	900
Ca	1520	1520	1000	1000
Mg	3000	3000	3000	3000
S	3013	3163	3663	4163
Cl	870	870	870	870
				μM

Table 6: MSR medium variants and their composition by the different solutions from Table 3. Their proportion is given in %

	MSR medium	Medium a	Medium b	Medium c
Solution 1	1%			
Solution 1a		1%		
Solution 1b			1%	
Solution 1c				1%
Solution 2	1%			
Solution 2a		3%	1%	
Solution 2b			3.4%	6.8%
Solution 3	0.5%	0.5%	0.5%	0.5%
Solution 4	0.5%	0.5%	0.5%	0.5%
Solution 5	0.1%	0.1%	0.1%	0.1%

4.1.7 Oligo nucleotides used in this study

Oligo nucleotides were designed using the Primer3plus web interface (<http://www.bioinformatics.nl/cgi-bin/primer3plus/primer3plus.cgi/>; Rozen & Skaletsky, 2000) and ordered at Sigma-Aldrich (Taufkirchen, Germany) or Metabion (Martinsried, Germany). The used primers are listed in Table 7.

Table 7: Oligo nucleotides used in this study

Primer name	Sequence (5'-3') ^a	Application
PMA5	CTCTCTTTTATACACACATTTC	Primer in backbone of pDR196sfi (Schübler <i>et al.</i> , 2006)
ADHclose	AATACGACTCACTATAGG	Primer in backbone of pDR196sfi (Schübler <i>et al.</i> , 2006)
GpyrAMT2-FWD1	CATATATTGGCAATTTAAGGAATG	Amplification of GpyrAMT2 3' fragment
GpyrAMT2-FWD2	GGCAATTTAAGGAATGCTTTCC	Nested to GpyrAMT2-FWD1
GpyrAMT2-REV1	TCAACAGGACCACCACCGGC	Amplification of GpyrAMT2 5' fragment
GpyrAMT2-REV2	ATTTCAACAGGACCACCACC	Nested to GpyrAMT2-REV1
PMA16FWD	CGGGCTGCAGGAATTCGG	Nested to PMA5
ADH109REV	CGACTCACTATAGGGCG	Nested to ADHclose
GpyrAMT2-REV3	CCAAATGCAATAGAAGATGAGG	Nested to GpyrAMT2-REV1
GpyrAMT2-REV4	GCAATGGCACCACACAGAATCCG	Nested to GpyrAMT2-REV1
GpyrAMT2-REV5	GGTCTTCTTGATGTCGCTTTCC	Nested to GpyrAMT2-REV1
GpyrAMT2-REV6	GACCTCGCTCTGCAGCCGAACC	Nested to GpyrAMT2-REV1
GpyrAMT2-5'UTR-FWD	GGGAAACCTAAAGTATTCTGCC	Amplification of GpyrAMT2 cDNA
GpyrAMT2-3'UTR-REV	CTGGGGAACATATGATAATCATTC	Amplification of GpyrAMT2 cDNA
GpyrAMT1-5'UTR-FWD	TTTTGAAATTTGCTCGGTGCC	Amplification of GpAMT1
GpyrAMT1-3'UTR-REV	AGTTTAAATTTCCCTTGGGTTT	Amplification of GpAMT1
X-S-EGFP-FWD	GGACTCGAGTAACACGGCCCGCTCGCCATGGTGAGCAAGGGCG AGG	Amplification of EGFP for cloning into pDR196
EGFP-A-REV	CATGGGCCCTTACTTGTACAGCTCGTCCATGCC	Amplification of EGFP for cloning into pDR196
GpyrAMT2-sfi-FWD	CCAGGCCATTACGGCCTACAAAATGGGCCATTATAATTC	Amplification and cloning of GpyrAMT2
GpyrAMT2-sfi-tag-REV	GATGGCCGAGGCGGCC GAATTTTCCTTGAAAGCACTCGA CAAGGCCATTACGGCCTACAAA ATGGCTTCGATAAATTC	Amplification and cloning of GpyrAMT2 without STOP
GpyrAMT1-sfi-FWD	GATGGCCGAGGCGGCC GAAAGAGACGGTTGCTGAAAGTCT CAAGGCCATTACGGCCTACAAA ATGGAGAGTCGAACTAC	Amplification and cloning of GpAMT1
GpyrAMT1-sfi-tag-REV	GATGGCCGAGGCGGCC GAAAGAGACGGTTGCTGAAAGTCT CAAGGCCATTACGGCCTACAAA ATGGAGAGTCGAACTAC	Amplification and cloning of GpAMT1 without STOP
ScMEP1-sfi-FWD	GATGGCCGAGGCGGCC GACCTATTGGCAGGATCTTCTTG	Amplification and cloning of ScMEP1
ScMEP1-sfi-tag-REV	GATGGCCGAGGCGGCC GACCTATTGGCAGGATCTTCTTG	Amplification and cloning of ScMEP1 without STOP
ORF-FWD	CGGCCACAAAATGTCGGCCGCT	Construction of the GFP negative control
ORF-REV	CGGCCGACATTTGTAGGCCGTAA	Construction of the GFP negative control
GpyrAMT1-REV	CAAAGCATCCATGTAATCCCAC	Sequencing of GpAMT1
GpyrAMT2-FWD-SEQ	GGAAATCTCGATTTTGTCTGGTGG	Sequencing of GpAMT2
GintAMT1-FWD	ATGCTGCTCCTCCGCTGCTGC	Sequencing of GintAMT1
GintAMT1-REV	TTATACAATTTGTGCATTTGCGTCAATTTG	Sequencing of GintAMT1
GintAMT1-539-FWD	CATGGAATCTTAATGGTTGGTCCGC	Sequencing of GintAMT1
GintAMT1-811-REV	GCTGATAAATTGGTTACAGCGATAGCC	Sequencing of GintAMT1
GintAMT1-290-REV	GCTAAACTGAAACCGATAGCCC	Sequencing of GintAMT1
GintAMT1-1136-FWD	CTGGAGGTGGCTTAATCAACATTG	Sequencing of GintAMT1
Gint-BTub1-FWD	GGCGATCTCAACAATTTGG	qPCR
Gint-BTub1-REV	CCCATATTGACAGCCAATTTTC	qPCR
Gint-rDNA-LSU-FWD	AGACCGATAGCGAACAAGTACC	qPCR
Gint-rDNA-LSU-REV	GACTGGCTCAATCGTTTC	qPCR
GintAMT1-405-REV	TGAATTGATACTACAGCCAAGGA	Sequencing of GintAMT1
GintAMT1-156-FWD	CTGCTGCAGAACCTAATCCA CCAGGCCATTACGGCCAAC ATGCTGCTCCTCCGCTGCTGC CCTAGGCCGAGGCGGCC	Sequencing of GintAMT1
GintAMT1-sfi-FWD	TTATACAATTTGTGCATTTGCGTCAATTTG	Amplification and cloning of GintAMT1
GintAMT1-sfi-REV	TTATACAATTTGTGCATTTGCGTCAATTTG	Amplification and cloning of GintAMT1
GintAMT3-FWD	CGAGTGGATATGCTCACCTCCGCTC	RACE for GintAMT3
GintAMT3-REV	AGCGTGTTCGGCTACACCTCCTACTG	RACE for GintAMT3
GintAMT3-FWD-nested	CACCTCCGCTCTGTAATTTTGG	RACE for GintAMT3
GintAMT3-REV-nested	TCCTACTGCATGAACAGCAAAAACA CCTAGGCCGAGGCGGCC TTAGCGTCCATTATGAAGAGGATAATGTAAG	RACE for GintAMT3
GpyrAMT2-D75-REV	TTAGCGTCCATTATGAAGAGGATAATGTAAG	Tranquating GpyrAMT2's c-Term by 75 AA

GpyrAMT2-D33-REV	<u>CCTAGGCCGAGGCGGCC</u> <u>TTAACGTTGCGTTCGTATTCAATAGAATTAC</u>	Tranquating GpyrAMT2's c-Term by 33 AA
GpyrAMT2-sfi-FWD2	<u>CCAGGCCATTACGGCCAAC</u> <u>ATGGCCGATTATAATTC</u>	Cloning of GpyrAMT2 Fwd Primer with different Kozak sequence
GpyrAMT1-sfi-FWD2	<u>CAAGGCCATTACGGCCAAC</u> <u>ATGGCTTCGATAAATTCGATATATTTTCG</u>	Cloning of GpyrAMT1 Fwd Primer with different Kozak sequence
GpyrAMT1-sfi-REV	<u>GATGGCCGAGGCGGCC</u> <u>TTAAAGAGACGGTTGCTGAAGTCT</u>	Cloning of GpyrAMT1 Rev Primer
GpyrAMT2-sfi-REV	<u>GATGGCCGAGGCGGCC</u> <u>TTAATTTTCCTTGAAAGCACTCGA</u>	Cloning of GpyrAMT2 Rev Primer
GintAMT3-REV2	<u>CGCCTCTAACATTTCATGAAGAATGC</u>	Genome Walking GintAMT3
uni24	<u>ACGACGTTGTAAAAAGACGGCCAG</u>	Sequencing of TOPO vectors (Brachmann <i>et al.</i> , 2001)
rev24	<u>TTCACACAGGAAACAGCTATGACC</u> <u>CCTAGGCCGAGGCGGCCG</u> <u>AACTAAGTATATATTGATTAGTGC</u>	Sequencing of TOPO vectors (Brachmann <i>et al.</i> , 2001)
GintAMT2-GFP-REV	<u>CCTAGGCCGAGGCGGCCG</u> <u>AAGAATAATGTATATGATCAATTGATTG</u>	Cloning GintAMT2 to GFP
GintAMT3-GFP-REV	<u>CCTAGGCCGAGGCGGCCG</u> <u>ATACAATTGTTGCATTTGCGTCATTTTG</u>	Cloning GintAMT3 to GFP
GintAMT1-GFP-REV	<u>CCTAGGCCGAGGCGGCCG</u> <u>ATACAATTGTTGCATTTGCGTCATTTTG</u>	Cloning GintAMT1 to GFP
gScMEP2_rev	<u>AGATGCTGTATATTATAGTGTGCACAG</u>	amplification and sequencing of the mep2 locus
gScMEP3_fwd	<u>CTTGTTAGAATAAGGTTGTGTGC</u>	amplification and sequencing of the mep3 locus
gScMEP3_rev	<u>GGCATATAGAATGGTGAGTAAAAA</u>	amplification and sequencing of the mep3 locus
gScMEP2_fwd	<u>CATTCCGAGCCACTTTTCTGC</u>	amplification and sequencing of the mep2 locus
GpyrAMT3_clone_Fwd	<u>CGGTTGGTTGGATTTAACG</u>	Amplification of GpyrAMT3 3' part
GpyrAMT3_clone_Rev	<u>CCCAGCAAGGAAACCAAATA</u> <u>CAAGCCATTACGGCCAAC</u>	Amplification of GpyrAMT3 5' part
GpyrAMT3_sfi_Fwd	<u>ATGGATTCTGTGGAAGATACGAATG</u> <u>GATGGCCGAGGCGGCC</u> <u>TTAAAAATGAGCAAATGTTCTTTCCG</u>	Amplification and cloning of GpyrAMT3
GpyrAMT3_sfi_rev	<u>CACAATGGATTCTGTGGAAGATACG</u>	Amplification and cloning of GpyrAMT3
GpyrAMT3_gen_fwd	<u>CAGAGCACAAAAATTTGCATTATTGCC</u>	Amplification of GpyrAMT3 genomic sequence
GpyrAMT3_gen_rev	<u>GGCTAACAGGCGACGGTTCATTTG</u>	Amplification of GpyrAMT3 genomic sequence
GpyrAMT3_331_rev	<u>GGCTAACAGGCGACGGTTCATTTG</u>	Sequencing of GpyrAMT3
GpyrAMT3_523_fwd	<u>ATGGGTGCTATCGATTTTGC</u>	Sequencing of GpyrAMT3
GpyrAMT3_695_rev	<u>AACCAACCGAACACATCAT</u>	Sequencing of GpyrAMT3
GpyrAMT3_1108_fwd	<u>GACCATCATTGGGAGCAAGT</u>	Sequencing of GpyrAMT3
GpyrAMT3_1341_rev	<u>TCGTAACCTCCCAAGTTCCAG</u>	Sequencing of GpyrAMT3
GpyrAMT1-StoC-FWD	<u>GTTTCATATGGCATGTGGAGCTGCTGCACTCG</u>	Mutation S ₁₇₃ C in GpyrAMT1
GpyrAMT1-StoC-REV	<u>CGAGTGCAGCAGCTCCACATGCCATATGAAC</u>	Mutation S ₁₇₃ C in GpyrAMT1
GpyrAMT2-CtoS-FWD	<u>GTACACATTTCTTCCGGAGCTGCTGTTTAG</u>	Mutation C ₁₇₈ S in GpyrAMT2
GpyrAMT2-CtoS-REV	<u>CTAAGCAGCAGCTCCGGAAGAAATGTGTAC</u>	Mutation C ₁₇₈ S in GpyrAMT2
GpyrAMT3 CtoS Fwd	<u>CTGTTTCATATTTCTTCCGGAGCTTCTGCAC</u>	Mutation C ₁₈₉ S in GpyrAMT3
GpyrAMT3 CtoS Rev	<u>GTGCAGAAGCTCCGGAAGAAATATGAACAG</u>	Mutation C ₁₈₉ S in GpyrAMT3
gGpyrAMT3 CtoS Fwd	<u>CTGTTTCATATTTCTTCCGGAGCTGCTGCAC</u>	Mutation C ₁₈₉ S in gGpyrAMT3
gGpyrAMT3 CtoS Rev	<u>GTGCAGCAGCTCCGGAAGAAATATGAACAG</u>	Mutation C ₁₈₉ S in gGpyrAMT3
GpyrAMT3_GFP_rev	<u>CCTAGGCCGAGGCGGCC</u> <u>AAAAATGAGCAAATGTTCTTTCCG</u>	Amplification and cloning of GpyrAMT3 without STOP
GintAMT1-Texasred-FWD	<u>TCGGTTTCAGTTTAGCATTTCG</u>	<i>In-situ</i> -PCR
GintAMT1-Texasred-REV	<u>AACCATTAAAGATTCCATGTCC</u>	<i>In-situ</i> -PCR
GintAMT3-Texasred-FWD	<u>ATCGCTTGTGGATTGGTTCG</u>	<i>In-situ</i> -PCR
GintAMT3-Texasred-REV	<u>TGCTGCTCTAGTATTGCTGCC</u>	<i>In-situ</i> -PCR
GintAMT2-Texasred-FWD	<u>AATGTTTGTTCAGTTACACC</u>	<i>In-situ</i> -PCR
GintAMT2-Texasred-REV	<u>GCCTAATTGTGCATACCATCC</u>	<i>In-situ</i> -PCR

^a Overhangs are underlined

4.1.8 Plasmids used in this study

Plasmid vectors used in this study are listed in Table 8. Intermediate plasmids for sequencing into TOPO vectors (Zero Blunt for sequencing, Invitrogen, Karlsruhe, Germany) are not mentioned.

Table 8: Plasmids used in this study

Plasmid	Backbone	Insert	Reference
pDR196sfi	pDR196	SfiI restriction sites	Schüßler <i>et al.</i> , 2006
pRU4		<i>EGFP</i>	Brachmann <i>et al.</i> , 2001
pBL101	pDR196sfi	<i>GpyrAMT1</i> with UTRs	This study
pBL102	pDR196sfi	<i>GpyrAMT2</i> with UTRs	This study
pBL103	pDR196sfi	<i>ScMEP1</i>	This study
pBL104	pDR196sfi	<i>ScMEP2</i>	This study
pBL105	pDR196sfi	<i>ScMEP3</i>	This study
pBL106	pDR196sfi	<i>GFP</i>	This study
pBL107	pDR196sfi	<i>GpyrAMT1-GFP</i>	This study
pBL108	pDR196sfi	<i>GpyrAMT2-GFP</i>	This study
pBL109	pDR196sfi	<i>ScMEP1-GFP</i>	This study
pBL110	pDR196sfi	<i>GpyrAMT1</i> ORF	This study
pBL111	pDR196sfi	<i>GpyrAMT2</i> ORF	This study
pBL112	pDR196sfi	<i>GpyrAMT2</i> $\Delta 33$ AA	This study
pBL113	pDR196sfi	<i>GpyrAMT2</i> $\Delta 75$ AA	This study
pBL130	pDR196sfi	<i>GpyrAMT1_S173C</i>	This study
pBL131	pDR196sfi	<i>GpyrAMT2_C178S</i>	This study
pBL134	pDR196sfi	<i>ScMEP2_S197C</i>	This study
pBL151	pDR196sfi	<i>GintAMT1</i>	This study
pBL152	pDR196sfi	<i>GintAMT3</i>	This study
pBL153	pDR196sfi	<i>GintAMT2</i>	This study
pBL154	pDR196sfi	<i>GintAMT1-GFP</i>	This study
pBL155	pDR196sfi	<i>GintAMT3-GFP</i>	This study
pBL156	pDR196sfi	<i>GintAMT2-GFP</i>	This study
pBL179	pDR196sfi	<i>GpyrAMT3</i> with UTRs	This study
pBL180	pDR196sfi	<i>cGpyrAMT3</i>	This study
pBL181	pDR196sfi	<i>cGpyrAMT3_C189S</i>	This study
pBL183	pDR196sfi	<i>gGpyrAMT3</i>	This study
pBL184	pDR196sfi	<i>gGpyrAMT3_C189S_A192S</i>	This study
pBL185	pDR196sfi	<i>gGpyrAMT3_C189S</i>	This study
pBL186	pDR196sfi	<i>gGpyrAMT3-GFP</i>	This study

4.2 Methods

4.2.1 Strains and Cultivations

Yeast strains

Mainly the *S. cerevisiae* strain Δ mep1-3 strain MLY131a/ α was used (genotype Mata/Mata mep1 Δ ::LEU2/mep1 Δ ::LEU2 mep2 Δ ::LEU2/ mep2 Δ ::LEU2 mep3 Δ ::G418R/mep3 Δ ::G418R ura3-52/ura3-52, Lorenz & Heitman, 1998a).

With this strain the complementation assays were performed (Ellerbeck, 2008; Ellerbeck, 2009).

It was cultivated on YPAD medium. After transformation with variants of the plasmid pDR196sfi it got prototroph and was cultured on HC-U medium lacking uracil. For characterization experiments it was grown in minimal medium without any nitrogen source despite the one mentioned in the experimental description ((NH₄)₂SO₄, NH₄Cl or proline).

Bacterial strains

For cloning and multiplication of plasmids *Escherichia coli* Top10 was used. Its genotype is F-; mcrA; Δ (mrr-hsdRMS-mcrBC); ϕ 80lacZ Δ M15; Δ lacX74; recA1; araD139; Δ (araleu)7697; galU; galK; rpsL(StrR); endA1; nupG; λ -

For selection for transformed organisms they were plated on LB medium complemented with respective antibiotics (mostly ampicillin, 100 μ g/ml).

For protein expression the strain *E. coli* Rosetta DE3 pLaql (Novagen) with the genotype F-, ompT, hsdSB(rB-mB-),gal, dcm (DE3) pLacIRARE (CmR) was used. It carries an additional plasmids encoding tRNA genes and a chloramphenicol resistance gene. This strain was cultivated on plates containing 100 μ g/ml ampicillin and 34 μ g/ml chloramphenicol.

Rhizophagus irregularis

The AM fungus *R. irregularis* DAOM 197198, Biosystematic Research Center, Ottawa, Canada (Chabot *et al.*, 1992) was cultivated in *in vitro* root organ culture with *A. rhizogenes* transformed *C. intybus* roots (Fontaine *et al.*, 2004). Culture was continued in the beginning by cutting the colonized roots into pieces and transferring them onto the root compartments (containing sugar) of new plates (Fortin & Bécard, 2002). However, a sophisticated new cultivation method including a liquid culturing step was developed (see results).

4.2.2 Molecular biological methods

DNA extractions

Genomic DNA from *R. irregularis* was extracted from ~1 million spores with a Plant-DNA-extraction-kit (Macherey & Nagel) following the manufacturer's protocol. DNA was resuspended in TE buffer and yield was estimated using the Nanodrop machine (Thermo Scientific).

Plasmid DNA from *E. coli* was extracted using either NucleoSpin Plasmid columns (Machery & Nagel) or GeneJet Plasmid Miniprep columns (Fermentas) following the manufacturer's protocol. Yield was estimated with the Nanodrop machine.

For larger amounts NucleoBond Midi or Maxi columns (Machery & Nagel) were used following the manufacturer's protocol.

Plasmid DNA from *S. cerevisiae* was extracted as formerly described (Dafinger, 2008; Ellerbeck, 2009). Cells of 2 ml over night culture were disrupted with glass beads and DNA was extracted using yeast mini-solution (2 % Triton X-100, 1% SDS, 100 mM NaCl, 10 mM Tris-HCl (pH 8,0), 1mM Na₂EDTA) followed by an isopropanol precipitation:

1. 2 ml yeast overnight cultures were spun down for 5 minutes at 3000 rcf.
2. 0.3 ml glass beads (Ø 0.3 mm) and 0.7 ml Yeast Mini Solution were added.
3. Yeast cells were lysed in a bead mill for 2 minutes at maximum speed.
4. Centrifugation for 3 minutes at 13000 rcf. 500 µl supernatant and 500 µl ice-cold isopropanol were mixed in a new 1.5 ml tube and incubated for 20 minutes at room temperature.
5. DNA was pelleted by centrifugation for 15 minutes at 20000 rcf and washed with 500 µl 70% Ethanol. Supernatant was removed and pellet dried.
6. DNA was resuspended in 20 µl H₂O.

Polymerase chain reactions (PCR)

PCRs for cloning were carried out with phusion polymerase (Finnzymes) following the manufacturer's protocol (in 20 µl instead of 50 µl, standard setup see below). Annealing temperature for oligonucleotides was calculated with OligoCalc (Kibbe, 2007). For oligonucleotides used see table 7.

Colony PCRs were performed with Taq polymerase (New England Biolabs) following the manufacturer's protocol in 10 µl. Colonies were picked with a sterile white pipette tip and transferred to a selective master plate before a as small as possible amount of cells was transferred directly to the PCR mix.

Phusion Standard Setup and Cycling Conditions:

Phusion Polymerase	(2 u/μl)	0.2 μl
5x Phusion Buffer HF	(1x)	4 μl
dNTPs	(10 mM)	0.4 μl
Primers	(0.5 μM each)	1 μl
Template DNA	1-250 ng	
H2O		ad 50 μl

98°C|30sec–[98°C|10sec – 55°C|30sec – 72°C|45sec] x 35 – 72°C|7min – 12°C|∞

Taq Standard Setup and Cycling Conditions:

Taq Polymerase	(5 U/μl)	0.1 μl
10x Taq Standard Buffer	(1x)	2 μl
dNTPs	(10 mM)	0.4 μl
Primers	(0.5 μM each)	1 μl
Template DNA	1-250 ng	
H2O		ad 50 μl

95°C|3min – [95°C|30sec – 55°C|30sec – 72°C|1min] x 35 – 72°C|7min – 12°C|∞

Primer annealing temperatures and elongation time were adapted to each reaction. For Phusion Polymerase 30 seconds per kb were estimated, for Taq Polymerase one minute per kb.

Gel Electrophoresis

SeaKem LE Agarose (Biozym) in SB or TAE buffer was used in different concentrations depending on the expected fragment size, usually 1% was chosen. Voltage ranged from 2 V/cm to 9 V/cm ,

Gels were run until the band of interest had past approximately 50%-60% of the gel.

4 μl or 5 μl NEB “100bp Ladder”, “1kb Ladder” or “2-log ladder” were used as standards. Normally, for analytic gels 100 ng DNA, for preparative gels as much DNA as possible were used. Whenever DNA concentrations were unknown 5 μl-10 μl were used.

Ethidium bromid (0.5 μg/ml) served as DNA staining agent and bands were detected and pictures taken under UV-light (darkroom hood by Herolab).

Recovery of DNA from Agarose Gels

DNA bands were excised from gels and purified with NucleoSpin Extract II (Macherey & Nagel) following the manufacturer’s protocol.

DNA Quantification

DNA concentration was determined by photospectroscopy (absorbance at 260 nm) using NanoDrop by PEQLAB.

Restriction Digestion Reactions

Enzymes and corresponding buffers by New England Biolabs were used according to the manufacturer's protocol:

Enzyme (different concentrations)	2-20 U
10x NEB Buffer	1x
100x BSA (10 mg/ml)	1x
DNA	500 ng to 1 µg
H ₂ O	ad 20 µl (analytic) ad 30 µl (preparative)

Incubation for one hour or over night at the indicated temperature, in most cases 37°C.

Dephosphorylation of DNA ends

Antarctic phosphatase (CIP) by New England Biolabs was used to remove 5'-phosphates in order to prevent religation of linearized plasmids. 1 u phosphatase per 1 µg DNA was added directly to the digestion reaction mixture and incubated for 1 h at 37°C. DNA was purified afterwards with NucleoSpin Extract II (Macherey-Nagel).

DNA Purification

DNA from PCR or digestion reactions was purified with NucleoSpin Extract II (Macherey-Nagel) following the manufacturer's protocol or performing a standard sodium acetate ethanol precipitation:

1. Sample was adjusted to 0.3 M sodium acetate by adding 1/10 volume of 3 M sodium acetate
2. 2.5 volumes Ethanol were added. 10 minutes incubation on ice.
3. Centrifugation for 15 minutes at 20000 rcf.
4. DNA pellet was washed in 70% Ethanol.
5. DNA was resuspended in 20 – 30 µl H₂O

Cloning and Ligation Reactions

For subcloning of PCR-products Zero Blunt TOPO PCR Cloning Kit (Invitrogen) was utilized following the manufacturer's protocol (devided by 4):

TOPO vector	0.25 µl
Salt Solution (0.06 M MgCl, 1.2 M NaCl)	0.25 µl
PCR product	1 µl

Incubation at room temperature for 5 minutes was followed by transformation into *E. coli* with the transformation mix.

In all other cases ligation reactions were performed with Quick Ligation Kit (NEB, protocol also devided by 4):

12.5 ng of vector backbone were mixed with a 3-fold molar excess of insert and adjusted to a total volume of 10 µl with H₂O. 10 µl of 2x Quick Ligation Buffer and 1 µl

of Quick T4 DNA Ligase were added. After 5 min incubation at room temperature direct transformation into E.coli strain TOP10.

E. coli Transformation

1. TOPO-cloning reaction mixture or ligation mix was added to 25 μ l or 50 μ l competent cells.
2. Incubation for 15 min on ice.
3. Heat shock at 42°C for 45 sec.
4. Incubation for 2 min on ice.
5. 120 dYT- or SOC-medium were added.
6. Incubation at 37°C for 30 minutes.
7. Cell suspension was plated on appropriate selection plates.
8. Incubation over night at 37°C.

Yeast Transformation

Two different protocols were used (Gietz & Schiestl, 2007a; Gietz & Schiestl, 2007b). The “High Efficiency Transformation” method was used whenever high numbers of transformants were needed or with difficult plasmids:

1. 5 ml YPAD were inoculated with yeast and incubated over night at 30°C and 240 rpm.
2. In a total volume of 50 ml YPAD, OD₆₀₀ was adjusted to 0.5 (~5x10⁶ cells/ml).
3. Cell suspension was incubated for c. 4 hours at 30°C and 180 rpm until cell titer had reached 2x10⁷ cells/ml.
4. Cells were harvested by centrifugation at 3000g for 6 min, then washed twice with 25 ml H₂O and resuspended in 1 ml H₂O.
5. Cell suspension was transferred to a 1.5 ml tube and centrifuged for 30 sec at 13000 rcf. Supernatant was discarded and H₂O was added to a final volume of 1ml.
6. For each transformation 100 μ l of this cell suspension were put in a 1.5 ml tube and centrifuged for 30 sec at 13000 rcf. Supernatant was removed.
7. The following transformation mix was added and the cell pellet resuspended (in brackets the stock solution concentration is given):

PEG 3350	(50% w/v)	240 μ l
LiAc	(1.0 M)	36 μ l
Boiled SS-carrier DNA (2 mg/ml)		50 μ l
Plasmid DNA plus Water		34 μ l
8. Incubation for 20-40 min at 42°C.
9. Centrifugation for 30 sec at 13000 rcf, supernatant was thoroughly removed.
10. One ml H₂O was added, the pellet resuspended and appropriate dilutions of the cell suspension were plated on selection media lacking uracil.
11. Incubation for 2 – 4 days at 30°C.

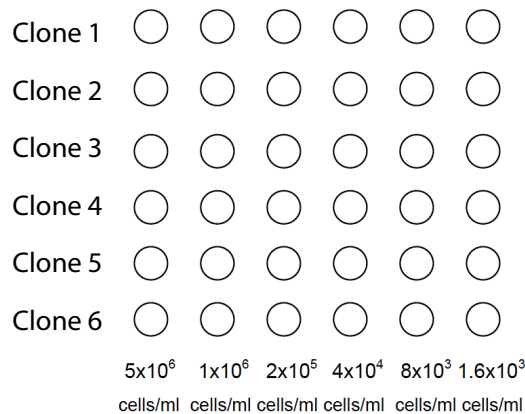
The “Quick and easy TRAF0 Protocol” was used whenever high transformation efficiency was not needed and/or easy plasmids were to be transformed:

1. 50 µl cells were scratched from plates and suspended in 1 ml H₂O.
2. Centrifugation for 30 sec at 13000 rcf, supernatant was removed.
3. The following Transformation Mix was added and the cell pellet resuspended:

PEG 3350	(50% w/v)	240 µl
LiAc	(1.0 M)	36 µl
Boiled SS-carrier DNA (2mg/ml)		50 µl
Plasmid DNA plus H ₂ O		34 µl
4. Incubation for 20 min at 42°C.
5. Centrifugation for 30 sec at 13000 rcf, supernatant was thoroughly removed.
6. One ml H₂O was added, the pellet resuspended and appropriate dilutions of the cell suspension were plated on selective media lacking uracil.
7. Incubation for 2 – 4 days at 30°C.

Yeast Dilution series

Yeast overnight cultures were adjusted to an OD₆₀₀ = 0.5 (5x10⁶ cells/ml). In six rows this cell suspension was diluted five times 1:5 following the scheme below:



With a 36-pinned stamp the dilutions of the six clones were transferred to different plates containing defined amounts of NH₄⁺ and HC-U as well as YPAD-plates. We calculated that each pin transferred about 2 µl, resulting in spreading of c. 3 cells in the highest dilution. Plates were incubated for indicated time periods at 30°C.

Sequencing

Sequencing reactions were performed using the Short BigDye Sequencing protocol for ABI 3730 provided by the Sequencing Service of the Department of Biology, LMU.

DNA Template	10 - 1000 ng
Sequencing Primer	3.2 pmol
H ₂ O	ad 7 µl

The cycling, cleaning and sequencing was done by the Sequencing Service of the department of biology, LMU, using an ABI 3730 (Applied Biosystems).

4.2.3 Biochemical methods

Methylammonium uptake assays

Methylammonium (MA) uptake assays were performed according to former protocols (Marini *et al.*, 1997; López-Pedrosa *et al.*, 2006). In brief, yeast cells expressing one of the investigated AMTs from the plasmid pDR196sfi were grown over night to an optical density (OD₆₀₀) of 0.5 to 0.7 in minimal medium without nitrogen (SD-N medium), containing 0.1% (w/v) of proline as sole nitrogen source, washed and concentrated to an optical density of 8 in phosphate buffer, pH6 or pH7, and stored on ice. Before addition of MA, cells were energized by addition of 0.1M glucose for 10 minutes and then incubated with varying MA concentrations for 30, 60, 120 and 240 seconds at 30° and 1000 rpm in an Eppendorf thermo shaker. Afterwards the cells were washed with 5 ml ice-cold phosphate buffer (20 mM), pH6 or pH7, respectively, containing 100 mM unlabeled MA once and with 5 ml sole ice-cold phosphate buffer twice, collected on a whatman filter and hydrolyzed in scintillation liquid. Radioactivity was measured by scintillation counting. From the number of disintegrations per minute (DPM) the amount of taken up MA in nmol per 10⁸ cells and minute was calculated.

Ammonium removal assays

Ammonium removal assays were performed as formerly described (Neuhäuser *et al.*, 2011). In brief, yeast cells expressing one of the investigated AMTs from the plasmid pDR196sfi were grown over night to an optical density of 0.5 to 0.7 in minimal medium without nitrogen (SD-N medium), containing 0.1% (w/v) of proline as sole nitrogen source, washed and concentrated to an optical density (OD₆₀₀) of 2 in 20 ml of SD medium containing 1 mM NH₄Cl as sole nitrogen source. After 0, 10, 30, 60, 120, 180, 240, 300 and 360 minutes 1 ml samples were taken, cells were pelleted (13,000 g, 30 seconds) and 40 µl of the supernatant were added to 760 µl OPA solution (containing 10% ethanol, 0.2 M NaPO₄-buffer pH7.3, 540 mg orthophthaldialdehyde [OPA] and 0.05% β-mercapto ethanol), incubated in the dark for 25 minutes and OD₄₃₀ was estimated with a photometer. The system was calibrated with SD-N containing 0 to 2

mM NH₄Cl to calculate the residual NH₄⁺ ions in the supernatant. Removal of ammonium was calculated over time and displayed in μmol per 2 x 10⁷ cells and hour.

Immune localizations

Immune localization was performed as formerly described (Perez-Tienda *et al.*, 2011). In brief, freshly harvested extraradical mycelium from the hyphal compartment of a ROC plate was fixed in 4% (w/v) paraformaldehyde in PBS, pH 7.3. After vacuum infiltration, fixation was performed overnight at 4 °C. The fixed samples were hand sectioned using a razor blade. Sections were washed three times in PBS and left to dry onto APTES (Sigma)-coated 8-well slides for 1 h at room temperature. After fixation, samples were firstly dried by dehydration–rehydration through a graded series of methanol (5 min each at 30%, 50%, 70% and 100% methanol in PBS, and 70%, 50%, 30% and 0% methanol in PBS, pH7.3). A permeabilization step was performed by partial digestion of the fungal cell walls with 0.05 U chitinase from *Streptomyces griseus* (Sigma) in 30 μl PBS, pH7.3, for 30 minutes at 37 °C. After digestion, samples were treated with 0.3% (v/v) Triton X-100 in PBS, pH7.3, at 37 °C for 10 minutes, washed three times with PBS, pH7.3 (5 minutes each), and blocked with 5% (w/v) BSA in PBS, pH7.3, at room temperature for 30 minutes. The slides were incubated for 1 hour at 37 °C in a humid chamber with the affinity purified antinodies (1:200 in PBS, pH7.3, containing 1% BSA). After three washes with 1% (w/v) BSA in PBS, pH7.3, (5 minutes each) and blocking with 5% (w/v) BSA in PBS, pH7.3, at room temperature for 10 minutes, slides were exposed to the secondary antibody (Alexa Fluor 647 anti-rabbit IgG; Sigma) applied 1:500 in PBS, pH7.3, for 45 minutes at room temperature in the dark. After five more washings in PBS, pH7.3, (5 minutes each), samples were incubated in 0.05 mg/ml WGA conjugated to Alexa Fluor 488 (Molecular Probes) in PBS, pH7.3, for 30 minutes at room temperature in the dark to stain the residual fungal cell wall. Finally, samples were washed twice with PBS, pH7.3. (5 minutes each) and once with desalted water, counterstained with DAPI (1 μg/ml in water) for 10 minutes at room temperature in the dark, washed twice with desalted water (10 minutes each) and mounted with DABCO (Roth, Karlsruhe), following the manufacturer's protocol.

Observations were performed on a confocal laser scanning microscope (CLSM) (Leica SP5) at the appropriate channels of excitation and emission corresponding to DAPI (to visualize the nuclei), WGA-Alexa488 (to visualize the fungal wall), and Alexa647 (to visualize the immune fluorescence signal). Z-series of optical sections of 0.5–1.0 μm intervals were collected. Images were taken from the projection of series of 15–20 optical sections. Differential Interference Contrast (DIC) images were also taken in most cases.

In-situ-RT-PCR

Detection of fungal transcripts *in situ* inside colonized roots by *in-situ*-RT-PCR was performed as formerly described (Seddas *et al.*, 2008).

Seeds of *M. truncatula* Gaertn. cv. Jemalong, line J5, were surface sterilized for 6 min in 98% sulphuric acid, rinsed 3 times (1 minute at each wash) in sterile water, 3 minutes in 100% Ethanol, then rinsed as described before. They were germinated for 3 days on 0.7% Bactogar (Difco Laboratories, Detroit) at 25°C and 355 μ E/m²/s for luminosity. Seeds were transplanted into 75 ml of a sterilized (autoclaved 2x6h at 180°C) mixture (2:3) of Sand (Sable) and Epoisse soil. Soil-based inoculum of *R. irregularis* was added as thin layer for mycorrhizal plants. Plants were grown under constant conditions (355 μ E/m²/s, 24 and 21°C, 16 and 8h, day and night, respectively, and 70% humidity) and fertilized with 5mL/ pot of Long-Ashton solution without phosphate twice a week. Plants were harvested at 21dai. Root systems of three plants per experiment were digested for 30 min in 10% KOH at 90°C and stained with 0.05% trypan blue for 15 minutes at 90°C, to evaluate mycorrhiza colonization according to the MYCOCALC program (www.dijon.inra.fr/mychintec/Mycocalc-prg/download.html, see Table 9).

Table 9: Fungal development on *Medicago truncatula* wild-type roots

J5	F%	M%	A%	m%	a%
Group1(Week 1)	68.3 \pm 8.8	21.9 \pm 11.0	31.1 \pm 12.7	96.2 \pm 3.9	21.0 \pm 10.4
Group2(Week 2)	83.3 \pm 0.0	29.5 \pm 19.0	35.4 \pm 22.9	95.6 \pm 2.1	28.4 \pm 18.8

Three plants were harvest from the pots and washed gently with cold water. Roots were put in a Petri dish with fixative solution (67% (v/v) absolute ethanol, 23% (v/v) acetic acid and 10% (v/v) DMSO) on ice and observed microscopically to ensure, that mycorrhized parts are taken for further processes. Root systems were cut to three parts and the middle part was taken and cut in 0.5-1cm pieces. Root pieces were put into glass tubes within 1ml fixative solution and 10 μ l RNAsin (Promega 40u/ μ l) and kept under vacuum for 1 hour. Roots were placed in fresh fixative solution containing RNAsin overnight at 4° C under slow rotation.

Fixed material was washed twice with 67% (v/v) absolute ethanol and 23% (v/v) acetic acid and once with DEPC-treated water. Fungal and plant cell walls were permeabilized by digestion with 0.1 U chitinase and 6 U pectinase, diluted in 100 μ l 25 mM Tris–HCl, pH7.6 for 15 minutes at 37° C per tube, followed by digestion with 0.1 U proteinase K (39u/mg, Sigma) in 100 μ l 50 mM Tris–HCl, pH7.6, for 30 min at 37°C.

Genomic DNA was digested for 1 h at 37 °C with 2 U HAE III (Promega) and 2 U Hpa II (Promega) in the presence of 1 μ l RNAsin (Promega) diluted in 100 μ l multicore buffer and BSA (Promega). Two samples were treated with 100 u RNase A in 25 mM Tris–HCl, pH7.6, for 1 hour at 37° C as control.

For reverse transcription, samples were incubated in 40 μ l RT mix:

dNTP 2.5mM	5 μ l
primer reverse (10 pmol/ μ l)	1 μ l
DEPC-treated water	34 μ l

and incubated for 5 minutes at 65° C then 5 minutes on ice

After addition of

10x RT buffer (Promega)	5 µl
RNAsine (Promega)	1 µl
M-MLV reverse transcriptase (Promega)	1 µl
DEPC-treated water	3 µl

Reverse transcription was performed at 42° C for 1 hour. One sample was excluded from reverse transcription as a control.

For the PCR, samples were incubated in 50µl PCR mix:

10x buffer	5 µl
dNTP 2.5mM	2.5 µl
5' Texas red labeled fwd primer (10 pmol/µl)	1.25 µl
5' Texas red labeled rev primer (10 pmol/µl)	1.25 µl
Taq polymerase (5U/µl)	0.25 µl
DEPC-treated water	39.75 µl

PCR conditions were chosen as follows:

95°C|2min – [93°C|1min – 58°C|1min – 72°C|1min] x 36 – 72°C|10min

After amplification samples were post-fixed in an ethanol gradient (100%, 75%, 50%, 2 minutes each) and washed in water at room temperature.

Samples were mounted with DABCO and kept in the dark (4° C) until observation with a Leica SP5 CLSM.

Poly acrylamide gel electrophoresis and coomassie staining

Proteins were size separated by poly acrylamide gel electrophoresis (PAGE) in 10% or 12% gels. Separating gel was casted in a vertical gel casting apparatus (BioRad) and one hour later the stacking gel was casted on top (Laemmli, 1970). 1 mg of yeast protein or as much as possible of *R. irregularis* protein was mixed with 6x loading dye (NEB) and loaded as 20 µl probes. Proteins were separated at 100V for 1.5 hours.

For Coomassie staining, gels were incubated in Coomassie solution for 20 minutes at room temperature followed by a short incubation in destaining solution and second incubation in destaining solution or water until background was clear.

Western Blots

10% poly acrylamide gels were loaded with either 1 mg protein per lane (yeast western blots) or as much protein as possible (*R. irregularis* western blots) and run at 100V for 1.5 hours. Separated protein was blotted on a nitro cellulose membrane in a tank

blotting system (BioRad) at 30V over night. Membrane was activated in ethanol for 5 seconds followed by incubation in cold transfer buffer together with 4 whatman papers, 2 sponges and the PAGE gel. A sandwich of these components was setup and blotted over night. After transfer the membrane was washed in TBS-Tween, blocked in TBS-Tween containing 5% of milk powder for at least two hours, washed and incubated with the first antibody diluted in TBS-Tween containing 5% milk powder for at least 2 hours at room temperature or at 4° C over night. Membrane was washed in TBS-Tween 3 times for 10 minutes and incubated with the second antibody diluted in TBS-Tween containing 5% milk powder for 1 hour at room temperature. After another 3 washing steps in TBS-Tween, detection took place either at the Odyssey infrared scanner (if the secondary antibody was IR700 or IR800 coupled for infra red detection) or by chemiluminescence detection following the manufacturer's protocol (if the secondary antibody was horse reddish peroxidase coupled for chemiluminescence detection).

Microscopy

DAPI-, GFP-, Alexa488-, Alexa647- and auto fluorescence were examined by confocal laser scanning microscopy with a Leica-TCS-SP5-AOBS confocal microscope. Sample excitation was performed with the 405 nm diode laser (DAPI), the 488 nm line of the argon gas laser (GFP, Alexa488) or the 633 nm helium neon laser (Alexa 647), emission was detected from 420 to 480 nm (DAPI), 495 to 550 nm (GFP, Alexa488) or 640 to 700 nm (Alexa 647). To avoid false detection of DAPI signal in other channels, sequential scans were performed.

5. References

- Akiyama K, Matsuzaki K, Hayashi H. 2005.** Plant sesquiterpenes induce hyphal branching in arbuscular mycorrhizal fungi. *Nature* **435**(7043): 824-827.
- Albrecht C, Geurts R, Lapeyrie F, Bisseling T. 1998.** Endomycorrhizae and rhizobial Nod factors both require SYM8 to induce the expression of the early nodulin genes *PsENOD5* and *PsENOD12A*. *Plant J.* **15**: 605-614.
- Altschul S, Madden T, Schäffer A, Zhang J, Zhang Z, Miller W, Lipman D. 1997.** Gapped BLAST and PSI-BLAST: a new generation of protein database search programs. *Nucleic Acids Res* **25**(17): 3389-3402.
- Amberg DC, Burke D, Strathern JN, Cold Spring Harbor Laboratory. 2005.** *Methods in yeast genetics : a Cold Spring Harbor Laboratory course manual.* Cold Spring Harbor, N.Y.: Cold Spring Harbor Laboratory Press.
- Andrade S, Dickmanns A, Ficner R, Einsle O. 2005a.** Crystal structure of the archaeal ammonium transporter Amt-1 from *Archaeoglobus fulgidus*. *Proc Natl Acad Sci U S A* **102**(42): 14994-14999.
- Andrade S, Dickmanns A, Ficner R, Einsle O. 2005b.** Expression, purification and crystallization of the ammonium transporter Amt-1 from *Archaeoglobus fulgidus*. *Acta Crystallogr Sect F Struct Biol Cryst Commun* **61**(Pt 9): 861-863.
- Andrade S, Einsle O. 2007.** The Amt/Mep/Rh family of ammonium transport proteins. *Mol Membr Biol* **24**(5-6): 357-365.
- Arcondeguy T, Jack R, Merrick M. 2001.** P_{II} signal transduction proteins, pivotal players in microbial nitrogen control. *Microbiol Mol Biol Rev* **65**(1): 80-105.
- Bago B, Pfeffer P, Abubaker J, Jun J, Allen J, Brouillette J, Douds D, Lammers P, Shachar-Hill Y. 2003.** Carbon export from arbuscular mycorrhizal roots involves the translocation of carbohydrate as well as lipid. *Plant Physiol* **131**(3): 1496-1507.
- Bago B, Pfeffer P, Shachar-Hill Y. 2000.** Carbon metabolism and transport in arbuscular mycorrhizas. *Plant Physiol* **124**(3): 949-958.
- Bago B, Pfeffer P, Shachar-Hill Y. 2001.** Could the urea cycle be translocating nitrogen in the arbuscular mycorrhizal symbiosis? *New Phytologist* **149**(1): 4-8.
- Bécard G, Fortin JA. 1988.** Early events of vesicular-arbuscular mycorrhiza formation on Ri T-DNA transformed roots. *New Phytologist* **108**(2): 211-218.
- Berg J, Tymoczko J, Stryer L. 2003.** *Biochemie:* Spektrum Akademischer Verlag.
- Besserer A, Puech-Pagès V, Kiefer P, Gomez-Roldan V, Jauneau A, Roy S, Portais J, Roux C, Bécard G, Séjalon-Delmas N. 2006.** Strigolactones stimulate arbuscular mycorrhizal fungi by activating mitochondria. *PLoS Biol* **4**(7): e226.
- Biswas K, Morschhauser J. 2005.** The Mep2p ammonium permease controls nitrogen starvation-induced filamentous growth in *Candida albicans*. *Mol Microbiol* **56**(3): 649-669.
- Boeckstaens M, André B, Marini A. 2007.** The yeast ammonium transport protein Mep2 and its positive regulator, the Npr1 kinase, play an important

- role in normal and pseudohyphal growth on various nitrogen media through retrieval of excreted ammonium. *Mol Microbiol* **64**(2): 534-546.
- Boeckstaens M, André B, Marini A. 2008.** Distinct transport mechanisms in yeast ammonium transport/sensor proteins of the mep/amt/rh family and impact on filamentation. *J Biol Chem* **283**(31): 21362-21370.
- Bougoure J, Ludwig M, Brundrett M, Grierson P. 2009.** Identity and specificity of the fungi forming mycorrhizas with the rare mycoheterotrophic orchid *Rhizanthella gardneri*. *Mycology Research* **113**(Pt 10): 1097-1106.
- Brachmann A, Parniske M. 2006.** The most widespread symbiosis on Earth. *PLoS Biol* **4**(7): e239.
- Brachmann A, Weinzierl G, Kämper J, Kahmann R. 2001.** Identification of genes in the bW/bE regulatory cascade in *Ustilago maydis*. *Molecular Microbiology* **42**(4): 1047-1063.
- Brody J, Kern S. 2004.** Sodium boric acid: a Tris-free, cooler conductive medium for DNA electrophoresis. *Biotechniques* **36**(2): 214-216.
- Brucker D 2008.** Screening einer cDNA-Bank aus *Geosiphon pyriformis* nach Ammoniumtransportern. In. Praktikumsprotokoll.
- Brucker D 2009.** Ammoniumtransporter und Kernfärbungen in *Glomus intraradices*. In. Diploma thesis in AG Brachmann.
- Campagnac E, Lounès-Hadj Sahraoui A, Debiane D, Fontaine J, Laruelle F, Garçon G, Verdin A, Durand R, Shirali P, Grandmougin-Ferjani A. 2009.** Arbuscular mycorrhiza partially protect chicory roots against oxidative stress induced by two fungicides, fenpropimorph and fenhexamid. *Mycorrhiza*.
- Cappellazzo G, Lanfranco L, Fitz M, Wipf D, Bonfante P. 2008.** Characterization of an amino acid permease from the endomycorrhizal fungus *Glomus mosseae*. *Plant Physiol* **147**(1): 429-437.
- Chabot S, Bécard G, Piché Y. 1992.** Life cycle of *Glomus intraradix* in root organ culture. *Mycologia*(84): 315-321.
- Crooks GE, Hon G, Chandonia JM, Brenner SE. 2004.** WebLogo: a sequence logo generator. *Genome Res* **14**(6): 1188-1190.
- Dafinger C 2008.** Isolation of *Geosiphon pyriformis* transporter genes by functional complementation of yeast mutant strains. In. Diploma thesis 2008 in AG Schüßler.
- Declerck S, Fortin JA, Strullu D-G, SpringerLink (Online service) 2005.** In Vitro Culture of Mycorrhizas. In. Berlin, Heidelberg: Springer-Verlag Berlin Heidelberg.
- Declerck S, Strullu DG, Plenchette C. 1998.** Monoxenic culture of the intraradical forms of *Glomus* sp. isolated from a tropical ecosystem: A proposed methodology for germplasm collection. *Mycologia* **90**(4): 579-585.
- Einsle O, Messerschmidt A, Stach P, Bourenkov G, Bartunik H, Huber R, Kroneck P. 1999.** Structure of cytochrome c nitrite reductase. *Nature* **400**(6743): 476-480.
- Ellerbeck M 2008.** Screen einer cDNA-Bank aus *Geosiphon pyriformis* nach Ammoniumpermeasen mit Hilfe von Hefe-Komplementation und degenerierter PCR. In. Praktikumsprotokoll.
- Ellerbeck M 2009.** Charakterisierung der putativen Ammoniumtransporter GpAmt1p und GpAmt2p aus *Geosiphon pyriformis*. In.

- Fellbaum CR, Gachomo EW, Beesetty Y, Choudhari S, Strahan GD, Pfeffer PE, Kiers ET, Bucking H. 2012.** Carbon availability triggers fungal nitrogen uptake and transport in arbuscular mycorrhizal symbiosis. *Proceedings of the National Academy of Sciences, USA* **109**(7): 2666-2671.
- Finlay R. 2008.** Ecological aspects of mycorrhizal symbiosis: with special emphasis on the functional diversity of interactions involving the extraradical mycelium. *J Exp Bot* **59**(5): 1115-1126.
- Fontaine J, Grandmougin-Ferjani A, Glorian V, Durand R. 2004.** 24-Methyl/methylene sterols increase in monoxenic roots after colonization by arbuscular mycorrhizal fungi. *New Phytologist* **163**(1): 159-167.
- Fortin J, Bécard G 2002.** Arbuscular mycorrhiza on root-organ cultures. In: *Can. J. Bot.* : 1-20.
- Franken P. 2002.** A plea for a concerted nomenclature for AM fungal genes. *Mycorrhiza* **12**(6): 319-319.
- Gallou A, De Jaeger N, Cranenbrouck S, Declerck S. 2010.** Fast track in vitro mycorrhization of potato plantlets allow studies on gene expression dynamics. *Mycorrhiza* **20**(3): 201-207.
- Gehrig H, Schüssler A, Kluge M. 1996.** *Geosiphon pyriforme*, a fungus forming endocytobiosis with *Nostoc* (cyanobacteria), is an ancestral member of the Glomales: evidence by SSU rRNA analysis. *J Mol Evol* **43**(1): 71-81.
- Genre A, Chabaud M, Faccio A, Barker D, Bonfante P. 2008.** Prepenetration apparatus assembly precedes and predicts the colonization patterns of arbuscular mycorrhizal fungi within the root cortex of both *Medicago truncatula* and *Daucus carota*. *Plant Cell* **20**(5): 1407-1420.
- Genre A, Chabaud M, Timmers T, Bonfante P, Barker D. 2005.** Arbuscular mycorrhizal fungi elicit a novel intracellular apparatus in *Medicago truncatula* root epidermal cells before infection. *Plant Cell* **17**(12): 3489-3499.
- Gerdemann J. 1963.** Spores of mycorrhizal *Endogone species* extracted from soil 673 by wet sieving and decanting. *Transactions of the British Mycological Society* **46**: 235-244.
- Gianinazzi-Pearson V. 1996.** Plant Cell Responses to Arbuscular Mycorrhizal Fungi: Getting to the Roots of the Symbiosis. *Plant Cell* **8**(10): 1871-1883.
- Gietz R, Schiestl R. 2007a.** Large-scale high-efficiency yeast transformation using the LiAc/SS carrier DNA/PEG method. *Nat Protoc* **2**(1): 38-41.
- Gietz R, Schiestl R. 2007b.** Quick and easy yeast transformation using the LiAc/SS carrier DNA/PEG method. *Nat Protoc* **2**(1): 35-37.
- Gonzales-Guerrero Mea. 2005.** Characterization of a *Glomus intraradices* gene encoding a putative Zn transporter of the cation diffusion facilitator family. *Fungal Genetics and Biology* **42**: 130-140.
- Govindarajulu M, Pfeffer P, Jin H, Abubaker J, Douds D, Allen J, Bücking H, Lammers P, Shachar-Hill Y. 2005.** Nitrogen transfer in the arbuscular mycorrhizal symbiosis. *Nature* **435**(7043): 819-823.
- Grossmann G, Opekarová M, Malinsky J, Weig-Meckl I, Tanner W. 2007.** Membrane potential governs lateral segregation of plasma membrane proteins and lipids in yeast. *EMBO J* **26**(1): 1-8.
- Grossmann G, Opekarova M, Novakova L, Stolz J, Tanner W. 2006.** Lipid raft-based membrane compartmentation of a plant transport protein expressed in *Saccharomyces cerevisiae*. *Eukaryot Cell* **5**(6): 945-953.

- Guether M, Neuhauser B, Balestrini R, Dynowski M, Ludewig U, Bonfante P. 2009.** A mycorrhizal-specific ammonium transporter from *Lotus japonicus* acquires nitrogen released by arbuscular mycorrhizal fungi. *Plant Physiol* **150**(1): 73-83.
- Gutjahr C, Radovanovic D, Geoffroy J, Zhang Q, Siegler H, Chiapello M, Casieri L, An K, An G, Guiderdoni E, Kumar CS, Sundaresan V, Harrison MJ, Paszkowski U. 2012.** The half-size ABC transporters STR1 and STR2 are indispensable for mycorrhizal arbuscule formation in rice. *Plant J* **69**(5): 906-920.
- Hackette S, Skye G, Burton C, Segel I. 1970.** Characterization of an ammonium transport system in filamentous fungi with methylammonium-¹⁴C as the substrate. *J Biol Chem* **245**(17): 4241-4250.
- Harrison M, van Buuren M. 1995.** A phosphate transporter from the mycorrhizal fungus *Glomus versiforme*. *Nature* **378**(6557): 626-629.
- Harrison MJ, Dewbre GR, Liu J. 2002.** A phosphate transporter from *Medicago truncatula* involved in the acquisition of phosphate released by arbuscular mycorrhizal fungi. *Plant Cell* **14**(10): 2413-2429.
- Helber N, Requena N. 2008.** Expression of the fluorescence markers DsRed and GFP fused to a nuclear localization signal in the arbuscular mycorrhizal fungus *Glomus intraradices*. *New Phytol* **177**(2): 537-548.
- Helber N, Wippel K, Sauer N, Schaarschmidt S, Hause B, Requena N. 2011.** A Versatile monosaccharide transporter that operates in the arbuscular mycorrhizal fungus *Glomus* sp is crucial for the symbiotic relationship with plants. *Plant Cell* **23**(10): 3812-3823.
- Hibbett D, Binder M, Bischoff J, Blackwell M, Cannon P, Eriksson O, Huhndorf S, James T, Kirk P, Lücking R, Thorsten Lumbsch H, Lutzoni F, Matheny P, McLaughlin D, Powell M, Redhead S, Schoch C, Spatafora J, Stalpers J, Vilgalys R, Aime M, Aptroot A, Bauer R, Begerow D, Benny G, Castlebury L, Crous P, Dai Y, Gams W, Geiser D, Griffith G, Gueidan C, Hawksworth D, Hestmark G, Hosaka K, Humber R, Hyde K, Ironside J, Kõljalg U, Kurtzman C, Larsson K, Lichtwardt R, Longcore J, Miadlikowska J, Miller A, Moncalvo J, Mozley-Standridge S, Oberwinkler F, Parmasto E, Reeb V, Rogers J, Roux C, Ryvarden L, Sampaio J, Schüssler A, Sugiyama J, Thorn R, Tibell L, Untereiner W, Walker C, Wang Z, Weir A, Weiss M, White M, Winka K, Yao Y, Zhang N. 2007.** A higher-level phylogenetic classification of the Fungi. *Mycol Res* **111**(Pt 5): 509-547.
- Higgins DG, Thompson JD, Gibson TJ. 1996.** Using CLUSTAL for multiple sequence alignments. *Methods Enzymol* **266**: 383-402.
- Hijri M, Sanders I. 2005.** Low gene copy number shows that arbuscular mycorrhizal fungi inherit genetically different nuclei. *Nature* **433**(7022): 160-163.
- Hsieh MH, Lam HM, van de Loo FJ, Coruzzi G. 1998.** A PII-like protein in *Arabidopsis*: putative role in nitrogen sensing. *Proc Natl Acad Sci U S A* **95**(23): 13965-13970.
- Ijdo M, Cranenbrouck S, Declerck S. 2011.** Methods for large-scale production of AM fungi: past, present, and future. *Mycorrhiza* **21**(1): 1-16.

- Jacobs P, Jauniaux J, Grenson M. 1980.** A cis-dominant regulatory mutation linked to the argB-argC gene cluster in *Saccharomyces cerevisiae*. *J Mol Biol* **139**(4): 691-704.
- Javelle A, Lupo D, Zheng L, Li XD, Winkler FK, Merrick M. 2006.** An unusual twin-his arrangement in the pore of ammonia channels is essential for substrate conductance. *J Biol Chem* **281**(51): 39492-39498.
- Javelle A, Morel M, Rodríguez-Pastrana B, Botton B, André B, Marini A, Brun A, Chalot M. 2003.** Molecular characterization, function and regulation of ammonium transporters (Amt) and ammonium-metabolizing enzymes (GS, NADP-GDH) in the ectomycorrhizal fungus *Hebeloma cylindrosporum*. *Mol Microbiol* **47**(2): 411-430.
- Javelle A, Severi E, Thornton J, Merrick M. 2004.** Ammonium sensing in *Escherichia coli*. Role of the ammonium transporter AmtB and AmtB-GlnK complex formation. *J Biol Chem* **279**(10): 8530-8538.
- Javot H, Penmetsa RV, Breuillin F, Bhattarai KK, Noar RD, Gomez SK, Zhang Q, Cook DR, Harrison MJ. 2011.** *Medicago truncatula* *mtpt4* mutants reveal a role for nitrogen in the regulation of arbuscule degeneration in arbuscular mycorrhizal symbiosis. *Plant Journal* **68**(6): 954-965.
- Javot H, Pumplin N, Harrison MJ. 2007.** Phosphate in the arbuscular mycorrhizal symbiosis: transport properties and regulatory roles. *Plant, Cell & Environment* **30**(3): 310-322.
- Jin H, Pfeffer P, Douds D, Piotrowski E, Lammers P, Shachar-Hill Y. 2005.** The uptake, metabolism, transport and transfer of nitrogen in an arbuscular mycorrhizal symbiosis. *New Phytol* **168**(3): 687-696.
- Jones ME. 1963.** Carbamyl Phosphate. *Science* **140**(3574): 1373-1379.
- Journet E-P, El-Gachtouli N, Vernoud V, de Billy F, Pichon M, Dedieu A, Arnould C, Morandi D, Barker DG, Gianinazzi-Pearson V. 2001.** *Medicago truncatula* *ENOD11*: A Novel RPRP-Encoding Early Nodulin Gene Expressed During Mycorrhization in Arbuscule-Containing Cells. *Molecular Plant-Microbe Interactions* **14**(6): 737-748.
- Katoh K, Kuma K, Toh H, Miyata T. 2005.** MAFFT version 5: improvement in accuracy of multiple sequence alignment. *Nucleic Acids Res* **33**(2): 511-518.
- Khademi S, O'Connell Jr, Remis J, Robles-Colmenares Y, Miercke L, Stroud R. 2004.** Mechanism of ammonia transport by Amt/MEP/Rh: structure of AmtB at 1.35 Å. *Science* **305**(5690): 1587-1594.
- Khademi S, Stroud R. 2006.** The Amt/MEP/Rh family: structure of AmtB and the mechanism of ammonia gas conduction. *Physiology (Bethesda)* **21**: 419-429.
- Kibbe WA. 2007.** OligoCalc: an online oligonucleotide properties calculator. *Nucleic Acids Res* **35**(Web Server issue): W43-46.
- Kirsten JH, Xiong Y, Davis CT, Singleton CK. 2008.** Subcellular localization of ammonium transporters in *Dictyostelium discoideum*. *BMC Cell Biology* **9**: 71.
- Kleiner D. 1981.** The transport of NH₃ and NH₄⁺ across biological membranes. *Biochim Biophys Acta* **639**(1): 41-52.
- Kleiner D. 1985.** Energy expenditure for cyclic retention of NH₃/NH₄⁺ during N₂ fixation by *Klebsiella pneumoniae*. *FEBS Lett* **187**(2): 237-239.
- Kleiner D, Fitzke E. 1981.** Some properties of a new electrogenic transport system: the ammonium (methylammonium) carrier from *Clostridium pasteurianum*. *Biochim Biophys Acta* **641**(1): 138-147.

- Krogh A, Larsson B, von Heijne G, Sonnhammer E. 2001.** Predicting transmembrane protein topology with a hidden Markov model: application to complete genomes. *J Mol Biol* **305**(3): 567-580.
- Krüger M, Krüger C, Walker C, Stockinger H, Schüßler A. 2012.** Phylogenetic reference data for systematics and phylotaxonomy of arbuscular mycorrhizal fungi from phylum to species level. *New Phytol* **193**(4): 970-984.
- Laemmli U. 1970.** Cleavage of structural proteins during the assembly of the head of bacteriophage T4. *Nature* **227**(5259): 680-685.
- Lamoureux G, Javelle A, Baday S, Wang S, Berneche S. 2010.** Transport mechanisms in the ammonium transporter family. *Transfus Clin Biol* **17**(3): 168-175.
- Larkin MA, Blackshields G, Brown NP, Chenna R, McGettigan PA, McWilliam H, Valentin F, Wallace IM, Wilm A, Lopez R, Thompson JD, Gibson TJ, Higgins DG. 2007.** Clustal W and Clustal X version 2.0. *Bioinformatics* **23**(21): 2947-2948.
- Lea PJ, Mifflin BJ. 1974.** Alternative route for nitrogen assimilation in higher plants. *Nature* **251**(5476): 614-616.
- Logi C, Sbrana C, Giovannetti M. 1998.** Cellular events involved in survival of individual arbuscular mycorrhizal symbionts growing in the absence of the host. *Appl Environ Microbiol* **64**(9): 3473-3479.
- Loos F 2008.** Großpraktikum Genetik. In: Praktikumsprotokoll.
- López-Pedrosa A, González-Guerrero M, Valderas A, Azcón-Aguilar C, Ferrol N. 2006.** *GintAMT1* encodes a functional high-affinity ammonium transporter that is expressed in the extraradical mycelium of *Glomus intraradices*. *Fungal Genet Biol* **43**(2): 102-110.
- Loqué D, Lalonde S, Looger L, von Wirén N, Frommer W. 2007.** A cytosolic trans-activation domain essential for ammonium uptake. *Nature* **446**(7132): 195-198.
- Loqué D, Ludewig U, Yuan L, von Wirén N. 2005.** Tonoplast intrinsic proteins AtTIP2;1 and AtTIP2;3 facilitate NH₃ transport into the vacuole. *Plant Physiol* **137**(2): 671-680.
- Loqué D, Mora S, Andrade S, Pantoja O, Frommer W. 2009.** Pore mutations in ammonium transporter AMT1 with increased electrogenic ammonium transport activity. *J Biol Chem* **284**(37): 24988-24995.
- Lorenz, Heitman. 1998a.** The MEP2 ammonium permease regulates pseudohyphal differentiation in *Saccharomyces cerevisiae*. *EMBO J* **17**(5): 1236-1247.
- Lorenz, Heitman. 1998b.** Regulators of pseudohyphal differentiation in *Saccharomyces cerevisiae* identified through multicopy suppressor analysis in ammonium permease mutant strains. *Genetics* **150**(4): 1443-1457.
- Lott G. 2011.** Ammoniumtransporter in *Geosiphon pyriformis*. *Bachelorarbeit*.
- Maillet F, Poinot V, Andre O, Puech-Pages V, Haouy A, Gueunier M, Cromer L, Giraudet D, Formey D, Niebel A, Martinez EA, Driguez H, Becard G, Denarie J. 2011.** Fungal lipochitoooligosaccharide symbiotic signals in arbuscular mycorrhiza. *Nature* **469**(7328): 58-63.
- Maldonado-Mendoza I, Dewbre G, Harrison M. 2001.** A phosphate transporter gene from the extra-radical mycelium of an arbuscular mycorrhizal fungus

- Glomus intraradices* is regulated in response to phosphate in the environment. *Mol Plant Microbe Interact* **14**(10): 1140-1148.
- Marini A, Matassi G, Raynal V, André B, Cartron J, Chérif-Zahar B. 2000.** The human Rhesus-associated RhAG protein and a kidney homologue promote ammonium transport in yeast. *Nat Genet* **26**(3): 341-344.
- Marini A, Soussi-Boudekou S, Vissers S, Andre B. 1997.** A family of ammonium transporters in *Saccharomyces cerevisiae*. *Mol Cell Biol* **17**(8): 4282-4293.
- Marini A, Vissers S, Urrestarazu A, André B. 1994.** Cloning and expression of the *MEP1* gene encoding an ammonium transporter in *Saccharomyces cerevisiae*. *EMBO J* **13**(15): 3456-3463.
- Marini A-M, Boeckstaens M, André B 2006.** From yeast ammonium transporters to Rhesus proteins, isolation and functional characterization. In. *Transfus Clin Biol*. 95-96.
- Marini AM, Urrestarazu A, Beauwens R, Andre B. 1998.** The Rh (rhesus) blood group polypeptides are related to NH₄⁺ transporters. *Trends Biochem Sci* **22**(12): 460-461.
- Martin F, Gianinazzi-Pearson V, Hijri M, Lammers P, Requena N, Sanders I, Shachar-Hill Y, Shapiro H, Tuskan G, Young J. 2008.** The long hard road to a completed *Glomus intraradices* genome. *New Phytol* **180**(4): 747-750.
- McDonald TR, Dietrich FS, Lutzoni F. 2012.** Multiple horizontal gene transfers of ammonium transporters/ammonia permeases from prokaryotes to eukaryotes: toward a new functional and evolutionary classification. *Mol Biol Evol* **29**(1): 51-60.
- Miller M, Pfeiffer W, Schwartz T. 2010.** Creating the CIPRES Science Gateway for inference of large phylogenetic trees *Proceedings of the Gateway Computing Environments Workshop*: 1-8.
- Mitaku S, Hirokawa T, Tsuji T. 2002.** Amphiphilicity index of polar amino acids as an aid in the characterization of amino acid preference at membrane-water interfaces. *Bioinformatics* **18**(4): 608-616.
- Mitsuzawa H 2006.** Ammonium transporter genes in the fission yeast *Schizosaccharomyces pombe*: role in ammonium uptake and a morphological transition. In. *Genes Cells*. 1183-1195.
- Monahan BJ, Askin MC, Hynes MJ, Davis MA 2006.** Differential expression of *Aspergillus nidulans* ammonium permease genes is regulated by GATA transcription factor AreA. In. *Eukaryotic Cell*. 226-237.
- Monahan BJ, Fraser JA, Hynes MJ, Davis MA 2002.** Isolation and characterization of two ammonium permease genes, *meaA* and *mepA*, from *Aspergillus nidulans*. In. *Eukaryotic Cell*. 85-94.
- Neuhäuser B, Dunkel N, Satheesh SV, Morschhauser J. 2011.** Role of the Npr1 kinase in ammonium transport and signaling by the ammonium permease Mep2 in *Candida albicans*. *Eukaryot Cell* **10**(3): 332-342.
- Ninnemann O, Jauniaux JC, Frommer WB 1994.** Identification of a high affinity NH₄⁺ transporter from plants. In. *EMBO J*. 3464-3471.
- Pantoja O. 2012.** High affinity ammonium transporters: molecular mechanism of action. *Front Plant Sci* **3**: 34.
- Parniske M. 2008.** Arbuscular mycorrhiza: the mother of plant root endosymbioses. *Nat Rev Microbiol* **6**(10): 763-775.
- Pawlowska T, Taylor J. 2004.** Organization of genetic variation in individuals of arbuscular mycorrhizal fungi. *Nature* **427**(6976): 733-737.

- Perez-Tienda J, Testillano PS, Balestrini R, Fiorilli V, Azcon-Aguilar C, Ferrol N. 2011.** GintAMT2, a new member of the ammonium transporter family in the arbuscular mycorrhizal fungus *Glomus intraradices*. *Fungal Genet Biol* **48**(11): 1044-1055.
- Pöggeler S, Masloff S, Hoff B, Mayrhofer S, KüCK U 2003.** Versatile EGFP reporter plasmids for cellular localization of recombinant gene products in filamentous fungi. In. *Current genetics*. 54-61.
- Pumplin N, Zhang X, Noar RD, Harrison MJ. 2012.** Polar localization of a symbiosis-specific phosphate transporter is mediated by a transient reorientation of secretion. *Proceedings of the National Academy of Sciences*.
- Redecker, Morton, Bruns. 2000.** Ancestral lineages of arbuscular mycorrhizal fungi (*Glomales*). *Mol Phylogenet Evol* **14**(2): 276-284.
- Rees D, Akif Tezcan F, Haynes C, Walton M, Andrade S, Einsle O, Howard J. 2005.** Structural basis of biological nitrogen fixation. *Philos Transact A Math Phys Eng Sci* **363**(1829): 971-984; discussion 1035-1040.
- Rees D, Howard J. 2000.** Nitrogenase: standing at the crossroads. *Curr Opin Chem Biol* **4**(5): 559-566.
- Remy W, Taylor T, Hass H, Kerp H. 1994.** Four hundred-million-year-old vesicular arbuscular mycorrhizae. *Proc Natl Acad Sci U S A* **91**(25): 11841-11843.
- Rice P, Longden I, Bleasby A. 2000.** EMBOSS: the European Molecular Biology Open Software Suite. *Trends Genet* **16**(6): 276-277.
- Riely BK, Ane JM, Penmetsa RV, Cook DR. 2004.** Genetic and genomic analysis in model legumes bring Nod-factor signaling to center stage. *Curr Opin Plant Biol* **7**(4): 408-413.
- Rose T, Henikoff J, Henikoff S. 2003.** CODEHOP (COnsensus-DEgenerate Hybrid Oligonucleotide Primer) PCR primer design. *Nucleic Acids Res* **31**(13): 3763-3766.
- Rose T, Schultz E, Henikoff J, Pietrokovski S, McCallum C, Henikoff S. 1998.** Consensus-degenerate hybrid oligonucleotide primers for amplification of distantly related sequences. *Nucleic Acids Res* **26**(7): 1628-1635.
- Rozen S, Skaletsky H. 2000.** Primer3 on the WWW for general users and for biologist programmers. *Methods Mol Biol* **132**: 365-386.
- Rutherford J, Chua G, Hughes T, Cardenas M, Heitman J. 2008.** A Mep2-dependent Transcriptional Profile Links Permease Function to Gene Expression during Pseudohyphal Growth in *Saccharomyces cerevisiae*. *Mol Biol Cell* **19**(7): 3028-3039.
- Saalbach G, Rosso M, Schumann U. 1996.** The vacuolar targeting signal of the 2S albumin from Brazil nut resides at the C terminus and involves the C-terminal propeptide as an essential element. *Plant Physiol* **112**(3): 975-985.
- Sambrook J, Russell DW. 2001.** *Molecular cloning : a laboratory manual*. Cold Spring Harbor, N.Y.: Cold Spring Harbour Press.
- Schüßler, Martin, Cohen, Fitz, Wipf. 2006.** Characterization of a carbohydrate transporter from symbiotic glomeromycotan fungi. *Nature* **444**(7121): 933-936.
- Schüßler A 2012.** The *Geosiphon-Nostoc* endosymbiosis and its role as a model for arbuscular mycorrhiza research. In Hook B. *The Mycota IX - Fungal Associations*. Heidelberg: Springer-Verlag. in press.

- Schüßler A, Kluge M 2001.** *Geosiphon pyriforme*, an endocytosymbiosis between fungus and cyanobacteria, and its meaning as a model system for AM research. In: B H ed. *The Mycota IX*: Springer Verlag, Berlin Heidelberg New York, 151-161.
- Schüßler A, Schwarzott D, Walker C. 2001.** A new fungal phylum, the Glomeromycota: phylogeny and evolution. *Mycology Research* **105**(12): 1413-1421.
- Schüßler A, Wolf E. 2005.** *Geosiphon pyriformis*—a glomeromycotan soil fungus forming endosymbiosis with cyanobacteria: Springer, Berlin Heidelberg.
- Seddas P, Arnould C, Tollot M, Arias C, Gianinazzi-Pearson V. 2008.** Spatial monitoring of gene activity in extraradical and intraradical developmental stages of arbuscular mycorrhizal fungi by direct fluorescent *in situ* RT-PCR. *Fungal Genet Biol* **45**(8): 1155-1165.
- Sedzielewska KA, Fuchs J, Tensch EM, Baronian K, Watzke R, Kunze G. 2011.** Estimation of the *Glomus intraradices* nuclear DNA content. *New Phytol* **192**(4): 794-797.
- Simon-Rosin U, Wood C, Udvardi MK. 2003.** Molecular and cellular characterisation of LjAMT2;1, an ammonium transporter from the model legume *Lotus japonicus*. *Plant Molecular Biology* **51**(1): 99-108.
- Smith D, Garcia-Pedrajas M, Gold S, Perlin M. 2003.** Isolation and characterization from pathogenic fungi of genes encoding ammonium permeases and their roles in dimorphism. *Mol Microbiol* **50**(1): 259-275.
- Smith S, Read D. 2008.** *Mycorrhizal Symbiosis*: Academic Press.
- Sohlenkamp C, Shelden M, Howitt S, Udvardi M. 2000.** Characterization of *Arabidopsis* AtAMT2, a novel ammonium transporter in plants. *FEBS Lett* **467**(2-3): 273-278.
- Sohlenkamp C, Wood C, Roeb G, Udvardi M. 2002.** Characterization of *Arabidopsis* AtAMT2, a high-affinity ammonium transporter of the plasma membrane. *Plant Physiol* **130**(4): 1788-1796.
- Soupe E, Lee H, Kustu S. 2002.** Ammonium/methylammonium transport (Amt) proteins facilitate diffusion of NH₃ bidirectionally. *Proc Natl Acad Sci U S A* **99**(6): 3926-3931.
- Stevenson R, Silver S. 1977.** Methylammonium uptake by *Escherichia coli*: evidence for a bacterial NH₄⁺ transport system. *Biochem Biophys Res Commun* **75**(4): 1133-1139.
- Stockinger H, Walker C, Schüßler A. 2009.** '*Glomus intraradices* DAOM197198', a model fungus in arbuscular mycorrhiza research, is not *Glomus intraradices*. *New Phytol* **183**(4): 1176-1187.
- Strenkoski LF, DeCicco BT. 1971.** pH-conditional, ammonia assimilation-deficient mutants of *Hydrogenomonas eutropha*: evidence for the nature of the mutation. *J Bacteriol* **105**(1): 296-302.
- Teichert S, Rutherford JC, Wottawa M, Heitman J, Tudzynski B. 2008.** Impact of ammonium permeases mepA, mepB, and mepC on nitrogen-regulated secondary metabolism in *Fusarium fujikuroi*. *Eukaryot Cell* **7**(2): 187-201.
- Thomas G, Coutts G, Merrick M. 2000.** The glnKamtB operon. A conserved gene pair in prokaryotes. *Trends Genet* **16**(1): 11-14.
- Thompson J, Higgins D, Gibson T. 1994.** CLUSTAL W: improving the sensitivity of progressive multiple sequence alignment through sequence weighting,

- position-specific gap penalties and weight matrix choice. *Nucleic Acids Res* **22**(22): 4673-4680.
- Tian C, Kasiborski B, Koul R, Lammers PJ, Bucking H, Shachar-Hill Y. 2010.** Regulation of the nitrogen transfer pathway in the arbuscular mycorrhizal symbiosis: gene characterization and the coordination of expression with nitrogen flux. *Plant Physiol* **153**(3): 1175-1187.
- Tisserant E, Kohler A, Dozolme-Seddas P, Balestrini R, Benabdellah K, Colard A, Croll D, Da Silva C, Gomez SK, Koul R, Ferrol N, Fiorilli V, Formey D, Franken P, Helber N, Hijri M, Lanfranco L, Lindquist E, Liu Y, Malbreil M, Morin E, Poulain J, Shapiro H, van Tuinen D, Waschke A, Azcon-Aguilar C, Becard G, Bonfante P, Harrison MJ, Kuster H, Lammers P, Paszkowski U, Requena N, Rensing SA, Roux C, Sanders IR, Shachar-Hill Y, Tuskan G, Young JP, Gianinazzi-Pearson V, Martin F. 2012.** The transcriptome of the arbuscular mycorrhizal fungus *Glomus intraradices* (DAOM 197198) reveals functional tradeoffs in an obligate symbiont. *New Phytol* **193**(3): 755-769.
- Valls LA, Winther JR, Stevens TH. 1990.** Yeast carboxypeptidase Y vacuolar targeting signal is defined by four propeptide amino acids. *J Cell Biol* **111**(2): 361-368.
- van Rhijn P, Fang Y, Galili S, Shaul O, Atzmon N, Wininger S, Eshed Y, Lum M, Li Y, To V, Fujishige N, Kapulnik Y, Hirsch AM. 1997.** Expression of early nodulin genes in alfalfa mycorrhizae indicates that signal transduction pathways used in forming arbuscular mycorrhizae and *Rhizobium*-induced nodules may be conserved. *Proceedings of the National Academy of Sciences* **94**(10): 5467-5472.
- Voets L, de la Providencia I, Fernandez K, Ijdo M, Cranenbrouck S, Declerck S. 2009.** Extraradical mycelium network of arbuscular mycorrhizal fungi allows fast colonization of seedlings under in vitro conditions. *Mycorrhiza* **19**(5): 347-356.
- von Wirén N, Merrick M 2004.** Regulation and function of ammonium carriers in bacteria, fungi, and plants. *Topics in Current Genetics, Molecular Mechanisms Controlling Transmembrane Transport*: Springer Berlin / Heidelberg, 95-120.
- Wang B, Qiu YL. 2006.** Phylogenetic distribution and evolution of mycorrhizas in land plants. *Mycorrhiza* **16**(5): 299-363.
- Wang S, Orabi EA, Baday S, Berneche S, Lamoureux G. 2012.** Ammonium Transporters Achieve Charge Transfer by Fragmenting Their Substrate. *J Am Chem Soc.*
- Woodmansee RG, Dodd JL, Bowman RA, Clark FE, Dickinson CE. 1978.** Nitrogen budget of a shortgrass prairie ecosystem. *Oecologia* **34**(3): 363-376.
- Zhang Q, Blaylock LA, Harrison MJ. 2010.** Two *Medicago truncatula* half-ABC transporters are essential for arbuscule development in arbuscular mycorrhizal symbiosis. *Plant Cell* **22**(5): 1483-1497.
- Zheng L, Kostrewa D, Berneche S, Winkler FK, Li XD. 2004.** The mechanism of ammonia transport based on the crystal structure of AmtB of *Escherichia coli*. *Proc Natl Acad Sci U S A* **101**(49): 17090-17095.

6. Appendix

6.1 Sequences of glomeromycotan AMTs and their genes

DNA (upper paragraphs) and protein (lower paragraphs) sequences of the glomeromycotan AMTs. Coding DNA sequence is written in capital letters.

GpyrAMT1 (JX535577)

```
aagcacacgactttgccacaattttcattatttttatgatttcttgacgatttgagggaaattttttattttgacaatttttgaaa
tttgtctgtgtccacaatttcctaagaactagtaaaatcctacaaattatttccctagcgtgagcaaaaaATGGCTTCGATAAATTC
GATATATTTTCGACTCAGGAGATACTGGCTTCGTTCTAATTTTCGACGGCATTAGTATGGTTTATGATACCGGGGGCTGGATATTTTTAT
AGTGGAAATGGCTCATCGAAAAAATGCACCTTCTCTCATCTTATTATGCATGGTAAGCGTTGCCGTGGTTACAGTGCAAagtaagttgag
acataatccagaagtttttattcaaacgccttgattgaaacaattttttcaaagttgacaaacaaaatcctttgacctgtcagTGGTTTT
TTTTCGGATACAGCTTGGCTTTTTCTAAAAGTGGGAATAAATTGATCGGAGGTTTTTCGCAAAGCCTTATTTCTTAATCTTGAGAAAGA
AGATCCATATCCAAATACAAATATCTCAGAATCAACCTTTGCCATATATCAATTAATGTTTGCAGCCATCACCCAGCTCTAGCAATT
GGATCAACAGCTGAACGAGCAAGAATATTTCCCAACGATTGTTTTTCATCTTTTTATGGACAACGTTGGTCTATGATCCAATTGCTTTTT
GGTTTTGGTCCGAACCGGCTGGGCCCATGATTTGGGAAGTCTGGATTTTGGCTGGTGGGACACCAGTTCATATGGCATCGGGAGCTGC
TGCACCTCGCTTATGCTTTAGTTTTGAAAAAAGAATGATTGAATCGGAAGAAGGGGAACCTAAACCAACAATGTTACAAATATTAT
CTTGGGACGATCATGCTTTGGTTTTGGATGGTTCGGGTTTTAATGGTGGTTCAGCTTTAGGTGCAAATCCTCGGCCACAAATGCTATTA
TTGTGACAAATTTGTCAGCATCTATCGGTGGGATTACATGGATGCTTTGGGATTATCGTCTGGAAGGTAAATTTTCAGCCTTGGGCTT
TTGTTGGGTGCGATTTCTGGGTTAGTTGCCATTACTCCTGCCTCTGGTTACGTTTTCGCCTCCATCAGCAATCGCCTTCGGTTTAGTA
AGTGGTTTTCTATGCAACTTGGCTACAAAATTGCGAAATATCTTTAATTACGACGATGCTTGTGATGATTTGCCGTGCATTTTGTGG
GTGGTTTTATTGGGAACATTCTCACAGCTATATTCGCTCAGAATCAATTTGTTTCAAGTTAGATGGTCACTCAGATCCGATCGATGGAGG
TTTTTTAGATCATAACTGGATTCAAATTGTATACCAACTAGCGAATCCCTTGTCTGGTGGACTCTATTCGTTCTTTGCAACACTCATG
ATTGTGTTGATTATGAATGAAATACCTGGGTTATCCCTTCGTGCAAGTCCCGATTCTGAAACATTGGGAATCGATCAATCAGAGCTTG
GTGAATCTGCCTATTACTTTCTTGATGAATTAATTATGGCTAATGTTTCAGACAGGCGAATACCATCAAATGCCAAGAGGTCTGTGTTCA
AACAAATGGAAATATAAGACAAAATGATGTGAGGATGGTAGACTTCAGCAACCGTCTCTTTAAaataactaattgtaaaaagtgattt
ttcatttgaattagagcaacactattagtagcatcagaagttagtttaatttgaacccaaaagaattaagattattgataaatt
taaaacccaaaggaatattaacctttgataatttgg
```

```
MASINSIYFDSGDTGFVLISTALVWFMI PGAGYFYSGMAHRKNALS LILLCMVSVAVVTVQWFFFGYSLA
FSKSGNKLI GGRKALFLNLEKEDPY PNTNISESTFAIYQLMFAAITPALAIGSTAERARIFPTIVFIFL
WTTLVYDPIAFVWVSEHGWAHDLGSLDFAGGTPVHMASGAAALAYALVLKRMIESEEGEPKPNNTNII
LGTIMLWFGWFGFNGGSALGANPRATNAIIVTNLSASIGGITWMLWDYRLEGKFSALGFCSGAI SGLVAI
TPASGYVSPPSAIAFGLVSGFLCNLTKLRNIFNYDDACDVFAVHFVGGFIGNILTAIFAQNSIVQLDGH
SDPIDGGFLDHNWIQIVYQLANSLAGGLYSFFATLMIVLIMNEI PGLSLRASPDSETLIDQSELGESAY
YFLDELIMANVQTGEYHQMPRGRVQTNGNIRQNDVEDGRLQQPSL
```

GpyrAMT2 (JX535578)

aaacttaaagtattctgcctggttgtaaggttccctttctttactttccgaaagttcacgaattcaggtcaacgggaaATGGCCGATT
ATAATTCGGGTGATATTTCCCTTCGTTTTGTTGTCGACTGCCTTGGTGTGGTTCATGATTCGCCGAGTGGGATACTTTTATAGCGGTAT
TTCACGTGAGAAGAATGCCTTATCTTTAATAATGTTAAGCGTTTTGTCGGTTGCCGTCGTTTCTTTCCAGtagaaaaatTTAATatt
ggttactatgacatttttcaaaattaatcttctcaattcgttacagTGGTTTTTTGGGGGTATAGCTTGACTTATGGCAAAGATAGC
GGCCCATATATTGGCAATTAAGGAATGCTTTCCTAATCTATGTCGAAAAAATCAAGATTGGTCAAGATAGCTCAATTACAGATATGA
CTTTCGCAATATATCAATGCATGTTTGCCTGCTATAACACCAGCTTTAGCTATGGTTCGGCTGCAGAGCGAGGTGCAATATTTCTGC
CATTTTCTTTTTTTTCATATGGTCAACACTTGTATACGATCCCATAGCGCATGGACATGGTCGCAAGATGGGTGGGGTAAAAACTC
GGAATTCGATTTTCTGCTGGTGGCACACCTGTACACATTTCTTGTGGTGTCTGCTGCTTTAGCCTATTGCCTAATACTCGAAAGCGAC
ATCAAGAAGACCATGAGGAATTTCCGCAGCATAACATTTCCGACACTGTTTTGGGCACTGTGATGTTATGGTTGGTTGGTTGGATT
TAATGGGGGTTCTGCATTGGCTGCTGGCCCTCAAGCCGTTAATGCATACACTGTAACAAATTTATCAGCATCTGTTGGTGGCCTTACT
TGGATGGCAATGGATTTTCGTGTTGAAAGAAAATTAACAACATCGGATTCTGTTGGTGGCATTGCTGGTTAGTAGTAATTACTC
CAGGAGCTGGATATGTTAGTCCCTCATCTTCTATTGCATTTGGATTTATTGGAGGATTTTTTTGTAATTTGGCAACAAATATTAACA
TTGGTTGATTTTGTATGATGCTATGGAAGTATTTCCAGTTCATTGTTGGTGGAAATTTATTGAAATATTTCCACCGGAATATTTGCC
CAGAAATCGATCGCAGCTCTTGATGGGAGGTTAGAAATGATGGTGGTTTGTAGATGGAATTTGGAAGCAAAATAGTTTACCAAATG
CTGGTCTTGTGCTGGCCTTGCAATTTCTTTTCGATTACTTACATTATCTCTTTCATAATGGACCGGTACCAGGTTTTCTTTGCG
TGTTAAGAAAGAAAATGAAACAAGCGGCTTTGATAAAACAGAGATCGGTGAATCAGCATACGATTTTGTGGATGAAGTAATTTCTATTG
AATACGAGAACGCAACGTGAACGAGTTCAACCTGAACCTCAAATCAAGAACTTCTATTAATGAAAGAGGAGTTGAGGTTGTACAAA
ACCGTTCGAGTCTTCAAGGAAAATTAAtataacttgaaagcttctctctcaaggactatcctggatataaatatactattcattt
atgatttatcaccacaatTTTTgaatgattatcatatggttccccag

MADYNSGDISFVLLSTALVWFMPGVGYFYSGISRQKNALSLIMLSVLSVAVVSFQWFFWGYSLTYGKDS
GPYIGNLNRNAFLIYVEKIKIGQDSSITDMTFAIYQCMFAAITPALAIGSAAERGRIFPAIFFFFIWSTLV
YDPIAHWTWSQDQWKKLGIILDFAGGTPVHISCGAAALAYCLILGKRHQEDHEEFRQHNI SHTVLGTVML
WFGWFNGGSALAAGPQAVNAYTVTNLSASVGLTWMAMDFRVERKLSTIGFCCGAIAGLVVITPGAGY
VSPSSSIAFGFIGGFNCLATNIKHWFDFDDAMEVFPVHCVGGIIGNILTGIFAQKSIAALDGRLEIDGG
LLDGNWKQIVYQIAGSCAGLAYSFSITYIILFIMDRVPGFSLRVKKNETSGLDKTEIGESAYDFVDEVI
LLNTRTQRERVQPEPSNQETSINERGVEVVQNRSSAFKEN

GpyrAMT3 (JX535579)

ggatttcacaATGGATTCTGTGGAAGATACGAATGTCACGTTACCATTCAAAAATGGATCTTCACCTGATTATAATCCTGGAGATGTT
GGATTCGTTTTAATGTCGACAGCTTTGGTGTTTTTATGGTGCCTGGAGTTGGATACTTTTATAGTGGGATGGCACGCAGTAAAAATG
CTCTGTCTCTAATATTGTTAAGCCTCCTATCAATTGCGGTAGTTTCATTTTCAGgtatattcttaaaaagggtatcttactatagttttt
atatttaattctttgtttctaaaaaatttttaattctattagTGGTGGTTTTGGGGCTTCAGTTTAAACATATAGCAAAGACAGCGGA
AAATTTATAGGAAATTTTCGTAATATATTCCTTGCAAAACGTTCAAAATGAACCGTCGCCTGTAGCCAAAAATTCAGATCTTGTTT
TTGCATTATACCAACTCATGTTTCGACGAATAACTCCAGCTCTGGCAATAGGGGAGCTGCCGAACGAGCAGCTTTATTTCCAACAAT
TATTTTCATTTTTGTCTGGACAACACTAGTATATGATGTAATTGCACATTGGGTTTTGGTCACCCAATGGATGGGCATATATGATGGGT
GCTATCGATTTTGTCTGGGGGAAACGCTGTTCATATTTCTTGCAGGAGCTGCTGCACCTGCTTATTGTATGATCCTTGGTAAACGAAACG
GCCATGGGACTGAAGAGTTTAGACCTCATAATGTTTCTAATATCGCACTTGGAACTGTGATGATGTGGTTCGGTTGGTTTGGATTTAA
CGGGGTTTCAGCATTATCTGCAAACTTCGTGCAGCAAATGCTATGTATGTCACCAATTTGTCGGCTTCTGTAGGTGGATTAACCTGG
ATGTTTTTAGATTATCGTCTCGAGCGCAAACCTTTCGACACTAAGTTTCTGTTCGGGTATCATCGCTGGTCTTGTAGCAATTAACCTCCAG
GATCTGGATATGTTAGCCCATCAGCAGCACTTTTTATTTGGTTTCCTTGTCTGGGCTTATCTGCAACCTTTCGGTAAAAATAAAAACATGT
TTTTGAATTTGACGACGCTTTGGATGTGTTTGCAGTTCACGGTGTGGTGGCATTCTTGGAAATCTTTTGACGGGAATATTTGCTCAA
AAATCCATTCCTTTTATGATAATCATGAGAGAATTAAGGTGGCTGGTTAGACCATCATTTGGGAGCAAATAGCTTACCAGCTAGCCA
CCTCAATGGCTGGTCTATTTTATTCATTTGCTGTACACATACATATATTATTTATCATGAATATACTACCTGGACTTCAATTCGTGC
TAGCCATGAAGCAGAAGTCAAAGGATTGATGAGTCTGAGATTGGTGAATAATGCCTATTATCAGTCCGACACTTATGGCCGCAAT
GCTAGAAGTGGGAGTTACGAACAATTCGAGAACTCAAAATTTTCAAAATACGTAGGAAAAATCGATCGAACCGAAAGAACATTTG
CTCATTTTTAActttttatttaacgcattttcgacttttaatttttattgtatttatcatgtaataatttaattttaactagcat
aatcttatgataaaagaagaattctagaatctaatttcaggatttttctaattataatgtaccaagattactgaacttttanaggcaa
taatgcaaatatTTTTgtgctctg

MDSVEDTNVTLPLFKNGSSPDYNPGDVGFLMSTALVFFMVPVGVGYFYSGMARSKNALSLILLSLLSIAVV
SFQWWFWGFSLTYSKDSGKFIGNFRNIFLQNVQNEPSPVSQKIPDLVFALYQLMFAAITPALAIGAAAER
ARLFPTIIFIFVWTTLVYDVIAHWVWSPNGWAYMMGAIDFAGGTPVHISCGAAALAYCMILGKRNGHGE
EFRPHNVSNIALGTVMMWFGWFGFNGGSALSANLRAANAMYVTNLSASVGGLTWMFLDYRLERKLSTLSF
CSGI IAGLVAITPGSGYVSPSAALLFGFLAGLICNLSVKLKHVFEFDDALDVFVHGVGGILGNLLTGIF
AQKSI AFYDNHERIKGGWLDHHWEQIAYQLATSMAGLFYSFAVTYIILFIMNILPGLSIRASHEAEVKGI
DESEIGENAYYHVARLMAANARTGELRTIRETSNFQNNVGKIDRTERTFHF

GintAMT1 (coding sequence: CAI54276)

ATGTCTGCTCCCGCTGCTGCTCCTGCTGCAGAACCTAATCCATTTCGATGGTGTTAATATAACAGAACTCATTGCAAATGTGTCAGCAT
TGTCTTCAGTTAACGATATTGATCAAGGACATACAGCATGGATTATGATGTCAACTGCTTTGGTATTTATTATGATTCCAGGTGTCGG
ATACTTTTACAGTGGTATGGCTAGAAAGTAAAAATGCATTATCCCTTATAATGTTAAGTGTTTATCCTTGGCTGTAGTATCAATTCAG
gtatgtttcttttcgataaaataaatggttttttttttttctttttagttagtttttttttttaatacatttgttttttctttctttt
atTTTTtaaaaaaagTGGTGGGCTATCGGTTTCAGTTTAGCATTCGGCCAGGCACAAGTGGTTATATCGGAACTTAAATTATGCT
TTCTTTATGGGTGTCGGTACTGAACCTCTTAATGGTGCTGTAAAAATCCAGGAATAGTTTTTGGCATGTATCAGTGTATGTTGCTG
CTATTACACCCGCACTTGCATCGGGTCTGCAGCTGAACGTGGTAGAATTTCCCAAGCATAATCTTCATTTTTATTGGTCAACTAT
TGTATATGATCCAATGCTTACTGGACATGAATCTTAATGGTTGGTCCGCAAAAATGGGTGGTCTCGATTTTCGCTGGTGGTACTCCC
GTACACATTTCTTCTGGTGTGCTGCTCTTCTTACTGTTAATCTTGGGTAAAAGAACTGGTCATGGAACGTGATGAATTTAACCTC
ATAATATTGCTAATGTTGTACTTGAACCGTTTTACTTTGGTTCGGTGGTGGTGGTTTCAACGGTGGTTCAGCTCTTAATCTACTTC
TCGTGCTGCTATGGCTATCGCTGTAAACCAATTTATCAGCTGCTGTTGGTGGTCTTACTTGGTGGTTATTGGATTATCGACTTGA
AAATTGTCAGCTCTAGCTTTCTGTTCCGGTGTGTTGCAGGACTTGTGCTATCACCCAGGTTCTGGTTATGTTGGTACCCAGCTG
CTGTTGCTTTTGGTTTCATTGCTGGAAATTTGTTGTAATTTGGCCGTTAAATTGAAGCACATCTTTGATTTTGATGACGCTTTGGATGT
TTTTCGCTGTTTCATGGAGTCCGGTGGTGTATTGGTAATATTTAACTGCTATTTTTGCTGAACAAAAAATGTTGCCCTTGACGAACT
GTTTTACCTGGAGGTTGGCTTAATCAACATTGGATACAAATGGGTCATCAACTCGCTGATTCAGTTACTGGTGTAGCTTATTCATTTG
TTGTTACATATTTAATCTTATTTATTATGGATAAAATCCCGGACTTCACTCAGAGCTGATCCTGAATCTGAAGCTAAAGGTTTGA
TGAAACTGAATTAGGAGAATGGCTTATTATCATGTCGATAGACTTGTAGCAGTAAATACACGAACCGGTGAGACAAAAACCGTAAAA
GAAGAAACAATTCACCAACAAAATGACGCAATGCAACAATGTATAA

MSAPAAAPAAEPNPFDFGVNITELIANVSALSSVNDIDQGHATAWIMMSTALVFIPIPGVGYFYSGMARSKN
ALSLIMLSVLSLAVVSIQWVAIGFSLAFPGTSGYIGNLNYAFFMGVGTPELNGAVKIPGIVFAMYQCMF
AAITPALAIGSAAERGRIFPSIIFIFIWSTIVYDPIAYWTWNLNGWSAKMGGLDFAGGTPVHISSGAAAL
AYCLILGKRTGHGTDEFKPHNIANVVLGTVLLWFGWFGFNNGSALNSTSRAAMIAVNTLSAAVGGTLWC
LLDYRLEKKLSALAFCSGAVAGLVAITPGSGYVGTAAVAFGFIAGICCNLAVKPKHIFDFDDALDVFAV
HGVGGVIGNILTAFIAEQKIVALDETVLPGGWLNQHWIQMGHQLADSVTGVAYSFVVTYLILFIMDKIPG
LSLRADPESEAKGLDETELGELAYYHVDRLVAVNTRTGETKTVKEETIHQQNDANATIV

GintAMT2 (coding sequence: CAX32490)

aatttggaaattacatcagtgcataattaatagggaaagcgtggaaccacataatgtatcatatgttggattaacggttaagtacta
caatgggtgattctatattatgttatctattgttctagttctagatggactaataatacataccatgtgtactatttactgatcaca
tgagtacaaaacactttaatctcatgatgatttcgtcaaaacttaatatcttcttttttttaattgattaattattaaatttgacaa
ccaaaaatgatctattaatattattgcggttaactctttattgatttccttaattttgatgaaataatgaaggtttagataagccatt
caagtttttgatactgcggtatgtttttactatgatacaacagtttaaatgaccgcaaaactaaaattctatttgcgatctacaat
agatcattgataatcatagttctttaaataataatattatggtctcatgattcgaaagagaatccacttctgagttctgatgttctaa
gtatagctgtataagatttaccaaagttggattatacgtgtaacggtaaccattgtataggggtaataaccgtataattccgaaattaa
gcacocatttttatgtataatgtcgggcaaggttatcataatgctggtaaaaaatcggaacaatcggttcccggtccgggatgcat
gaatggaattttaaacaaagttataaagcaagtttttttagagttcatggcgtcaaaagatctttacacaaattatcttacgaccta
gttttcccatgataccatctaaaatcgaagaactcttcaataaacattatcctcaaatgcaattgaaaatcaacaaatacaacattca
tgtataataattgtaatatctcctcttttcgaaataaataattcctctgcgccatagttttaaattgtttcatttcttcatgttggccaat
acagtatttaccgttacccttattgatgtatgtatatttattatgaaacatattaatatctacggaacatcatcacggttgaacatgcy
gatatttattttgagttacaatttatattaatgtgcatctcaatcgcatctacttttaattccatggccatgtcctttaactaaatt
ggattcctaattaacaattgatgggtgtttatagataaataatagtaatttataatcttgggttatgtacctttgagttatct
tatcttttaattttaaacaatctttaatatcatcaaaatgtgactcttgttatttcaattaagaactgtactgttattatcgttatacc
cgattattttgtttgtttatattataatagcattacattttccattcaagaaataaaaggtgatcttaaccgttttat
acataattttttgattatgttaataatataatatt
ttccttcatgatgcaactgctgcatctatcattgagaacacaaaatatttattttcccttcatatcggaatttttttgataaggtta
atattataaataacttctgctattcgaagctcggattttctttttgatcgtttcatttgaattgctcctttcaatataagactttatat
tacttatatagttaaacagatacaatcttatacatt
gtatccttctctcattatattttgttcaactagttccctttatagtttatgaaaaATGTCCACAGCTACACCCTAGACGACTCTATGT
TAGTAGAGAATAAATATTTTCCAGGAGATATAGCATGGGTGTGGTGTAGTACCGGCTTGTGTGGCTTATGgtaatttgacttttct
aatttcgagtttgaatt
agATTCCTGGTGTAGTTTTTTTTTATAGTGGTATGGCAAGAAGTAAGAATGCTCTCTCTCATTCTGCTTTGCGTCTTTGTGGTGC
CGTAGTTACTGTACAGGtaaaagagttcttagaatctcattatgtgtagcataatttattttttcagcctaagtgttaacaattatt
ataataaatttttagTGGTTTATTATAGGATATTCTCTCACATTTAGTACAATGGAAATGGTTTCATGGTAATGTAGATCACGCTTT
TTTTCGAAATCTCAAAGGAAATCCATCATTGCCAGTCAAAGAATTCAGATATATATATATGCAGTATATCAAGGAATGTTTGTCTCA
GTTACACCAGCATTAGCAATGGTGCAGCTGCCGAAAGAGCAAGAGTAGTTCCATTGCTAATATTTGTGTTTGTATGGACAACCTTAG
TATATGATGTTATTGCATCATGGTCATGGTCAGAAAAAGGATGGTATGCACAATTAGGCGGATTAGATTTTCCCGGAGGTACGCCAGT
ACATATAACATCAGGTGCAGCTGCATTAGCATATTGTATTAATAGGAAAGAGACACGGTCATGGTACGGATGAATTTAAACCGCAT
AATGTAGCAAATGTAATATTAGGCACCACTATGTTATGGTTTGGATGGTTTGGATTCAATGGAGGTAGTGCCAATGCCGCTAACATAA
GAGCAATAATGGCATTAACTCTAGTAATTTAGCAGCTTCTGTAGGTGGAATAACATGGATGTTAATAGATTATAGGTTAGAAAGAAA
ATTATCTGCTTTGGGATTTCTGTTCTGGCGCGTAGCAGGATTTGGTGTGTGTACACCAGGGAGCGGATATTAATGTACCATCAGCT
ATAGCATTTTGAATTTGGAGGTACATCATGTAATTTTGTGTTAAATTTAAACATTTATAGATTTTGTATGATGATGATGATGATGATG
TTGCTGTACATGGGTTGGTGGTATATGTGAAATATTTTAAACCGtaaggaagtaataaacttttttttttttttttttttttttttttt
aaagaatagtaattaagcatt
GTTGGTTAGATGGTCATTGGGTTCAAATACTTTATCAACTTGCTGATAGCTGTGCTGGTTTACTTTATAGCTTTTGTGTTACATATAT
GATTTTATTATAATGGATAAAATTCCTGGTTTACATTTAAGGGTTGATATTGAGGCCGAAGAACAAGGTATTGATGATACTGAATTG
GGTGAATGGCTTATATCACGTTGATCGTCTGCGGTTTACTTAATTCAAATATCTAAATAACTCAACCAATACTCCGCTACTA
TGACTAATATTAATAGTGGTAACTTCCAATACAGCAAGGCACTAATCAATATATACTTAGTTAattagtagctatttaaacaaaaaa
aaaaaaaaaaaaaa

MSTATPLDDSMLENKYFPGDIWVVLVSTGLVWLMIPGVGFFYSGMARSKNALSLILLCVLCGAVVTVQW
FIIGYSLTFSTNGNGFIGNVDHAFRNLKGNPSFASQRI PDILYAVYQGMFASVTPALAIIGAAAERARVV
PLLI FVFVWTTLVYDVIA SWSWSEK GWYAQLGLDLFAGGTPVHITSGAAALAYCIKLGKRHGHGHTDEFKP
HNVANVILGTTMLWFGWFGFNGGSANAANIRAIMALTSSNLAASVGGITWMLIDYRLERKLSALGFCSGA
VAGLVCVTPGSGYINVPSAIAFGIVGGTSCNFAVKLKHLLDFDDALDVFVHGVGGICGNILTGFIFAQKE
VAALGGQVIQGGWLDGHVWQIILYQLADSCAGLAYSCVYTMILFIMDKIPGLHLRVDIEAEEQGIDDTTEL
GELAYYHVDRLAGLLNSNYLNNSTNTSATMTNINSGKLP IQQGTNQYILS

6.2 List of figures

Figure 1: Steps in AM formation.	13
Figure 2: Root organ culture for cultivation of AM fungi.	15
Figure 3: The <i>G. pyriformis</i> symbiosis and its comparability to AM.	18
Figure 4: Metabolic fluxes in AM.	20
Figure 5: Fixation of Ammonium.	21
Figure 6: Amino acid sequence and predicted topology of GintAMT1.	24
Figure 7: Distinct transport mechanisms for Amt proteins.	25
Figure 8: Proposed transport mechanism of MEP2-like AMTs.	26
Figure 9: Topologies of glomeromycotan AMTs and AMT genes and their relationship.	29
Figure 10: Phylogenetic analysis.	31
Figure 11: Yeast complementation capability of glomeromycotan AMTs.	32
Figure 12: Localization of GFP-tagged AMTs in <i>S. cerevisiae</i> .	34
Figure 13: Methylammonium uptake kinetics of ScMEP1, GintAMT1, GpyrAMT1 and GpyrAMT2.	36
Figure 14: GpyrAMT1 transports ammonium but not methylammonium.	37
Figure 15: Ammonium removal assays.	39
Figure 16: Mutation of cysteine 173 to serine restores transport capacity of GpyrAMT2.	40
Figure 17: Antibody test on yeast cells expressing AMT-GFP fusion proteins.	42
Figure 18: Immune localization of beta-tubulin in a fungal hypha and a plant root.	44
Figure 19: Immune localization of GintAMT1 in extraradical mycelium.	44
Figure 20: Immune localization of GintAMT2 in extraradical mycelium.	46
Figure 21: Immune localization of GintAMT3 in extraradical mycelium.	47
Figure 22: Immune localization of GintAMT1 in extraradical mycelium on medium lacking NH ₄ ⁺ .	49
Figure 23: Summary of immune localization data in varying extraradical fungal structures	49
Figure 24: Immune localization of GintAMT1 in colonized roots.	51
Figure 25: Immune localization of GintAMT2 in colonized roots.	52
Figure 26: Immune localization of GintAMT3 in colonized roots.	54
Figure 27: GintAMTs are not located to arbuscules.	55
Figure 28: Summary of immune localization data in varying intraradical fungal structures	56
Figure 29: <i>In-situ</i> -RT-PCR controls on colonized <i>M. truncatula</i> roots.	58
Figure 30: <i>In-situ</i> -RT-PCR on colonized <i>M. truncatula</i> roots.	59
Figure 31: Comparison of mycorrhization level and ROC success rate.	61
Figure 32: Biomass production of mycorrhizal chicory roots in ROL with different phosphate concentrations.	62
Figure 33: Comparison of high-P and low-P ROLs.	63
Figure 34: Continuous ROL cycles are stable.	64
Figure 35: Influence of gellan gum and sucrose concentration on ROC success rate.	65
Figure 36: Experimental setup and time management.	66
Figure 37: Transformed <i>R. irregularis</i> spore expressing GFP.	67
Figure 38: Structural model of the hydrophilic pore in GpyrAMT2.	70

6.3 List of Tables

Table 1: Antibody tests on yeast cells expressing AMT-GFP constructs.	43
Table 2: glomeromycotan AMTs can be classified into three functional groups.	73
Table 3: For this work prepared and used buffers and solutions	82
Table 4: Media used in this study	87
Table 5: Nutrient compositions of MSR medium variants.	89
Table 6: MSR medium variants and their composition.	89
Table 7: Oligo nucleotides used in this study	90
Table 8: Plasmids used in this study	92
Table 9: Fungal development on <i>Medicago truncatula</i> wild-type roots	101

6.4 Abbreviations

°C	degree(s) Celsius
A	Adenine
AA	amino acid
AM	arbuscular mycorrhiza (symbiosis)
AMF	AM fungus/AM fungi
AMT	ammonium transporter
BLAST	basic local alignment search tool
bp	nucleic acid base pair(s)
C	Cytosine
c.	circa
cDNA	complementary DNA
CLSM	confocal laser scanning microscope
d	day(s)
DNA	deoxyribonucleic acid
dNTPs	desoxynucleotides
dpi	days post inoculation
dpm	disintegrations per minute
EDTA	ethylenediaminetetraacetic acid
e.g.	for example
EGFP	enhanced GFP
G	Guanine
g	gram(s)
g/l	grams per liter
GFP	green fluorescent protein
h	hour(s)
HC (medium)	Hartwell's complete (medium)
HC	hyphal compartment
kb	kilo basepair(s)
KCl	potassium chloride
K	Michaelis constant
KOH	potassium hydroxide
l	liter(s)
LSU	large ribosomal subunit
M	molar
MA	methylammonium
MEP	methylammonium permease
min	minute(s)
ml	milliliter(s)
mm	millimeter(s)
mM	millimolar
mRNA	messenger RNA
MY	million years
N	nitrogen
ng	nanogram
NH ₃	ammonia
NH ₄ ⁺	ammonium
nm	nanometer(s)
nmol	nanomol
OD ₆₀₀	optical density at a wavelength of 600 nm
ORF	open reading frame
P	phosphorus
PCR	polymerase chain reaction
PHG	pseudohyphal growth
PPA	prepenetration apparatus
RACE	rapid amplification of cDNA ends
RC	root compartment
rcf	relative centrifugal force
RNA	Ribonucleic acid
rpm	rounds per minute
RT-PCR	reverse transcription of RNA
SD	standard deviation
sec	seconds

T	Thymine
TE	Tris EDTA
TMD	transmembrane domain
U	uracil
UTR	untranslated region
UV	ultra violet
V_{\max}	maximal reaction rate
v/v	volume per volume
w/v	weight per volume
yeast	<i>Saccharomyces cerevisiae</i>
μl	microliter(s)
μm	micrometer
μM	micromolar

Curriculum Vitae

Personal Data

Name: Matthias Ellerbeck
Born: 26th September 1983, Munich, Germany
Nationality: German

Education

Apr. 2009 – present:
Doctoral student at the Ludwig-Maximilians-Universität (LMU) München
Topic: Identification and characterization of glomeromycotan ammonium transporters. Supervisor: Prof. Martin Parniske

Oct. 2004 – Jan. 2009:
Diploma in Biology (Grade 1,3) at the LMU München
Major subject: Genetics. Minor Subjects: Microbiology, Biochemistry

May 2008 – Jan. 2009:
Diploma thesis about “Charakterisierung der putativen Ammonium-transporter GpAmt1p und GpAmt2p aus Geosiphon pyriformis”.
Supervisors: Prof. Martin Parniske and Dr. Andreas Brachmann

Sep. 1995 – Jul. 2003:
Secondary school (Grade 1,8) at the Adolf-Weber-Gymnasium München

Conferences

Oral presentation

Ellerbeck, M., Dafinger, C., Brucker, D., Schüßler, A. and Brachmann, A.: Nitrogen transport in the arbuscular mycorrhiza symbiosis. International mycological congress 9, 1st – 6th Aug. 2010, Edinburgh, United Kingdom.

Poster presentations

Ellerbeck, M. and Brachmann, A.: Nitrogen transport in arbuscular mycorrhiza symbiosis. Interact 2010 symposium, 23rd Mar. 2010, Munich, Germany.

Ellerbeck, M., Brucker, D., Dafinger, C., Loos, F., Schüßler, A. and Brachmann, A.: Ammonium transport in arbuscular mycorrhiza symbiosis. 11th European conference on fungal genetics, 30th Mar. – 2nd Apr. 2012, Marburg, Germany.

Ellerbeck, M., Brucker, D., Dafinger, C., Loos, F., Schüßler, A. and Brachmann, A.: Ammonium transport in arbuscular mycorrhiza symbiosis. 1st Molecular mycorrhiza meeting, 6th – 7th Sep. 2012, Munich, Germany.